T1-mapping as a Novel Technique for Myocardial Tissue Characterisation Using Cardiovascular Magnetic Resonance – From Method Development to Clinical Validation and Application

Vanessa Ferreira MD FRCPC BSc

Merton College

Department of Cardiovascular Medicine

University of Oxford

Thesis submitted for the Degree of

Doctor of Philosophy

Trinity Term 2012

I dedicate this thesis to my parents, Mr. Roberto Augusto Ferreira Jr. and Mrs. Mabel Hawkett Ferreira – this is as much an accomplishment yours as it is mine because without you, I would never be where I am today.

In loving memory of my grand-father, Mr. Roberto Augusto Ferreira Sr., and my grand-mother, Mrs. Lucy Teresa Ferreira, both of whom passed away peacefully during the course of my DPhil, I will always remember the good times we had together.

Acknowledgements

To my Oxford supervisor **Prof. Stefan Neubauer** – thank you for accepting me into your unit, where I learned all about CMR from you and some of the very best people in the field. I truly enjoyed my time in OCMR and it is arguably the most productive time of my life. Taking everything into account, this DPhil was tougher than my four years at MIT. Thank you for guiding me through it and providing such a stimulating environment. You have been a wonderful mentor.

To my Calgary supervisor **Prof. Matthias Friedrich** – thank you for spending all that time introducing me to CMR back in 2005 at the Stephenson CMR Centre. You inspired me to go into the field, and I can never thank you enough for leading me to Oxford where I developed many skills and advanced as a CMR specialist and researcher. I hope to pay tribute to you by continuing to do great research.

To my Oxford co-supervisor **Dr. Matthew Robson** – thank you for taking me, a non-physicist, on as a DPhil student so that I got an opportunity to do such a fascinating project with you and your team. Thank you and Nicky for Christmas dinner in 2010 when I was stuck here as Heathrow shut down because "the runways are frozen." As a Canadian, I will never understand what happened there.

To my close collaborator **Dr. Stefan Piechnik** – what can I say? Thank you for ShMOLLI and for bringing colour to CMR! As Sairia Dass put it, everyone has an angel during their DPhil, and you were definitely mine. Can't even count how many hours you've spent on ShMOLLI, and those crazy Excel spreadsheets! Thanks for the sandwiches, early scans, late scans, weekend scans, listening to my 3T rants and witnessing my melt-downs. Just remember you promised me the original ShMOLLI phantoms as souvenirs.

To my Oxford co-supervisor **Dr. Theo Karamitsos** – thank you for all your practical advice and support on the projects. As resilient as you may be, I don't think you will ever get used to the British weather compared to what you can get in Greece!

To **Dr. Cameron Holloway** – thank you for always being there for the more junior members coming into the unit. I will not forget how you drove me back and forth from Christ Church to OCMR every day when I first came here for an interview in 2007. Your hospitality and day-to-day help made my transition so much easier and knowing that I could come over for dinner impromptu with you and Ian was always comforting. I shall see the both of you in Sydney!

To **Dr. Erica Dall'Armellina** – thank you for being my partner-in-crime, recruiting all those acute patients and running around like crazy women. I learned lots from you, including scanning at 3T, and portering skills, of course. I'm just glad we took turns having melt-downs, but never both at the same time, and thanks for humouring me on those 6:30 pm discussions (I think you call them "sun-downing").

To **Dr. Sairia Dass** – it was so much fun to have another girly girl in the office to laugh and online-shop with. In response to your DPhil Acknowledgement section, I think I need to break this to you now: "to-do lists" are a delusion – they just keep growing (and can be a constant reminder that you are a failure) until one of two things happen (1) things start dropping off the list and they become a non-issue, or (2) things drop off the list but if they were really that important, they come back to haunt you. Clearly, however, you have done very well, including completing a DPhil and having 2 children during that time. You are truly a remarkable woman.

To **Dr. Sacha Bull** – I didn't believe you when you said you gained 10 pounds during your first year of your DPhil, until it also happened to me. Not sure what to do because I still love going to Dong Dong's with you for Cantonese-style sticky ribs. Thank you for making the office fun and cheerful, and for all your "eggs on the head", "office chair rides" and scalp massages with that special device. I will be returning to Zurich for more Raclette with you.

To **Dr. Ntobeko Ntusi** – thanks for keeping me company during those horrible hours of data processing and circle drawing. I stopped estimating how many circles I needed to draw when my calculator showed 42,000. I think you have double that – Good Luck! No amount of running will fix this one.

I want to thank my family for their continual support and love: my sister **Joanne Michelle Ferreira**, who shares laughter, rants, and pretty much everything with me, including our birthdays (we're not even twins!), and my husband **Wei-Pin Shen**, music conductor and entrepreneur, who introduced me to the wonderful world of music and tolerates nerds.

Last but not least, I want to thank my special friends in the background for keeping me sane and the world magical – CW, JJS and ZZ.

For the pursuit of this degree, I was funded by the Alberta Innovates Health Solutions Clinical Fellowship and the University of Oxford Clarendon Fund Scholarship.

Declaration

The work in this thesis is my own. Drs Matthew Robson and Stefan Piechnik provided physics support and developed the technical aspects (including sequence design, computer programming, computer simulation and phantom experiments) of the novel sequence named "Shortened Modified Look-Locker Inversion Recovery" or "ShMOLLI" for T1-mapping, to which they hold patent rights. Dr. Erica Dall'Armellina provided data on patients with myocardial infarction in chapter 3 for the initial validation of the ShMOLLI method in patients with gadolinium contrast imaging. Drs. Ntobeko Ntusi and Cameron Holloway contributed to data on normal human volunteers for the results in chapters 5 and 6.

Abbreviations

ACUT2E = Acquisition for Cardiac Unified T2 Edema

bpm = beats per minute

CAD = Coronary artery disease

CMP = Cardiomyopathy/Cardiomyopathies

CMR = Cardiovascular Magnetic Resonance

CNR = Contrast-to-noise ratio

ECG = Electrocardiogram

EDV = End-diastolic volume

EF = Ejection fraction

ESV = End-systolic volume

FOV = Field of view

Gd-DPTA = Gadolinium-Diethylene triamine pentaacetic acid

GRAPPA = Generalised autocalibrating partially parallel acquisition

IR = Inversion Recovery

LGE = Late gadolinium enhancement

LV = Left ventricle/ventricular

LVOT = Left ventricular outflow tract

MI = Myocardial infarction

MOLLI = Modified Look-Locker Inversion Recovery

NMR = Nuclear magnetic resonance

RF = Radiofrequency

ROC = Receiver operator characteristic

ROI = Region of interest

RV = Right ventricle/ventricular

SD = Standard deviation

ShMOLLI = Shortened Modified Look-Locker Inversion Recovery

SI = signal intensity

SNR = Signal-to-noise ratio

SSFP = steady-state free precession

STIR = short-tau inversion recovery

SV = stroke volume

T = Tesla

TCM = Takotsubo cardiomyopathy

TD = Delay time

TE = Echo time

TI = Inversion time

TR = Repetition time

TSE = Turbo spin echo

T1 = longitudinal or spin-lattice relaxation

T2 = transverse or spin-spin relaxation

Table of Contents

ACKNOWLEDGEMENTS **1**

DECLARATION **3**

ABBREVIATIONS **4**

TABLE OF CONTENTS **6**

THESIS ABSTRACT **10**

CHAPTER 1 **13**

INTRODUCTION **13**

1.1 Overview 13

1.2 T1-mapping 14

1.3 Goals of this research 18

CHAPTER 2 **20**

GENERAL METHODS **20**

2.1 General Methods 21

2.2 Background and Rationale 21

2.3 Study Participants 23

2.3.1 Inclusion Criteria 24

2.3.2 Exclusion Criteria 25

2.4 Clinical assessment 27

2.5 CMR Scan Protocols 27

2.5.1 T1-mapping 28

2.5.2 Anatomical and functional imaging 28

2.5.3 Dark-blood T2-weighted CMR Imaging 29

2.5.4 Bright-blood T2-weighted CMR Imaging 31

2.5.5 Late gadolinium enhancement (LGE) imaging 32

CHAPTER 3 ..... **33**

SHORTENED MODIFIED LOOK-LOCKER INVERSION RECOVERY (SHMOLLI) FOR CLINICAL MYOCARDIAL T1-MAPPING AT 1.5 AND 3 T WITHIN A 9 HEARTBEAT BREATH-HOLD **33**

3.1 Introduction 34

3.2 Methods 35

3.2.1 Simulation and Sequence design 35

3.2.2. Processing 36

3.2.3. Phantom Studies 39

3.2.4 In Vivo Studies 39

3.2.5 Statistical Analysis 41

3.3 Results 41

3.3.1 Simulation and Phantom Studies 41

3.3.2 Normal Human Subjects 43

3.3.3 Gadolinium contrast application 45

3.4 Discussion 49

3.5 Conclusion 55

CHAPTER 4 ..... **57**

T1-MAPPING DETECTS ACUTE MYOCARDIAL OEDEMA WITH HIGH DIAGNOSTIC ACCURACY: A COMPARISON TO T2-WEIGHTED CARDIOVASCULAR MAGNETIC RESONANCE IMAGING **57**

4.1 Introduction 58

4.2 Methods 59

4.2.1 Ethics and Study Population 59

4.2.2 CMR image acquisition and analysis 61

4.2.3 Statistical Analysis 62

4.3 Results 62

4.3.1 Study Population Characteristics 62

4.3.2 CMR Findings 63

4.3.3 Receiver operating characteristic analysis 63

4.3.4 Intra- and inter-observer agreement of T1-mapping 71

4.4 Discussion 71

4.4.1 CMR for the detection of acute myocardial oedema 74

4.4.2 ShMOLLI T1-mapping: a novel method for imaging myocardial oedema 75

4.4.3 Quality and reliability of ShMOLLI T1-maps 77

4.5 Limitations 79

4.6 Conclusion 80

CHAPTER 5 ..... **81**

THE DIAGNOSTIC PERFORMANCE OF T1-MAPPING AND T2-WEIGHTED CARDIOVASCULAR MAGNETIC RESONANCE IN ACUTE MYOCARDITIS **81**

5.1 Introduction 82

5.2 Methods 83

5.2.1 Study population. 83

5.2.2 CMR image acquisition and analysis 84

5.2.3 Statistical Analysis 84

5.3 Results 85

5.3.1 Study population characteristics 85

5.3.2 Detection of myocardial changes by CMR in acute myocarditis 86

5.3.3 Relationship between myocardial T1 and other measures of acute myocardial injury. 86

5.3.3 Diagnostic performance of CMR methods in the detection of acute myocarditis. 89

5.4 Discussion 92

5.4.1 Dark-blood T2-weighted imaging 92

5.4.2 Bright-blood T2-weighted imaging 93

5.4.3 Late Gadolinium Enhancement (LGE) imaging 96

5.4.4 T1-mapping 97

5.4.5 Combination approach 97

5.5 Limitations 98

5.6 Conclusion....99

CHAPTER 6 **....100**

TISSUE CHARACTERISATION OF ACUTE MYOCARDITIS USING T1-MAPPING: INSIGHTS INTO MYOCARDIAL INJURY FROM QUANTITATIVE CARDIOVASCULAR MAGNETIC RESONANCE **....100**

6.1 Introduction....101

6.2 Methods....102

6.2.1 Study Population....102

6.2.2 CMR image acquisition and analysis....102

6.2.3 Statistical analysis....102

6.3 Results....103

6.3.1 Study Population characteristics....103

6.3.2 Quantification of myocardial injury in acute myocarditis using CMR....108

6.3.3 Patterns of myocardial injury revealed by T1-mapping using incremental thresholds....113

6.4 Discussion....115

6.4.1 Insights from T1 characterisation of acute myocarditis....115

6.4.2 Clinical Implications....116

6.6 Conclusion....117

CHAPTER 7 **....118**

GENERAL CONCLUSIONS AND FUTURE DIRECTIONS **....118**

INDEX OF TABLES AND FIGURES **....121**

APPENDIX 1: R^2 MAPS **....124**

APPENDIX 2: PUBLISHED ABSTRACTS **....130**

APPENDIX 3: PUBLICATIONS **....132**

BIBLIOGRAPHY **....133**

Thesis Abstract

Cardiovascular magnetic resonance (CMR) is superior to other cardiac imaging modalities in its ability to perform multiparametric myocardial tissue characterisation. Commonly applied techniques include T2-weighted (T2W) imaging for detecting oedema and late gadolinium contrast enhancement imaging for detecting fibrosis, allowing characterisation of most cardiac conditions encountered in the clinical setting. While these techniques have proven useful, conventional MR images acquired by these techniques are displayed on an arbitrary scale and only semi-quantitative with some inherent deficiencies. Quantitative techniques, such as T1-mapping, allow direct quantification of tissue properties and may circumvent many of the issues of conventional MR imaging, with potential to offer more insight into diseased myocardium. Although T1-mapping has been well-established for brain T1-mapping, cardiac T1-mapping has been slow to mature due to technical and practical challenges. The aim of this thesis was to develop a novel method for cardiac T1-mapping that is robust and clinically applicable so that cardiac T1-mapping can transition from a research tool into clinical practice. Further, cardiac T1-mapping using this new technique was validated in normal and disease states, including its ability to detect regional and global myocardial oedema and acute myocarditis.

This work developed a novel MR sequence for cardiac T1-mapping, named Shortened Modified Look-Locker Inversion Recovery (ShMOLLI). The conventional method (MOLLI) required 17 heart-beats (a 17 second breath-hold for a patient with a heart rate of 60 bpm) for the acquisition of one slice of T1-map. This is difficult to achieve for patients, especially those who are acutely ill and if whole heart coverage (~8 slices) were desired. One of the goals in the design of ShMOLLI was to bring the breath-hold time down to below 10 seconds so that patients may tolerate the protocol. The design of ShMOLLI was successful in breaching the

10-second breath-hold time without compromising the accuracy of T1 measurements compared to the conventional method; further, unlike MOLLI, ShMOLLI did not exhibit increasing error with increasing T1 or heart rates, making it advantageous in measuring long T1 values and at fast heart rates. These features of ShMOLLI make it a very attractive method ready for clinical application.

The ShMOLLI method was then further applied to disease states, starting with models of acute myocardial oedema. ShMOLLI T1-mapping was performed in patients with acute stress-induced cardiomyopathy (model of global oedema) and in patients with regional oedema without infarction, and compared to T2W imaging. T1-mapping demonstrated an excellent diagnostic performance compared to the T2W methods in detecting acute myocardial oedema, whether it was global or regional. ShMOLLI T1-mapping was well-tolerated by acute cardiac patients and showed promise in its application to other conditions in which oedema would be a major component in the pathophysiology.

ShMOLLI T1-mapping was next applied to patients presenting with acute myocarditis, in which oedema and inflammation are major components. Compared to the conventional MR methods of T2W and LGE imaging, T1-mapping again showed superior diagnostic performance to T2W imaging and equivalent performance to LGE imaging in detecting acute myocarditis. Further, T1-mapping was able to detect a larger extent of injury compared to both of these methods, and provided topographic information such as the non-ischemic patterns of injury similar to that seen on LGE imaging, but without the need for exogenous contrast agents.

In conclusion, this thesis reports the development of a novel method for cardiac T1-mapping, its validation and clinical application to detect myocardial oedema and characterise

acute myocarditis without the need for exogenous contrast agents. ShMOLLI T1-mapping holds promise in quantitative tissue characterisation in a wide range of myocardial diseases.

Chapter 1

Introduction

1.1 Overview

Cardiovascular magnetic resonance for myocardial tissue characterisation

Cardiac disease remains the leading cause of death in developed nations, including the United States of America (1) and the United Kingdom (2). In addition to conventional diagnostic tools, such as electrocardiography, echocardiography and nuclear imaging, that aid in the work-up of heart disease, cardiovascular magnetic resonance (CMR) is an ideal tool for examining the heart in both ischaemic and non-ischaemic aetiologies. It provides an accurate and reproducible method for the assessment of ventricular mass and cardiac chamber sizes, regional and global left ventricular (LV) function. General advantages of CMR over other non-invasive cardiac imaging modalities include its improved accuracy, that image quality is not adversely affected by body habitus and that it does not involve ionising radiation or radioactive isotopes. Notably, the main strength of CMR is its superior capability for multiparametric tissue characterisation with a wide range of techniques. Selected examples include contrast-enhanced CMR, which is an accurate imaging tool for quantifying myocardial necrosis, previously possible only post-mortem, and T2-weighted imaging, which detects myocardial oedema indicative of acute inflammation and/or injury. CMR has been proven useful in distinguishing ischaemic from non-ischaemic heart disease, as well as amongst the non-ischaemic aetiologies (3). Thus, CMR is a powerful tool to characterise cardiac

phenotypes, enabling accurate measurements of cardiac indices, function and myocardial tissue characterisation.

1.2 T1-mapping

In magnetic resonance (MR) imaging, tissue contrast is generated by a combination of intrinsic tissue properties such as flow, proton density, spin-lattice (T1) and spin-spin (T2) relaxation times, and extrinsic properties such as imaging sequence, imaging coils and settings. Consequently, signal intensity on conventional MR images is displayed on an arbitrary scale, and is not suitable for comparison between subjects.

Quantitative techniques, on the other hand, aim to provide a quantitative surrogate marker for the cellular environment of the myocardium, allowing direct comparison between patients and examinations. T1-mapping is one such technique, which provides pixel-resolved estimates of the T1 relaxation time of the underlying tissue. As discovered by Nobel laureates Felix Bloch and Edward Purcell in 1946, there is a small preference of nuclei with uneven molecular spin numbers to align with the direction of an externally applied magnetic field. These aligned spins exhibit what is known as longitudinal magnetisation (Mz). Mz can be perturbed by selected radiofrequency (RF) pulses, which constitutes the underlying mechanism of nuclear magnetic resonance (NMR) and magnetic resonance imaging (MRI). Among the many different parameters that describe NMR processes, T1 refers to the relaxation time which Mz returns to the thermodynamic equilibrium after the externally applied RF pulse has been released. Specifically, T1 relaxation time refers to the time it requires for 63% of the longitudinal magnetisation (Mz) to recover from the initial disturbance in longitudinal magnetisation (4), as shown in Figure 1.1. T1 relaxation times depend on the composition of tissues and cellular environment of water, and each tissue type exhibits a characteristic range of normal values at a selected magnetic field strength (5). T1 relaxation

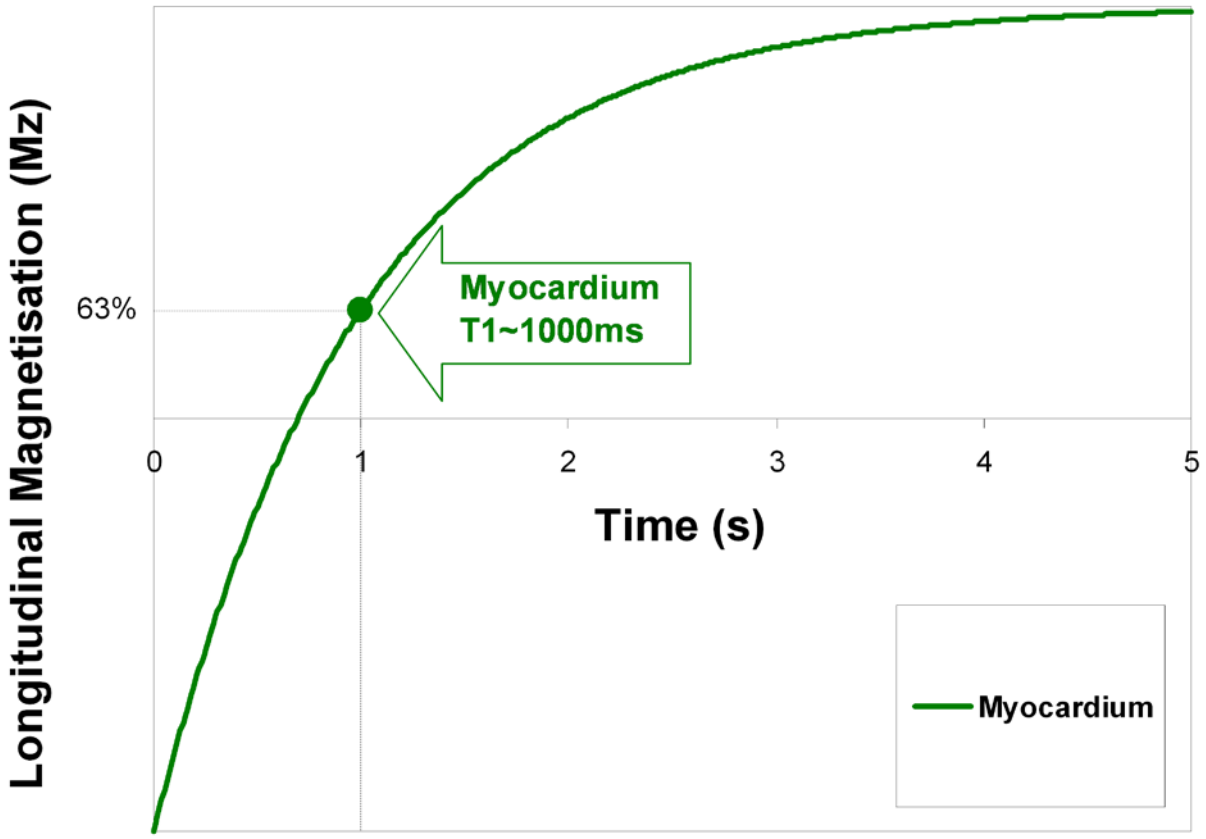


Figure 1.1 T1 relaxation curve of normal human myocardium at 1.5 Tesla.

times, or T1 values, calculated on a pixel-by-pixel basis (Figure 1.2A), can be generated into a parametric T1-map (Figure 1.2B). Deviation from established normal ranges in a particular tissue, such as the myocardium, can thus be used to quantify the effects of pathological processes.

There are a number of advantages to T1-mapping compared to existing methods. Conventional CMR techniques for tissue characterisation, such as T2-weighted and late gadolinium enhancement (LGE) imaging, require a reference region of interest (ROI) in order to detect signal intensity changes within the myocardium, meaning that measured signal changes are always relative and displayed on an arbitrary scale (see also Chapter 2). T1-mapping, on the other hand, allows direct quantification of tissue characteristics, as the T1 value of a pixel is representative of the T1 relaxation time of that underlying tissue. This eliminates the need for reference ROIs and also minimises subjectivity. T1-mapping allows direct comparison of signal changes between different subjects or within the same subject over different examinations over time. Further, no exogenous contrast agent is required for the high resolution tissue characterisation of this type, which is especially useful for patients who cannot tolerate gadolinium-based contrast agents.

Despite these advantages, myocardial T1-mapping has been slow to mature into widespread clinical application. T1-mapping had been well-established for the brain using the conventional Look-Locker (LL) inversion recovery method developed in 1970 (6) . While widely-applied for brain T1-mapping, the LL method was not well-suited for cardiac T1-mapping due to the fact that it acquires data continuously throughout the cardiac cycle without taking into account cardiac motion (7). In the 1980s, there were isolated experimental work on myocardial T1-mapping using ischaemic canine models and a clinical study examining T1 relaxation times in hypertrophic cardiomyopathy and systemic lupus erythematosus using other T1-mapping methods (8,9). It was not until 2004 that a technically-

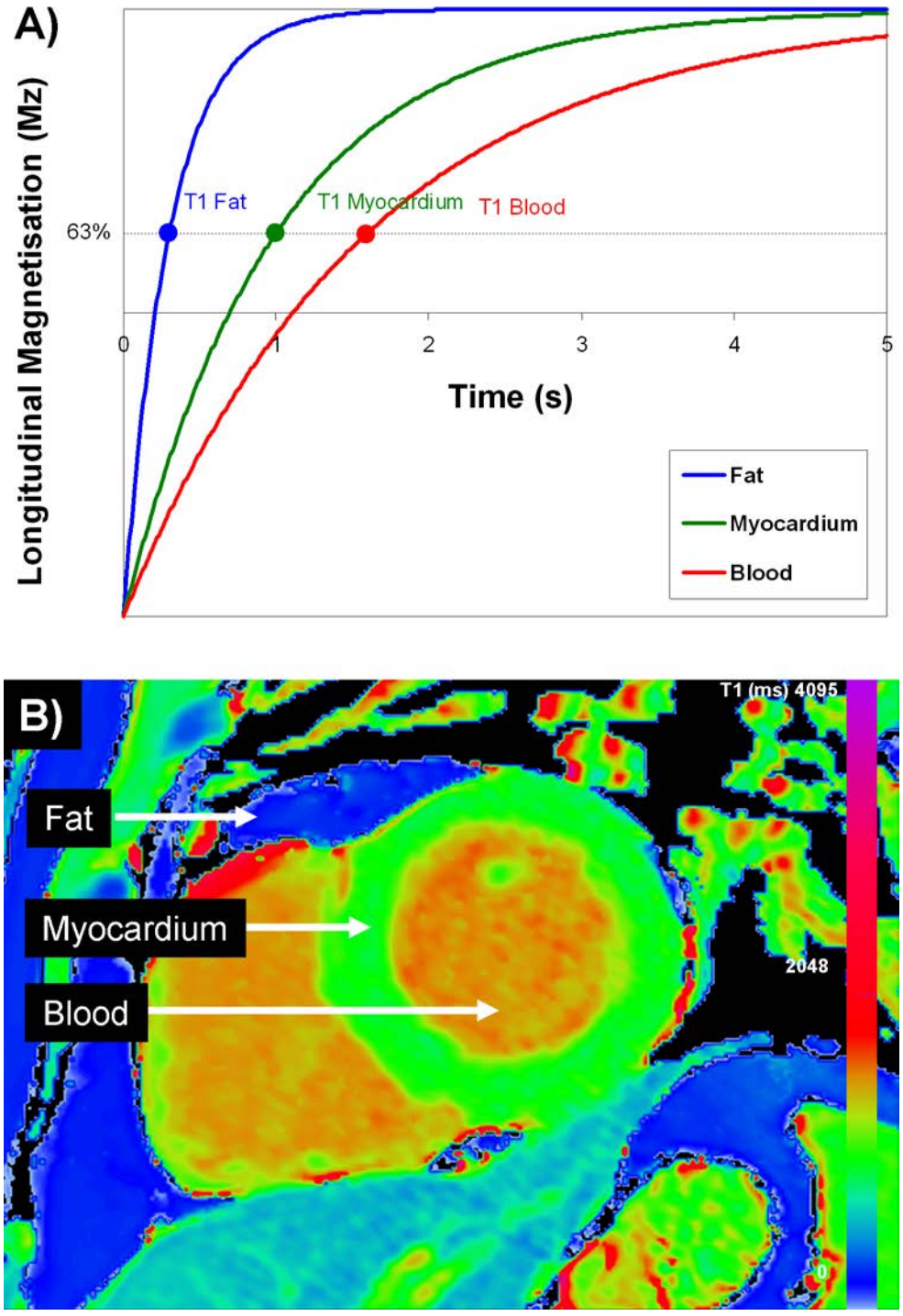


Figure 1.2 (A) T1 relaxation curves of fat, myocardium and blood. (B) Colour T1-map.

improved sequence for cardiac T1-mapping, named Modified Look-Locker Inversion Recovery (MOLLI), was introduced which allowed myocardial T1-maps to be acquired within a single, but relatively long breath-hold (~17-20 seconds, depending on the subject's heart rate)(7). Nevertheless, T1-mapping remained a research tool primarily, perhaps due to a few practical and technical challenges. Our research team felt that it is a promising method with excellent potential, and thus set out to accomplish a number of goals towards bringing T1-mapping into the clinical realm.

1.3 Goals of this research

This work aimed to develop a method for T1-mapping that is clinically applicable from a technical and practical standpoint, and to perform clinical validation and application of the technique. Specifically, the following were explored:

1. Devise a T1-mapping sequence that would significantly shorten the breath-hold time, ideally to under 10 seconds, such that typical clinical patients will be able to comply with ease. This is described in chapter 3 where the new sequence design, initial validation in computer simulation and phantoms, and clinical validation in normal volunteers and selected patients with myocardial infarction are presented.

2. Perform clinical validation of the novel T1-mapping method in normal human volunteers and to obtain normal T1 values in the human myocardium. This is presented in chapter 3 where clinical validation of the new method against the conventional method for T1-mapping in estimating myocardial T1 in normal volunteers are presented.

3. Test the novel T1-mapping method in disease states. We have initially tested the method in a few cases of acute myocardial infarction in the early clinical validation stage (Ch.3).

We then focused on acute non-ischaemic cardiac pathologies, starting with acute myocardial oedema without infarction, in order to test the ability of T1-mapping to detect pure myocardial oedema, and then acute myocarditis, to test whether T1-mapping can diagnose and further characterise this disease. These studies are described in chapters 4, 5 and 6.

Chapter 2

General Methods

2.1 General Methods

Research procedures received a favourable opinion from the Oxfordshire REC B Committee (REC reference: 09/H0605/64) of the National Research Ethics Service (NRES) representing the NRES Directorate within the National Patient Safety Agency and Research Ethics Committees in England. All subjects gave written informed consent for all study procedures.

2.2 Background and Rationale

General background

This thesis focused mainly on the application of novel and conventional CMR methods in the study of patients presenting with non-ischaemic aetiologies of acute myocardial injury, defined as those admitted to hospital with acute chest pain, abnormal rise in Troponin levels and normal or minimally-diseased coronary arteries by coronary angiography. This cohort of patients often presents a challenge to clinicians, and account for up to 10% of patients presenting to hospital with chest pain and positive troponins (10). Acute myocarditis is the top cause of myocardial injury in this cohort (11), but can also include stress-induced (Takotsubo) cardiomyopathy, myocardial stunning or infarction potentially due to ruptured coronary plaques, coronary embolism or vasospasm (11). The main challenge lies in accurately locating and diagnosing the cause of myocardial injury, which in turn can affect the management plan for these patients. Oftentimes, a definitive diagnosis is never confirmed in this clinical conundrum, and the patient is managed without any standardised approach. Cardiovascular magnetic resonance (CMR) is an ideal non-invasive diagnostic tool in this cohort. Not only can cine CMR enable an accurate assessment of left ventricular function and morphology, conventional tissue characterisation techniques such as late gadolinium

enhancement (LGE) imaging can identify patterns of myocardial necrosis/fibrosis, and T2-weighted CMR allows detection of myocardial oedema reflective of acute inflammation/injury.

Current limitations and rationale for investigation

At the start of this project in 2008, the most recent and largest study performed in this cohort using CMR (performed at 1-90 days) revealed a diagnosis in 65% of the cases, with myocarditis being the most common aetiology (50%), followed by myocardial infarction (12%) and non-ischemic cardiomyopathies (3.4%); 35% of patients had a normal CMR scan and thus still did not have a diagnosis, but significant pathologies, such as myocardial infarction, fibrosis and inflammation were ruled out (11). This study demonstrated that CMR adds incremental value in addition to traditional diagnostic modalities in the work-up of this challenging group of patients. However, the fact that 35% of cases still remained undiagnosed was intriguing, and may have been due to a couple of factors, including: (1) an early diagnostic window may have been missed by not scanning all patients as early as possible; some CMR features, which could have revealed a possible aetiology such as acute myocarditis, may have resolved by the time of scanning (12); (2) Selection of patients – those patients who had a normal CMR scan and remained non-diagnostic also were more likely to have only modest levels of troponin-elevation; conventional techniques such as dark-blood T2W imaging have known limitations (such as signal drop out in the posterior wall, low signal-to-noise ratio), and may not have the resolution to detect very small areas of injury; on the other hand, some patients may have had only oedema but no LGE, and if these patients were scanned at a later date when oedema has already resolved, the initial area of injury would not have been identified. Thus, scanning these patients early, and the use of novel techniques, such as quantitative pixel-wise T1-mapping, may add diagnostic value in detecting small areas of acute injury in this cohort.

2.3 Study Participants

Patients

Patients were those admitted to hospital presenting with acute chest pain, myocardial injury (as defined by abnormal elevation of at least 2 serial troponin levels) and coronary angiography showing normal or minimally-diseased coronary artery disease. Patients were identified through referrals by their treating physicians at the John Radcliffe Hospital and Milton Keynes Hospital (UK). Investigators or the patients' physicians approached and provided them with a PIL. Patients may contact their physician or study investigators to express interest in participation. Recruitment and study procedures took place at the John Radcliffe Hospital.

In Chapter 3, for the initial in-vivo validation of the novel T1-mapping method ShMOLLI, four patients with acute ST-elevation myocardial infarction treated with primary percutaneous coronary intervention (PCI), who belonged to another research study led by Dr. Erica Dall-Armellina, were studied. Their inclusion/exclusion criteria are also included below.

Healthy Volunteers

Healthy volunteers were recruited to serve as controls, as some CMR features explored in this study are novel. Healthy volunteers were identified via local advertising approved by the ethics committee and upon contacting the investigators were provided with a participant information leaflet (PIL) and screened for eligibility.

2.3.1 Inclusion Criteria

Patients (acute chest pain, positive troponins, un-obstructed coronary arteries)

- Male or female, at least 18 years of age.
- Patient is willing and able to give informed consent for participation in the study
- New-onset chest pain, present at rest.
- Abnormal troponin elevation of at least ≥ 0.04 ug/L
- Coronary angiography demonstrating normal or minimally-diseased coronary arteries, defined as < 50% stenosis in the main- and side-branch arteries, for patients aged 40 years or older. For patients aged 18-39 years-old, if their clinicians deem that coronary blockages are unlikely based on the patient's clinical profile and presentation, significant coronary artery disease may be excluded on clinical grounds without the need of a coronary angiogram.

Patients (acute myocardial infarction treated with 1º PCI, in Chapter 3)

- Male or Female, aged 18 years or above.
- No previous history of cardiovascular disease (including hypertrophic cardiomyopathy, dilated cardiomyopathy, myocarditis, moderate to severe valvular disease).
- Diagnosed acute myocardial infarction within 12 hours from symptoms onset. Myocardial infarction was defined as follows: ST-elevation MI : Patients with typical cardiac ischaemic chest pain ongoing for ≥ 30 minutes and/or ECG positive for ST elevation of 2 mm in 2 consecutive ECG leads (1 mm in peripheral leads) or 2-fold increment of CK-MB or increment in Troponin

Healthy Volunteers

- Male or female, at least 18 years of age.
- No known cardiac disease, hypertension, diabetes mellitus or chronic systematic diseases known to have or at high risk for cardiac involvement (e.g. amyloidosis, sarcoidosis, systemic lupus erythematosus)
- Normal cardiac examination
- Normal resting ECG

2.3.2 Exclusion Criteria

All patients

- Age < 18 years-old
- Contraindications to magnetic resonance imaging (including severe claustrophobia, cardiac pacemaker, internal cardiovertor-defibrillator, cranial aneurysm clips, metallic ocular foreign bodies, inability to lie flat, etc)
- Patients with significant renal impairment (GFR < 60mL/minute).
- Patients who have had or are undergoing liver transplantation
- Patients with known allergies to contrast (gadolinium-contrast containing agents).
- Female who is pregnant, lactating or planning pregnancy during the course of the study.
- Patients who are unstable, critically or terminally ill.

Patients (acute chest pain, positive troponins, un-obstructed coronary arteries)

- Patients who have known, pre-existing heart disease of any aetiology, including coronary artery disease, previous myocardial infarctions, significant valvular disease, history of

myocarditis prior to the current admission, and cardiac dysfunction of any other known aetiology.

- Patients found to have significant coronary artery disease, defined as ≥50% stenosis in the main- or side-branch arteries on coronary angiography.
- Patients found to have non-stenotic coronary artery disease as a cause of troponin elevation (e.g. coronary vasospasm, left-anterior descending coronary artery muscle bridge, coronary artery dissection)
- Patients requiring coronary interventions.
- Patients presenting with hypertensive emergencies.
- Patients who may have suffered myocardial contusion(s) due to accidents consistent with the mechanism of injury (e.g. motor vehicle accidents, deceleration injuries)
- Patients diagnosed with non-cardiac causes of elevated troponin (including pulmonary embolism, COPD exacerbation, septicaemia, cerebral vascular accident or other neurologic catastrophes)
- Recent or current septicaemia or septic shock.
- Patients with a history of chronic troponin elevation.
- Chronic systematic diseases known to have or at high risk for cardiac involvement (e.g. amyloidosis, sarcoidosis, systemic lupus erythematosus)
- History of treatment with chemotherapy or radiation therapy to the chest wall.

Patients (acute myocardial infarction treated with 1º PCI, in Chapter 3)

- Patients with CV events occurring in the first 12 hours post reperfusion (moderate to severe congestive heart failure symptomatic for shortness of breath leading to incapability to lay on the scan table; dangerous arrhythmias, reoccurrence of angina/NSTEMI with indication for catheterization)

2.4 Clinical assessment

On the day of scanning, all subjects underwent a focused clinical assessment. This included history for:

- Inclusion and exclusion criteria as above.
- Drug history including allergies

The following study procedures were also performed:

- Blood pressure measurements using a manual sphygmomanometer
- 12 lead electrocardiogram, (ECG)
- Height (cm) and weight (kg) using calibrated scales.
- Blood test for Troponin I if not already performed during hospital admission
- Creatinine check to measure glomerular filtration rate.

2.5 CMR Scan Protocols

Subjects underwent CMR scanning which included the following:

(1) Left ventricular function

(2) T1-mapping

(3) Dark-blood T2W imaging to assess for oedema

(4) Bright-blood T2W imaging to assess for oedema

(5) Late gadolinium enhancement (LGE) to assess for cell necrosis/fibrosis

CMR studies were performed using a 1.5T MR system (Siemens Avanto, Germany). A 32-channel phased-array chest coil was used for all data acquisition, except for STIR imaging for which the body coil was used. T1-mapping and oedema imaging were acquired before the administration of contrast agents. Imaging performed with the methods listed above was acquired with matching short-axis images for comparison.

2.5.1 T1-mapping

Myocardial T1-mapping was performed using the novel sequence Shortened Modified Look-Locker Inversion Recovery (ShMOLLI), which was newly developed in this unit as part of this thesis in collaboration with the Cardiac Physics team Drs Matthew Robson and Stefan Piechnik. This is discussed in further detail in chapter 3.

2.5.2 Anatomical and functional imaging

Cardiac volumes were acquired using Steady State Free Precession (SSFP), retrospectively-gated imaging. Scan parameters are typically: voxel size 2.0x2.0x8.0mm, FOV=380x380mm, TR/TE 39.6/1.12ms, flip angle 55^{o}, matrix 192x192, GRAPPA=3, 24 reference lines, segments=15, concatenations=1). Pilot, horizontal long axis, vertical long axis and short axis stack images were acquired with the patient in the supine position. The slices were obtained during a breath-hold at the end of normal expiration to minimise the effects of respiratory motion.

Using Argus post-processing software package software (Version 2002B, Siemens Medical Solutions), LV short axis epicardial and endocardial borders were manually contoured at end diastole and end systole. LV end systolic (ESV) and end diastolic (EDV) volumes are used to calculate stroke volume (SV). Ejection fraction (EF) and cardiac output (CO) are calculated (EF = SV/EDV, CO=SV x HR). Myocardial mass was also calculated by subtracting the endocardial volume from the epicardial volume. LV mass was calculated based on prior knowledge of myocardial specific gravity (1.05 g/cm^{3}). Regional wall motion was visually-scored using in-house software MC-ROI (programmed by SKP in IDL v.6.1, www.ittvis.com). Segments were graded as: normal=1, hypokinetic=2, akinetic=3, or dyskinetic=4.

2.5.3 Dark-blood T2-weighted CMR Imaging

T2-weighted turbo spin echo images were acquired using an ECG-triggered Short-Tau Inversion Recovery (STIR) sequence with fat and moving blood suppression (13,14) in the short axis view covering the left ventricle from base to apex using the body coil. Scan parameters are typically: voxel size 1.9x1.5x10.0mm (no gap between slices), FOV=380x309mm, matrix=166x256, TE=61ms, TR 80-85% of RR interval during breath-hold, flip angle 180^{o}, TI=170ms, dark blood thickness 200%, dark blood flip angle 180^{o}, turbo factor 25, echo trains per slice=7, phases=1, concatenations=1.

As previously described (14), the short axis T2-weighted TSE image through the base of the left ventricle is reviewed for the presence of an adequate cross-section through skeletal muscle for later placement of a reference ROI. If a satisfactory reference region is not available, the initial T2 TSE image is used to revise the graphic prescription by shifting the field of view more off-centre towards the left shoulder to include a suitable sample of chest wall / left shoulder / left upper arm skeletal muscle, adjusting the size of the field of view as necessary.

Quantitative analysis was performed by comparing the LV myocardium in short axis against 2 reference regions of interest: (1) in remote myocardium, and (2) within adjacent skeletal muscle in the same slice, verified on a corresponding SSFP image (Figure 2.1). The T2 signal intensity (SI) ratio was calculated as: (1) T2 $SI_{myo:remote}$= $SI_{myocardium}$/$SI_{remote\ myocardium}$ and (2) T2 $SI_{myo:skeletal}$=$SI_{myocardium}$/$SI_{skeletal\ \ muscle}$, as previously published (15). Care was taken to exclude non-suppressed blood pool signal due to slow-flow adjacent to the subendocardium.

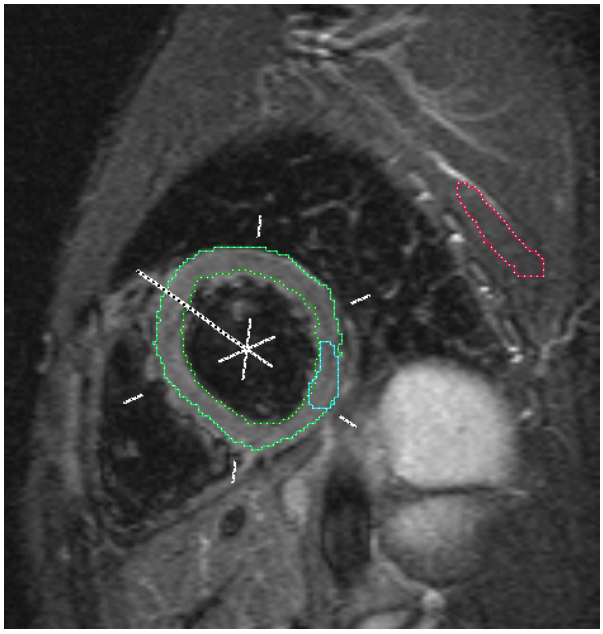


Figure 2.1 Dark-blood T2-weighted image with myocardial contours (green contours) and regions of interests over remote myocardium (blue contour) and skeletal muscle (red contour).

2.5.4 Bright-blood T2-weighted CMR Imaging

Bright-blood T2W images were acquired using ACUT2E, a turbo spin echo-steady state free precession (TSE-SSFP) hybrid sequence for T2-weighted imaging of oedema in the heart (16), in the short axis view covering the entire left ventricle from base to apex. Scan parameters were typically: voxel size 1.9 x 1.5 x 8.0mm, FOV=380x309mm, matrix=165x256, TR/TE=229.70/1.78ms, effective TE=98ms, flip angle 180^{o}, T2 prep duration=24ms, segments=33, 5 shots per slice, phases=1, concatenations=1, bandwidth=781 Hz/Px).

Quantitative analysis was performed the same way as for STIR images on coil intensity normalised and distortion corrected images (Figure 2.2). If no suitable reference skeletal muscle were available on a slice (i.e. affected by artefacts), then a ROI with a mean SI and SD similar to that of skeletal muscle of the nearest neighbouring slice is placed on the index slice.

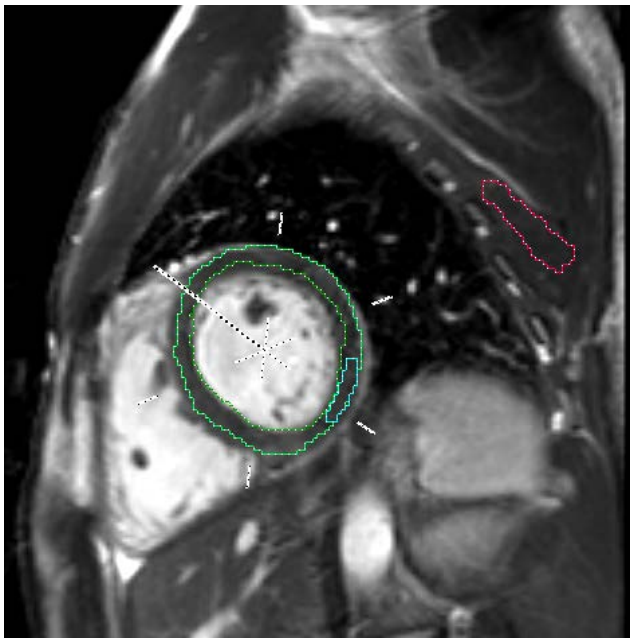


Figure 2.2 Bright-blood T2-weighted image with myocardial contours (green contours) and regions of interests over remote myocardium (blue contour) and skeletal muscle (red contour).

2.5.5 Late gadolinium enhancement (LGE) imaging

Delayed enhancement imaging was acquired using a T1-weighted phase-sensitive inversion recovery sequence 8-10 minutes after the administration of top up intravenous contrast agent (Gadodiamide, Omniscan, GE Healthcare, UK, total 0.13mmol/kg body weight at 6ml/s) and provides quantification of fibrotic tissue. The inversion time was adjusted for optimal nulling of remote normal myocardium.

The scan parameters were typically: voxel size 2.0 x 1.5 x 8.0 mm, matrix 144x256, FOV=380x285mm, TR/TE=800.20/3.36ms, flip angle 25^{o}, GRAPPA=2, 24 reference lines, segments=25, phases=1, concatenations=1, measurements=1, bandwidth=130Hz/Px). Images were evaluated qualitatively by two experienced cardiologists for the presence or absence, pattern (subendocardial, midwall, subepicardial, transmural) and regional distribution of LGE areas. In addition, focal areas of LGE were defined quantitatively using the MC-ROI software as hyper-enhanced pixels of at least 40 mm^2 with a SI ≥ 2.0 standard deviations above the mean SI of normal myocardium in the same image (Figure 2.3).

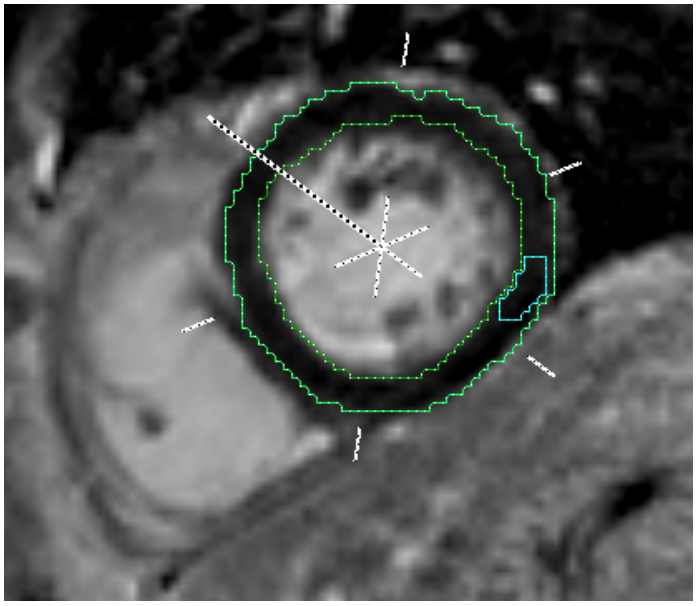


Figure 2.3 Late gadolinium image with myocardial contours (green contour) and region of interest over remote myocardium (blue contour).

Chapter 3

Shortened Modified Look-Locker Inversion recovery (ShMOLLI) for clinical myocardial T1-mapping at 1.5 and 3 T within a 9 heartbeat breath-hold

3.1 Introduction

The work presented in this chapter on the development of the novel sequence for T1-mapping, named Shortened Modified Look-Locker Inversion Recovery (ShMOLLI), has been published in the Journal of Cardiovascular Magnetic Resonance (2010;12:69) (17) on which Dr. Stefan Piechnik is the first author and I am the second author. I was not involved in the design of the sequence, computer programming, computer simulation or phantom experiments; I recruited all normal volunteers, performed all CMR scans on the volunteers, analysed all the T1-maps of the human subjects and contributed significantly to the drafting of the manuscript. Dr. Erica Dall'Armellina provided data on patients with acute myocardial infarction. The ShMOLLI method described in this thesis is novel and distinct from the Short MOLLI (11 heart-beat) variant available on the Siemens Work-In-Progress (WIP) package; prior to 31st January, 2013, ShMOLLI was not available via the Siemens WIP package and was available only to 4 other centres via research C2P agreements.

As discussed at the beginning of this thesis, the previously established method for myocardial T1-mapping is the modified Look Locker inversion recovery (MOLLI) pulse sequence (7). It merges images from three consecutive inversion-recovery (IR) experiments into one data set (Fig. 3.1A), generating single-slice T1 maps of the myocardium (7,18). Clinical use of MOLLI was demonstrated in myocardial infarction (19,20). One barrier to the clinical adoption of this method is the 17 heart beat breath-hold required to obtain the T1 map. This is usually acceptable for normal subjects who can hold their breath for 20.9s (range 13-74s) in end-expiration (21) (the respiratory phase in which CMR is usually performed). However, pulmonary compromised cases could achieve such breath holds for only 9.1 (range 2-16) seconds (21), and problems are exacerbated in old age due to frequent respiratory comorbidities (22) and in patients on beta-blockers where the lower heart rate translates into breath holds of over 20 seconds. Therefore, a significant improvement in

speed over the MOLLI method is required to achieve T1 mapping for sequential slice by slice heart coverage in routine clinical practice.

We hypothesised that it is possible to determine T1 maps of the heart with high precision in a short breath-hold. We thus present a shortened alternative to MOLLI (ShMOLLI) that can generate rapid and high-resolution myocardial T1-maps in a single short breath-hold of only 9 heartbeats. We investigate the accuracy of T1 measurements by ShMOLLI against MOLLI in simulation and gel phantom experiments over a wide range of heart rates and T1 values. The findings are validated *in-vivo* for normal human myocardium at 1.5T and 3T. To extend the *in-vivo* validation range we also present findings in four human subjects with recent myocardial infarction and four normal subjects after gadolinium contrast.

3.2 Methods

3.2.1 Simulation and Sequence design

Simulations were performed in IDL (Interactive Data Language ver. 6.1, ITT Visual Information Solutions) by implementing equations for the piece-wise calculation of longitudinal magnetisation (Mz(t)) and the signal samples generated by a train of arbitrarily-spaced ideal excitation pulses. Inversion pulses are assumed to be perfect 180º excitations; readouts are simulated as single pulses of 35º. Both sequences had three IR epochs. Simulations were performed for MOLLI based on its optimised variant (23), which collects 3+3+5 samples in three consecutive IR epochs separated by long recovery periods, which are approximated as being fully recovered in the reconstruction. The shortest effective TI (7) in each IR are 100, 180 and 260ms; incremented by heart beat period for subsequent samples (Fig. 3.1A). ShMOLLI (Fig. 3.1B), uses a similar effective TI principle but collects

only 5+1+1 samples and IR epochs are separated by only one T_{RR} (R-R interval), which does not approximate to full recovery of the magnetisation.

Simulations using simplified pulse sequences outlined in Fig. 3.1 were performed for T1 ranging from 50 to 2700 ms (50ms increments) and for HR between 40-100 bpm (20 bpm increments). For each combination of parameters, we analysed 200 sample trains with noise representative of our phantom measurements.

3.2.2. Processing

Significant shortening of the recovery epochs means that Mz can be severely affected by preceding IR epochs in the excitation sequence as demonstrated for long T1 values in Fig.3.2B (thick grey line). Consequently, the signal samples from the 2nd and 3rd IR of ShMOLLI do not fit the simple method of pooling data together into a single IR equation as outlined for MOLLI (7) and would produce significant errors if used in reconstruction. This problem is circumvented by conditional data analysis according to the algorithm presented in Fig. 3.2. In essence, in regions of long T1, samples 1-5 are fitted using (7). For shorter T1 ($0.4T_{RR} < T1 < T_{RR}$) samples 1-6 are used. For very short T1 ($< 0.4T_{RR}$), samples 1-7 are utilised. As the T1 is not known accurately the inclusion thresholds $0.4T_{RR}$ and T_{RR} are modified depending on the fit error.

On-the-scanner implementation: The MOLLI and ShMOLLI acquisitions used a research sequence provided by Siemens (Siemens Healthcare, Germany) utilising the optimised parameter set for MOLLI (23) and ShMOLLI. T1s were fitted using the algorithms described above with an AMOEBA optimisation method (24). This reconstruction fitting was coded in C++ directly into the scanner's multi-threaded parallel processing image pipeline. As a result, T1-maps are available for viewing in about 10 seconds following image acquisition.

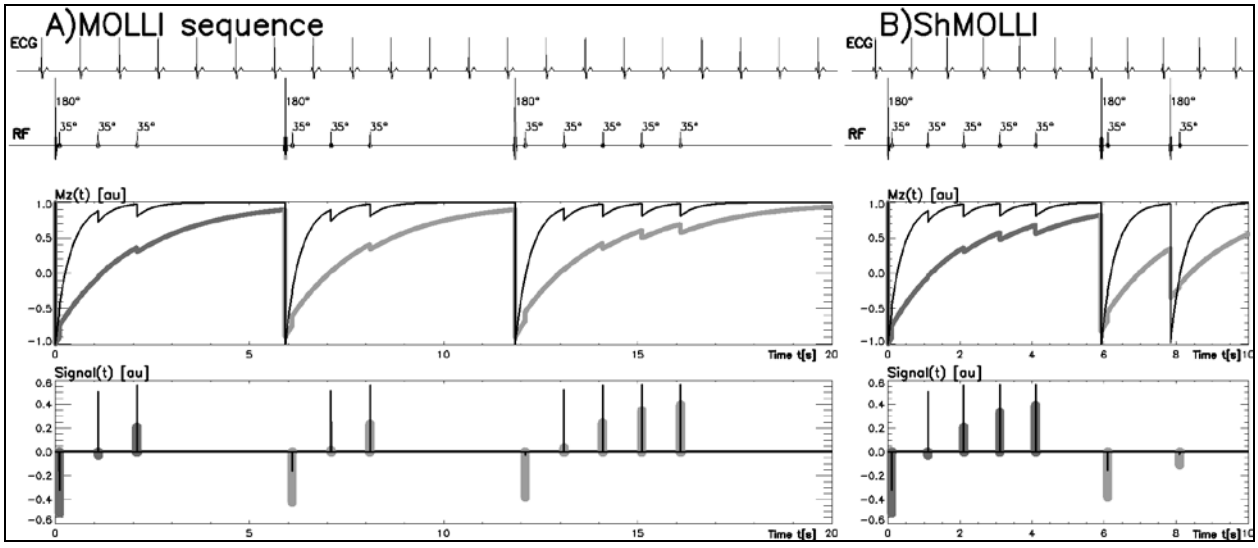


Figure 3.1 ECG-gated pulse sequence schemes for simulation of A) MOLLI and B) ShMOLLI at a heart rate of 60 bpm. SSFP readouts are simplified to a single 35^{o} pulse each, presented at a constant delay time TD from each preceding R wave. The 180^{o} inversion pulses are shifted depending on the IR number to achieve the desired first TI of 100, 180 and 260ms in the consecutive inversion recovery (IR) experiments. The plots below represent the evolution of longitudinal magnetisation (Mz) for short T1 (400ms, thin lines) and long T1 (2000ms, thick lines). Note that long epochs free of signal acquisitions minimise the impact of incomplete Mz recoveries in MOLLI so that all acquired samples can be pooled together for T1 reconstruction. In ShMOLLI the validity of additional signal samples from the 2nd and 3rd IR epochs is determined by progressive nonlinear estimation.

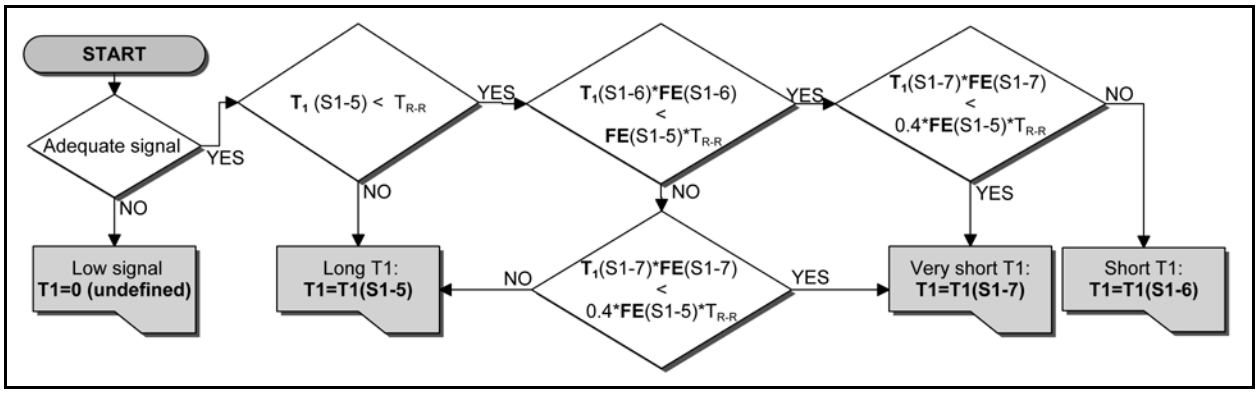


Figure 3.2 ShMOLLI conditional data analysis. Simplified algorithm for inclusion of samples to circumvent the impact of short recovery epochs in T1 estimation. "FE" is the fit error calculated as the square root of the sum of squared residuals divided by number of samples minus one. "S1-5" denotes the set of samples from the first inversion recovery, "S1-6" and" S1-7" are supplemented by samples from consecutive IR experiments. T_{R-R} is a heart beat interval.

3.2.3. Phantom Studies

Fifteen 50ml Agarose and NiCl gel phantoms (25) with T2~50 ms and T1 ~100-2500 ms were studied at 1.5T (Avanto, Siemens Healthcare, Germany) using a 32 channel body array and at 3T (Trio, Siemens Healthcare) using a 16 channel body array. The artificially generated ECG scanner triggers were used to validate HR range from 40-100 bpm with 10 bpm increments. Imaging parameters were the same for MOLLI and ShMOLLI: FOV=300x300 mm, voxel size=1.17x1.17x8mm, matrix=256x256 (interpolated from 128x128 acquisition matrix, 95 phase encoding steps), flip angle=35^{o}, TR/TE=1.96/0.98ms.

Reference T1 relaxation times were calculated offline based on images collected using slice-selective IR with non-segmented spin echo readout. TI=33, 100, 300, 900, 2700, 5000 ms. TR/TE=10 s/6.3 ms; 80 phase encoding steps with total image acquisition time of 13 minutes. Sizing and positioning were identical to the studied MOLLI methods. ROI were placed in each tube using an automated method and reference T1s were fitted per pixel and a mean T1 determined.

3.2.4 In Vivo Studies

Ethics approval was granted for all subjects and informed consent was obtained.

Human Volunteers: 10 normal volunteers (7 men; age 35±7years, normal ECGs without history of cardiac diseases or symptoms) underwent CMR imaging at 1.5T and 3T on the same day. Following standard planning, end-expiration basal, mid-cavity and apical short-axis images using MOLLI and ShMOLLI were collected. Images for specific TI were collected using exactly the same SSFP readouts for both methods to allow direct comparisons, typically: TR/TE=2.14/1.07 ms, flip angle=35º, FOV=340x255mm, matrix=192x144, 107 phase encoding steps, interpolated voxel size=0.9x0.9x8mm, GRAPPA=2 with 24 reference

lines, cardiac delay time TD=500ms; 206 ms acquisition time for single image. A single slice, which was judged to have the “best quality” at the time of scanning, was repeated twice at the end of the protocol to assess short-term intra-scan variability of the T1 measurements; this was not performed in the first pilot case. Offline post-processing involved manual tracing of endo- and epi-cardial contours for analysis of the T1 measurements in myocardial segments 1 to 16 of the American Heart Association (AHA) 17-segment model (26) using in-house software.

Gadolinium contrast application

Matching pairs of ShMOLLI and MOLLI pre-contrast and post-contrast T1 maps were obtained in 4 female subjects (61±3 years old) without pre-existing cardiac disease who underwent a separate research protocol at 1.5T. Subjects underwent adenosine stress perfusion at 140µg/kg/min for 3 min, followed by a bolus of Gd (Gadodiamide, Omniscan, GE Healthcare, Amersham, UK, 0.03mmol/kg body weight). After 20 minutes, resting perfusion imaging was performed using 0.03mmol/kg of Gd followed immediately by a top-up Gd of 0.10mmol/kg for LGE imaging. Matching T1-maps were obtained at baseline and ~14 minutes after adenosine stress perfusion. Finally, 4 pairs of images were collected before, and one after, the LGE image stack. The dynamic evolution of T1 recovery after the final Gd bolus was corrected with 3rd order polynomial for the purpose of constructing Bland-Altman plots

Patients with Recent Myocardial Infarction: 4 patients (3 men; age 53±10 years) underwent CMR imaging at 3T following the diagnosis of a first acute ST-elevation type myocardial infarction (STEMI) post primary percutaneous coronary intervention (PCI). LGE images were obtained 24-48 hours post acute infarct (27). T1-maps using ShMOLLI and MOLLI were obtained 5-17 days after the ischaemic event at a single representative slice

replicating settings from the normal control volunteer study. Manual contouring of the endo- and epicardium was followed by calculation of the distribution of T1 values within the defined myocardium. The resulting distributions were clearly bi-modal and were fitted using a two-component Gaussian model in order to assess T1 in injured and unaffected myocardium.

3.2.5 Statistical Analysis

Unless stated otherwise, the results are presented as mean±SD/mixed SD, where the "mixed SD" is estimated as the independent combination of average individual SD and the inter-individual SD. For estimation of the relative variability we use the coefficient of variation (CV=100%*SD/Mean). The term "noise penalty" is used to describe the expected relative increase in CV resulting from predicable factors, i.e. the reduced number of samples. Significance of the differences between population means is calculated using 2-tailed Student T-tests, paired whenever possible, and quoted when $p < 0.05$.

3.3 Results

3.3.1 Simulation and Phantom Studies

The accuracy of both methods is dependent on the T1 and heart rate. Generally, as HR and T1 increase, the T1 measurements diverge increasingly from the ideal identity line (Fig 3.3). This is observed in both simulation (Fig. 3.3 A, C) and phantom measurements with excellent agreement at both field strengths (Fig. 3.3 B, D). Fig. 3.3 C, D demonstrate a clear dependence of MOLLI estimates on HR, with relative underestimation reaching -30% for the highest HR and longest T1 studied. In contrast, ShMOLLI calculation (Fig. 3.3 A, B) demonstrates tight overlap of the values with significant reduction in dependence on the heart rate. For T1s longer than approximately 800ms the deviation of ShMOLLI estimates from the identity line is proportional to T1. The corresponding relative error of underestimation by ShMOLLI in this range is effectively a constant of -4%.

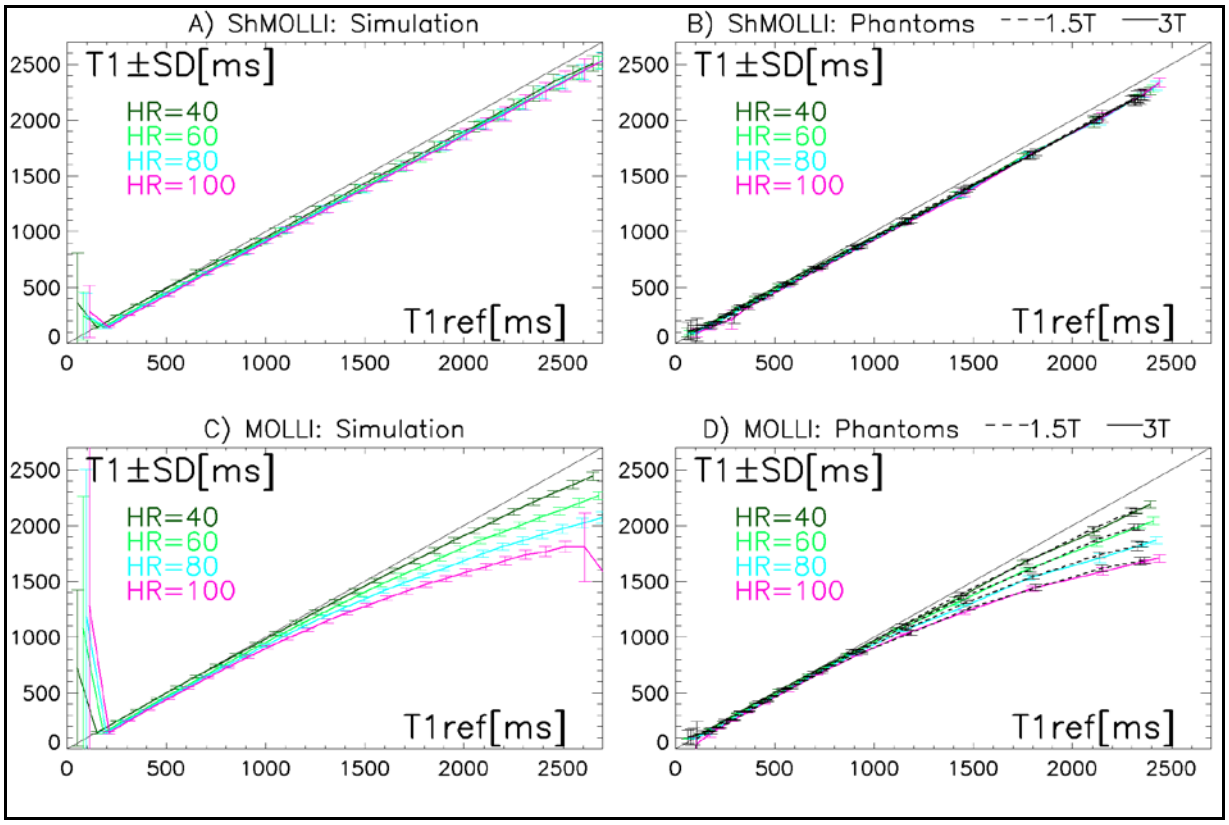


Figure 3.3 Relationship between T1 measurements for ShMOLLI (top row) and MOLLI (bottom row) and the corresponding reference T1 (T1ref) depending on selected simulated heart rates (HR). Diagonal line represents the ideal identity line. Simulation (A&C) and Phantom (B&D) measurements in 3T and 1.5T (dashed lines) overlap and are in close agreement with simulation results. NOTE. The lines are offset by 15ms horizontally for each HR value to reduce the overlap between lines.

The variability of T1 measurements across all simulations or pixels is shown as whiskers in Fig. 3.3. For long T1s, measurements by ShMOLLI are based on 5 samples whereas MOLLI measurements are based on 11 samples. Therefore ShMOLLI has a predicted noise penalty of 48% versus MOLLI (√(11/5)). For shorter T1s, 6 or 7 TI samples are used with a predicted noise penalty of 35% and 25%. Inclusive of the heavily nonlinear processing, for the reference T1 range of 300-2600ms, we find the simulated average CV is 2.7% for ShMOLLI and 2.1% for MOLLI, translating to an overall 28% noise penalty for using ShMOLLI. In phantom studies, the noise penalty for ShMOLLI is 21% at 3T (Fig. 3.3B) and 61% at 1.5T (Fig 3.3C).

3.3.2 Normal Human Subjects

In normal control volunteers, the myocardial ShMOLLI and MOLLI T1-maps did not show any visual differences (Fig. 3.4). The imaging time was 9.0±1.1s and 17.6±2.9s, respectively. Both methods utilise the same imaging SSFP sequence and suffered from occasional localised image artefacts. These were more severe at 3T where the maximum CV over the worst single segment reached 79% for MOLLI and 47% for ShMOLLI. Aside from the extreme outliers, the accuracy of T1 measurements benefited both from the increase in field strength and the number of samples included. CV was below 10% in 97% of the segments for MOLLI and 94% for ShMOLLI at 3T. At 1.5T the proportions were 89% and 85%, respectively. The median CVs were 4.7% (MOLLI, 3T), 5.5% (ShMOLLI, 3T), 6.1% (MOLLI, 1.5T) and 7.4% (ShMOLLI, 1.5T). Overall, ShMOLLI carried a 10% noise penalty at 1.5T ($p<0.001$) but was the same as MOLLI at 3T (3%, $p=0.8$). The lack of statistical significance in the latter comparison was attributed to outliers, which was addressed by removing 3 (out of 160) data points from further analysis. This returned the expected differences ($p<0.001$) between methods indicating an 18% noise penalty for ShMOLLI at 3T and 14% at 1.5T. There was a

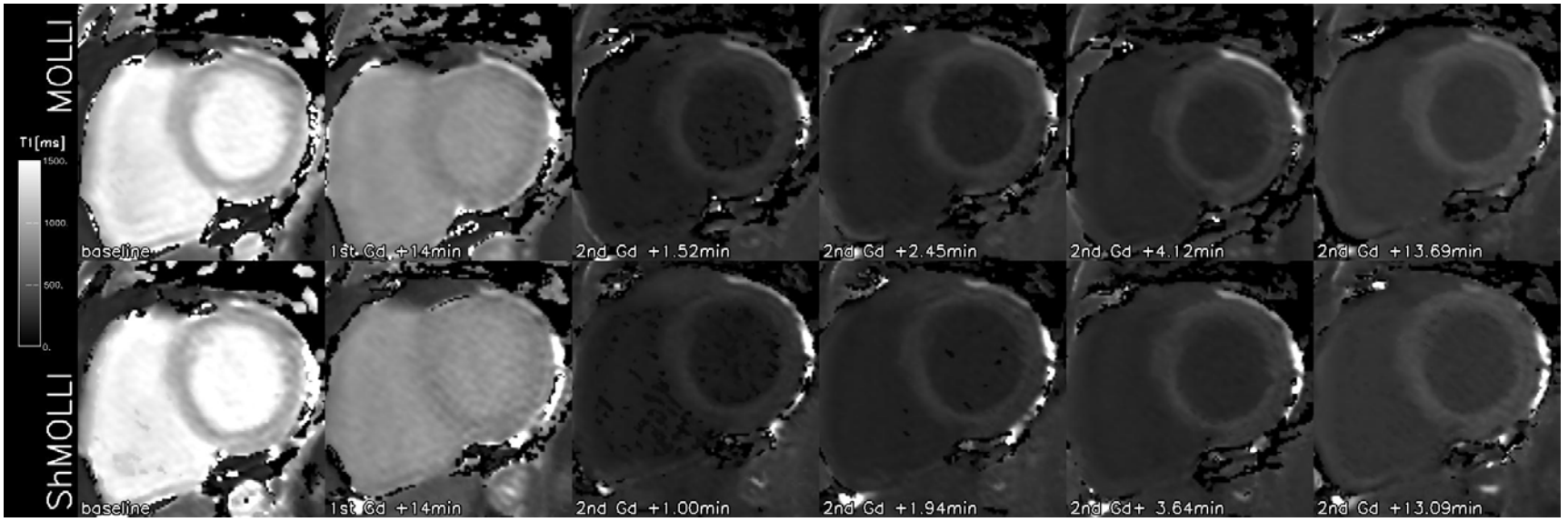


Figure 3.4 Representative short axis slice T1 maps of the normal myocardium obtained using MOLLI (top row) and ShMOLLI (bottom row) at 1.5T at the baseline and following Gd administration for perfusion imaging (1st Gd) and after top-up (2nd Gd) at times shown in panel labels.

clear benefit of using high field MR in a 33% reduction in CV for MOLLI and 24% for ShMOLLI ($p<0.001$, both differences) despite the use of a better coil array at 1.5T.

The average T1 values for myocardial segments derived using both ShMOLLI and MOLLI at 1.5T and 3T are presented in Fig. 3.5. At 1.5T, average myocardial T1s by ShMOLLI were 966±48/88 ms and 976±46/80 ms by MOLLI. T1 values for normal myocardium by both methods compared closely to previously published T1 values at 1.5T (18). At 3T, average myocardial T1s were similar for ShMOLLI and MOLLI (1166±60/91 ms and 1169±45/73 ms). Analysis of differences between methods (Fig. 3.6) revealed that myocardial ShMOLLI T1s were shorter than MOLLI T1s by 10±16ms (relative 1±1.6%, $p<0.001$) at 1.5T. At 3T both methods produced similar values (Δ=-0.2±16ms or 0.02±1.3%, $p=0.13$). Given that the average HR was 63±8 bpm (1.5T) and 61±7 bpm (3T), for the closest emulated HR of 60 bpm, we predict from phantoms the difference between methods to be -12.5 ms (for normal myocardial T1=1000ms at 1.5T) and +0.5 ms (for normal myocardial T1=1200ms at 3T). Analysis of intra-scan variability showed that the average repetition error was similar to the spread of differences between methods, approximately ±16ms (~1.6%) between any pair of repeated measurements at 1.5T (Fig. 3.7). At 3T the intra-scan variability was ±29ms (2.4%) for ShMOLLI and ±76ms (7%) for MOLLI. The latter was due to the 3 myocardial segments characterised by excessive CV of over 38%. When these were removed, MOLLI repetition accuracy improved to ±18ms (1.5%).

3.3.3 Gadolinium contrast application.

None of the subjects demonstrated LGE lesions with resting T1 values 982±28ms comparable with other controls at 1.5T. Depending on the dose and time point the T1 showed expected shortening with lowest average myocardial T1 of 135±33ms and subsequent recovery towards normal values (Fig. 3.4). The differences between the ShMOLLI and MOLLI measurements are

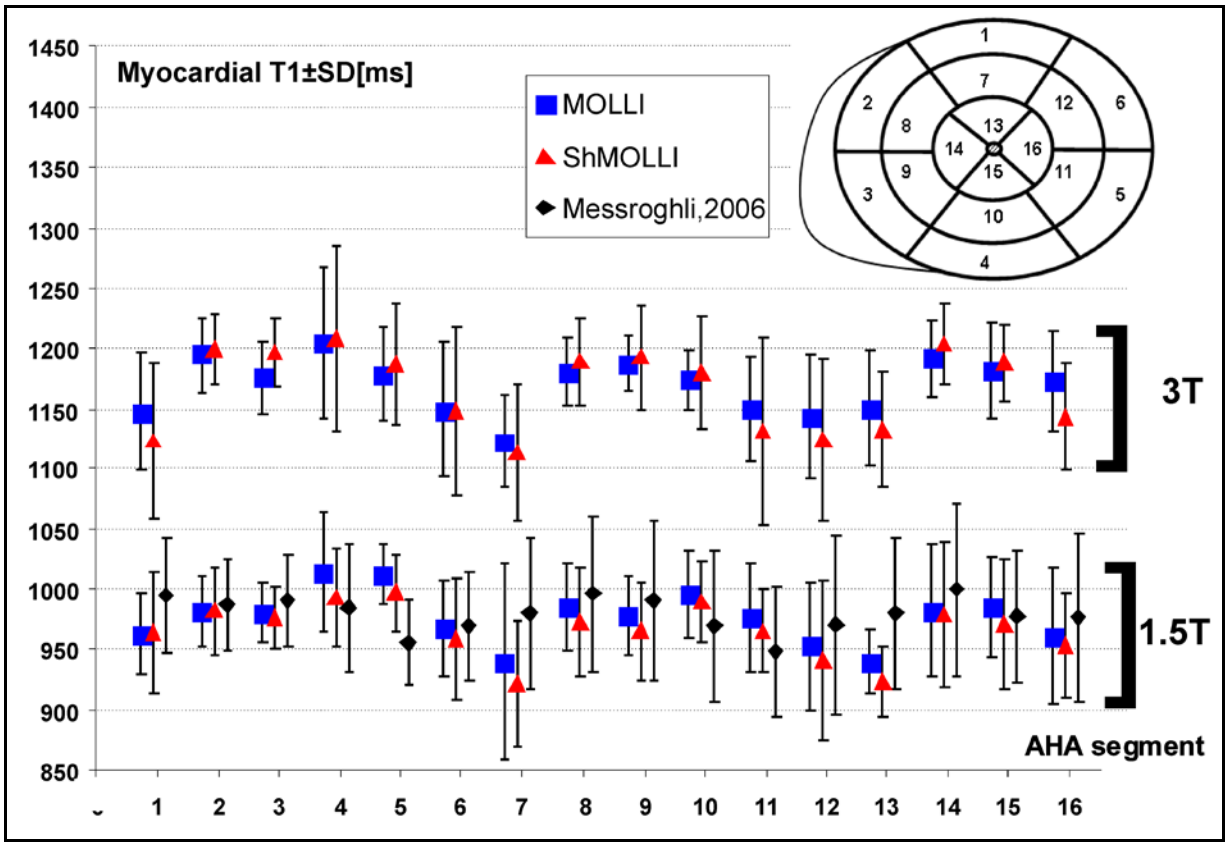


Figure 3.5 T1 values for AHA myocardial segments 1-16 (see insert) at 1.5T and 3T using ShMOLLI and MOLLI. Results of current study as compared to previously published values at 1.5T (18).

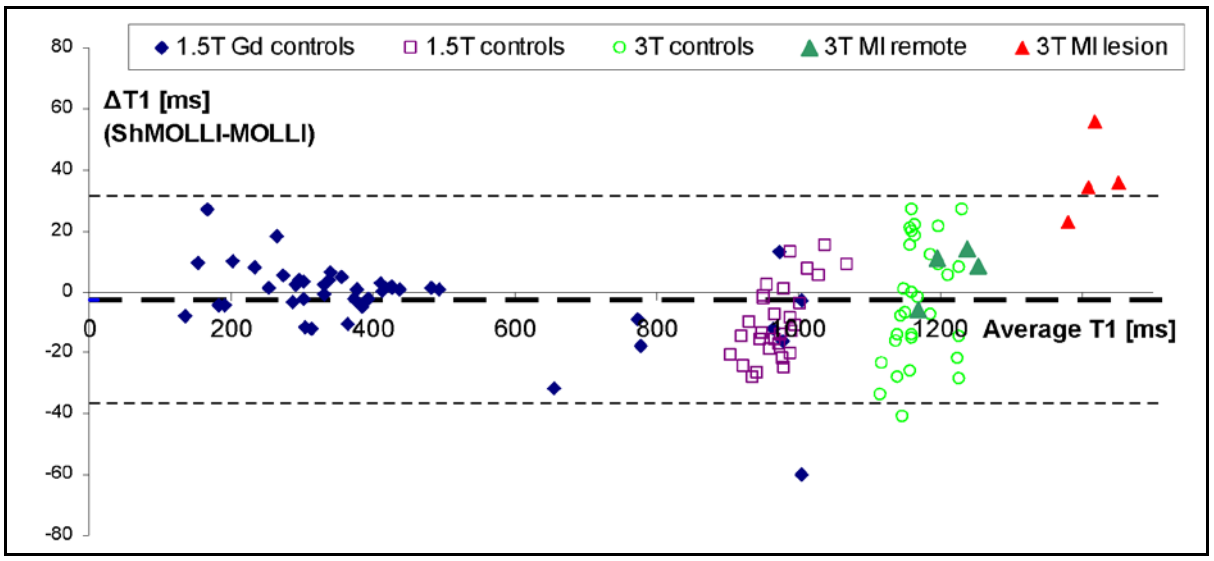
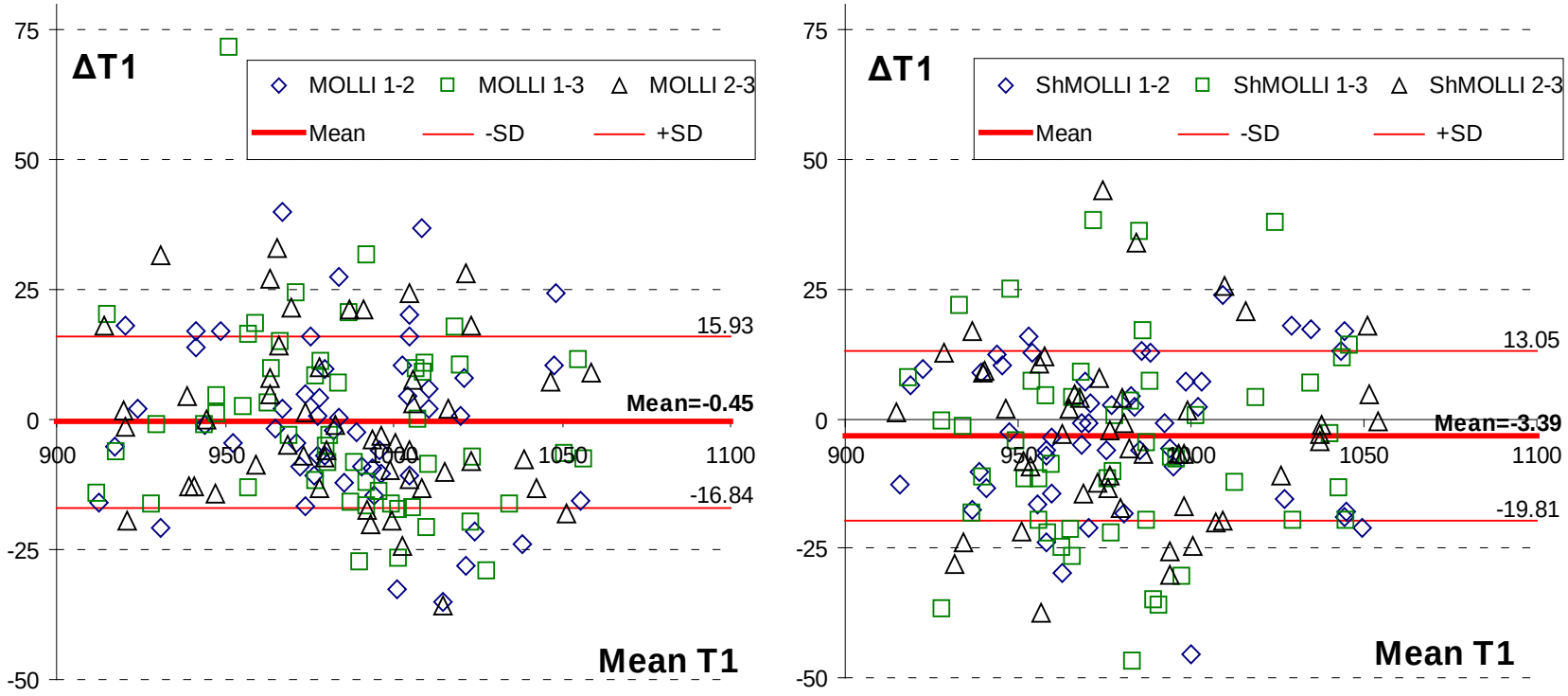


Figure 3.6 Bland-Altman plot shows good agreement between the average ShMOLLI and MOLLI myocardial T1 values pooled across our material obtained at 1.5T and 3T. Note that the distribution of differences at approximately ±17 ms is also representative of the repetition accuracy for either method. Note that the majority of outliers relate to the infarct data at 3T where the demonstrated MOLLI bias dominates over noise considerations even at normal heart rates. Thick dashed line represents overall average difference between measurements (-3ms), thin dashed lines represent 2SD range.



MOLLI: 11 TI samples
Difference=-0.5 ± 16ms

ShMOLLI:5-7 TI samples
Difference=-3.9 ± 16ms

95% confidence bounds = ±32ms (~3% myocardial T1)

Figure 3.7. Short-term intra-scan variability of MOLLI vs. ShMOLLI at 1.5T. The Bland-Altman plots demonstrate that the standard deviation (SD) of the differences is the same at 16 ms, with both methods having similar 95% repeat confidence interval at ± 32ms (~3% of resting myocardial T1 values).

shown together with the remaining *in-vivo* data in figure 3.6 and confirm good agreement *in-vivo* in the low T1 regime predicted in simulation and phantom measurements.

Patients with Recent Myocardial Infarction

As in normal controls, the image acquisition in patients was much faster using ShMOLLI (9.9±1.6s) than with MOLLI (18.3±3.0s) without visually perceivable impact on the reconstructed myocardial T1 maps. Fig. 3.8 shows an example of recent transmural inferior infarct 4 days following the primary PCI, as demonstrated by LGE at 3T. Table 3.1 shows T1 values for injured and unaffected normal myocardium measured by distinct T1 distribution peaks in all 4 cases. Unaffected myocardium had T1 values showed no significant difference to those of healthy volunteers at 3T measured by ShMOLLI (1216±42ms, p=0.09) and MOLLI (1209±35ms, p=0.1). Injured myocardium had increased T1 ($p<0.001$) of 1432±33ms (ShMOLLI) and 1396±27ms (MOLLI). The relative difference in T1 values between injured and unaffected myocardium were 17.8±6% (ShMOLLI) and 15.5±5% (MOLLI), which was statistically different between methods ($p<0.04$). The width of identified T1 distribution peaks, indicative of noise penalty, was on average 20% larger for ShMOLLI than for MOLLI ($p<0.02$). The area of injured myocardium as identified by T1-maps was on average 4±10% (range -3 to +19%) larger than the area identified by LGE.

3.4 Discussion

To exploit benefits of quantitative T1 mapping we sought to develop an accurate practical method characterised by a shorter breath-hold of the order of 10 seconds, which is easily achievable for patients. Figure 3.9A demonstrates that such drastic shortening of the MOLLI sampling scheme results in significant errors when a straightforward T1 reconstruction (7) is used. The novelty in ShMOLLI approach arises from simulations prior to this study, where we

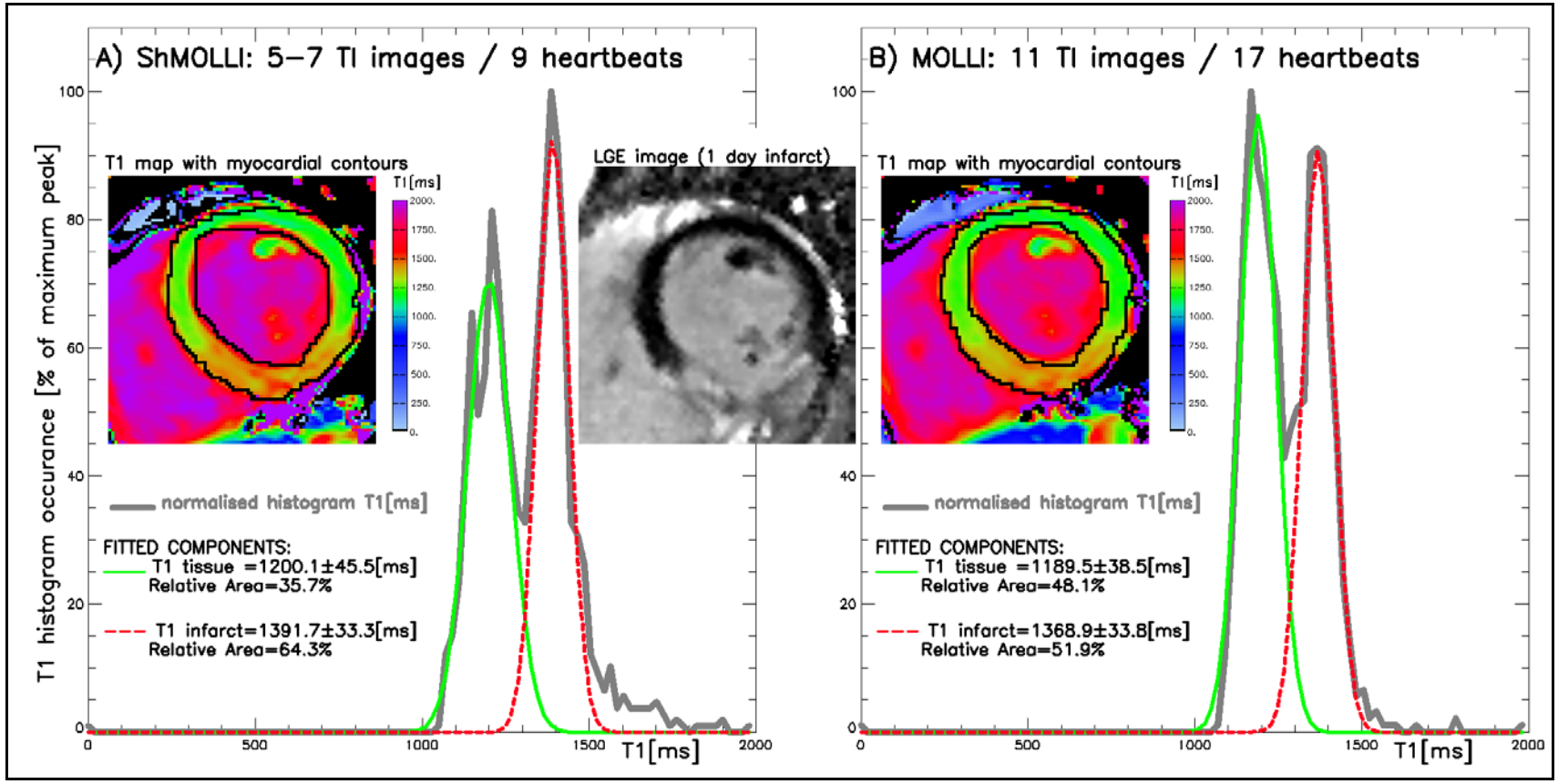


Figure 3.8 The distribution of T1 in case #1 at 3T using A) MOLLI and B) ShMOLLI reveals two distinct populations of values within the myocardium, which can be fitted using two Gaussian curves, corresponding to injured (long T1) and unaffected (normal T1) myocardium. Regions of increased T1 demonstrate spatial co-localisation with LGE 4 days earlier (image insets).

Table 3.1 Assessment of myocardium by T1-mapping and LGE at 3T in acute STEMI treated by 1º PCI

Case	Gender (age years)	T1-mapping	T1 [ms]		Injured myocardium[%]	
		Method	*Unaffected*	*Injured*	*T1-based*	*LGE (days prior)*
1	F(50)	ShMOLLI	1200 ± 46	1392 ± 33	64%	39%(-4d)
		MOLLI	1189 ± 39	1369 ± 34	52%	
2	M(49)	ShMOLLI	1269 ± 69	1425 ± 21	50%	44%(-14d)
		ShMOLLI	1244 ± 50	1418 ± 30	38%	
		MOLLI	1248 ± 47	1391 ± 21	47%	
3	M(68)	ShMOLLI	1244 ± 51	1445 ± 45	58%	48%(-16d)
		MOLLI	1230 ± 33	1389 ± 46	44%	
4	M(45)	MOLLI	1171 ± 47	1433 ± 48	41%	46%(-14d)
		ShMOLLI	1165 ± 55	1469 ± 59	40%	
	53 ± 10	***Averages***	**1217 ± 37**	**1424 ± 23**	**48 ± 9%**	**44 ± 4%**

observed that just a single Look-Locker IR is sufficient to accurately estimate long T1 values that are longer than the T_{RR} (28) (Fig. 3.9C). Conversely, inclusion of additional samples from subsequent IRs is essential for the accurate estimation of short T1 values but does not require long epochs for complete recovery of longitudinal magnetisation. Thus, our final design of ShMOLLI is based not only on an abbreviated TI sample set and a drastic reduction of the recovery periods between subsequent inversion recovery experiments. Side effects of such rapid sampling are compensated with a novel concept of conditional data processing to distinguish between long and short T1 relaxation times in order to optimally utilise the available TI samples for accurate non-linear T1 estimation over a wide range of T1 (Fig. 3.9D).

We used both methods to measure a wide range of T1 applicable to 1.5 and 3T, encompassing values corresponding to contrast enhanced myocardium (T1~150-500ms), fat (T1~200ms), liver (~700ms), skeletal muscle and myocardium (~1000ms), blood (~2000ms) and lymph or pericardial effusion (~3000ms). ShMOLLI demonstrates robust T1 measurement properties across a wide range of T1 values and heart rates in simulation and phantoms. While both ShMOLLI and MOLLI slightly underestimate true T1 values, MOLLI shows prominent dependency on heart rate. An empirical correction for MOLLI has been proposed that addresses specifically the normal myocardial T1 values at 1.5T (18,23). In contrast, ShMOLLI underestimation is consistently ~4% for any T1 above 800ms. This permits easier adjustment to calculate the true T1 values in wide range independently of heart rate:

$$T_1^{True} = \frac{T_1^{Measured}}{1 + relativeError} \approx 1.04 \cdot T_1^{Measured}$$

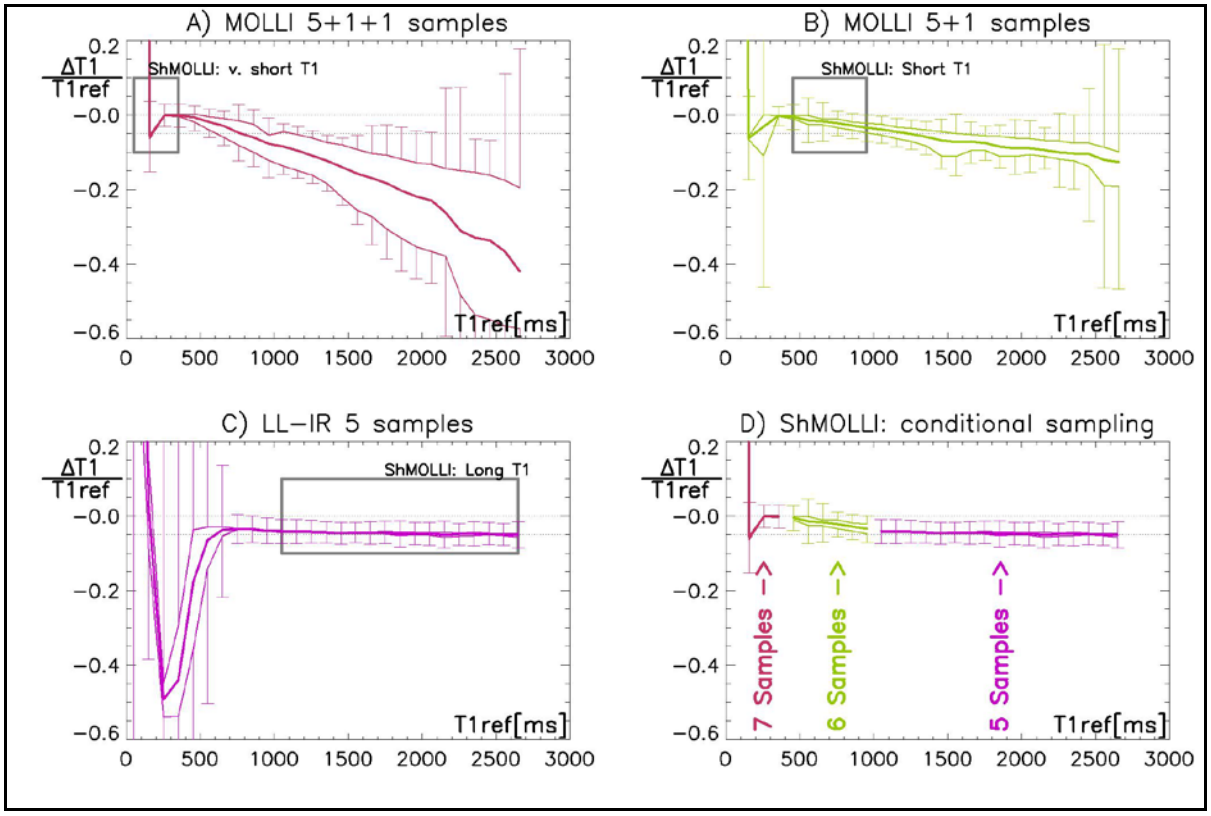


Figure 3.9 Simulated average relative T1 estimation error (thick lines) with boundaries characterising dependence on heart rate (thin lines) and measurement noise (whiskers) as a function of reference T1ref. A) Standard MOLLI reconstruction applied to the proposed ShMOLLI sampling scheme demonstrates very large errors reaching -60%, with accuracy acceptable only within the shortest T1 range (grey rectangle). B) Accuracy is improved for short T1 range when the last sample is removed from analysis; however very short T1estimates suffer increased variability and the longer T1 are affected by heart rate dependent bias and noise. C) Simple Look-Locker IR experiment has adequate accuracy only for long T1. D) Concept of conditional use of the marked parts of reconstructions A/B/C to obtain the wide range of ShMOLLI T1 estimates with the average bias within 5% range (dotted lines).

Excluding any such corrections (as no corrected values are presented in this thesis), the measurements of myocardial T1 by ShMOLLI at 1.5T are in good agreement with in-vivo data published in the literature (29), particularly with previous measurements using the MOLLI sequence (18). The observed minor differences between the two methods conform closely to simulation and phantom validation. Under reasonably normal heart rate conditions (e.g. HR 50-80 bpm) and for T1 800-1200ms, ShMOLLI and MOLLI T1 agree well with each other, with the former exhibiting an acceptable lower SNR (discussed further below) in exchange for a significantly shorter breath-hold time for easy clinical application.

The purpose of the limited in-vivo material was to directly compare ShMOLLI performance with MOLLI over a wide range of clinically relevant scenarios. This included measurements in normal myocardium, following shortening of T1's as a result of contrast administration and T1 prolongation related to myocardial infarction. T1 measurements agreed in healthy controls within ±17ms noise boundaries for normal myocardium and after Gd administration. Our MI data is consistent with previously published reports (7,19,23,30) showing that the area of infarct demonstrates increased T1 values on non-contrast T1 maps. LGE images were acquired 4-16 days prior to T1-maps, which precludes direct comparisons of infarct size assessment by LGE imaging and T1-mapping. Nonetheless, it is clear that the distribution of T1 values within the myocardium shows two distinct peaks of normal and long T1s, the latter co-localising to the area of injured myocardium as seen on LGE. ShMOLLI showed a 15% larger T1 difference between injured and unaffected myocardium, which can be directly attributed to its superior quantification of long T1s.

Noise considerations

Typically, the penalty for reducing the number of images collected for T1 reconstruction is increased variability within the resulting T1 maps. Our simulation and phantom measurements predicted the noise penalty for ShMOLLI to be as much as 61%. However, in-

vivo T1 measurements by ShMOLLI showed noise penalty of only 14% (1.5T) and 18% (3T) as compared to MOLLI T1s. The repetition error was 1.6% for both methods at 1.5T (as shown in Figure 3.7) and only excluding the worst measurements brought out the expected noise advantage of MOLLI at 3T. We found that while MOLLI benefited from more samples for the majority of measurements, the higher SNR was bought at the cost of more prominent outliers, especially at 3T. This may be due to the ShMOLLI conditional processing acting as an error checker, but detailed analysis of such effects exceeds the scope of this work. Overall, for most of the T1 values tested, the in-vivo noise penalty for ShMOLLI due to a shorter imaging time is only 10-20%. We attribute this favourable observation mostly to the beneficial effect of the short breath-hold, which limits the incidence of breathing motion, estimated as the cause for 31% of image artefacts (18). The small reduction in precision of ShMOLLI T1 maps in-vivo is an excellent trade-off for halving the imaging time and breath-hold, rendering the ShMOLLI both accurate and clinically acceptable.

The ShMOLLI technique holds promise for wider application of non-contrast T1-mapping towards cardiac conditions in which there are focal changes, such as myocardial infarction and myocarditis. It may be pivotal in studying conditions in which there are diffuse myocardial changes, such as chronic heart failure, hypertrophic cardiomyopathy and infiltrative diseases such as cardiac amyloidosis and sarcoidosis. The presented comparisons warrant the ongoing ShMOLLI deployment on its own merit in several more comprehensive patient validation studies.

3.5 Conclusion

The novel ShMOLLI sequence for myocardial T1-mapping generates robust, high resolution quantitative T1 maps in agreement with published data in the literature in just 9 heart-beats across a wide range of heart rates and T1 values. Single short breath holds are typical for

routine examinations to make them easily achievable for patients and permit wider clinical application of quantitative mapping. Implementation of nonlinear T1 fitting directly in the scanner image reconstruction pipeline yields immediate access to T1-maps for viewing, allowing for re-acquisition if necessary. In patients presenting with recent myocardial infarction, preliminary data demonstrates ShMOLLI superiority in distinguishing injured from normal myocardium, with areas of long T1 co-localizing with injured myocardium as assessed by LGE. ShMOLLI provides a valuable clinically applicable tool for myocardial tissue characterisation with or without the use of contrast agents.

In this chapter, we have presented a novel method for T1-mapping that is feasible in one single short breath-hold of under 10 seconds without compromising the accuracy of T1 measurements. In fact, two other technical advantages of ShMOLLI over the previous method MOLLI are that ShMOLLI is T1-indenepdent and heart-rate independent, which render ShMOLLI a better method especially in measuring long T1s (such as in acute oedema) and during fast heart rates. These features make ShMOLLI highly suitable and ready for clinical application.

Chapter 4

T1-mapping detects acute myocardial oedema with high diagnostic accuracy: a comparison to T2-weighted cardiovascular magnetic resonance imaging

4.1 Introduction

Oedema is a common feature of acute myocardial injury in a number of cardiac diseases encountered in the clinical setting. In this chapter, we explore and validate how T1-mapping may be used to detect different models of acute myocardial oedema in comparison to T2-weighted cardiovascular magnetic resonance (T2W-CMR).

T2W-CMR is the standard imaging technique for detecting acute myocardial oedema in vivo (31). It is used for differentiation of acute from chronic MI (32), assessment of the area-at-risk (33,34), myocarditis (14) and increasingly as a surrogate end-point in clinical trials (35).

T2W-CMR techniques are sensitive to an increase in myocardial water content and/or free water fractions (14,31,35,36). Conventional T2W images are acquired using the short-tau inversion recovery (STIR) sequence at 1.5T (13). Limitations of this technique include signal drop-out, bright signals adjacent to the subendocardium due to slow-flow blood, image quality impairment in tachyarrhythmias, and long breath-holds (14,37). Furthermore, there is need for a “normal” reference region of interest (ROI), either in remote myocardium, or in adjacent skeletal muscle for conditions with diffuse oedema. The use of an ROI outside the myocardium typically requires the body coil to be used to minimize spatial inhomogeneity (14), which gives a lower SNR than would normally be achieved with phased-array coils. In systemic conditions like viral myocarditis, the reference skeletal muscle may also be inflamed, leading to false negative results (14). The bright-blood T2-weighted sequence ACUT2E (16) has been shown to be superior to dark-blood STIR in assessing acute myocardial infarction and area-at-risk (33), but has not been tested in subjects with diffuse or patchy oedema using reference ROIs outside the myocardium.

T1-mapping may provide a quantitative means to detect myocardial oedema without the need for reference ROIs. Each tissue type exhibits a characteristic range of normal T1 relaxation times at a particular magnetic field strength (5). T1 and T2 times track closely together such that myocardial oedema, which prolongs T2, also prolongs T1 (31,35,38). Increased T1 values have been shown in ischaemic tissue from dog hearts, which largely reflected increased free water content (9), and in humans with acute myocardial infarction (20,39). However, the ability of T1-mapping to detect oedema in the absence of infarction has not been systematically compared to T2W-CMR.

In the study described in this chapter, we compared T1-mapping using the novel ShMOLLI sequence (17), dark-blood and bright-blood T2W-CMR in the detection of acute myocardial oedema. Patients presenting with Takotsubo cardiomyopathy (TCM) and regional oedema in the absence of infarction were included. This allowed testing of the performance of each method in detecting both global and regional oedema. We hypothesised that quantitative T1-mapping would be superior to T2-weighted methods that require reference ROIs.

4.2 Methods

4.2.1 Ethics and Study Population

All subjects gave written informed consent and ethical approval was granted for all study procedures.

Consecutive patients demonstrating CMR features of acute Takotsubo cardiomyopathy or acute myocardial oedema without infarction were prospectively enrolled. The diagnosis of Takotsubo cardiomyopathy was based on the proposed Mayo Clinic criteria (40):

(1) an acute cardiac event presenting with chest pain and/or dyspnoea;

(2) transient systolic dysfunction with marked LV contraction abnormality (akinesis or dyskinesia of the LV apical and/or mid-ventricular or basal segments) extending beyond a single coronary perfusion bed;
(3) absence of significant (>50%) obstructive coronary artery disease or angiographic evidence of acute plaque rupture;
(4) new ECG abnormalities (either ST elevation or T wave inversion) or elevation in cardiac troponin level (upper limit Troponin I=0.04 ug/L);
(5) absence of phaeochromocytoma; and
(6) absence of myocarditis or typical ischaemic subendocardial/transmural LGE on CMR.

Patients with acute myocardial oedema without infarction not fulfilling the regional distribution criteria for TCM all had:

(a) an acute cardiac event presenting with chest pain and/or dyspnoea;
(b) acute regional systolic dysfunction;
(c) absence of significant (>50%) obstructive coronary artery disease;
(d) new ECG abnormalities (ST elevation or T wave inversion) and/or elevation in cardiac troponin level (upper limit Troponin I = 0.04 ug/L);
(e) absence of myocarditis or typical ischaemic subendocardial/transmural LGE on CMR.

Exclusion criteria included contraindications to CMR, known coronary artery disease, previous myocardial infarction, myocarditis or any chronic cardiac conditions. In addition**,** healthy volunteers with no prior cardiac history or known cardiac risk factors, not on cardiovascular medications and with a normal ECG underwent CMR, including cine, ShMOLLI T1-mapping, STIR and ACUT2E imaging.

4.2.2 CMR image acquisition and analysis

CMR studies were performed using a 1.5T MR system (Siemens Avanto, Germany). CMR scans assessed LV function, T1-mapping, oedema and LGE, with matching short-axis images. T1-mapping was performed using the novel sequence ShMOLLI (17); dark-blood and bright-blood T2w-CMR were performed with the STIR (13), and the ACUT2E (16) sequences, respectively. These are described in detail in chapters 2 and 3.

Image Analysis

Image quality was assessed and matching short axis slices were compared across cine, ShMOLLI T1-mapping, STIR and ACUT2E and LGE imaging. These were described in detail in chapters 2 and 3.

Quality assessment of T1-maps.

As T1-maps are derived from non-linear estimation based on a sequential series of SSFP images acquired after an inversion pulse (17), factors such as off-resonance artefacts, breathing motion and poor T1 model fit may lead to falsely high or low T1 values. The presence of off-resonance artefacts and diaphragmatic movement was assessed by examination of the raw T1-weighted SSFP images. To assess for how well T1 model fitting was achieved for each T1-map, we used parametric maps of the goodness-of-fit (R^2 maps; see Appendix for further explanation and examples). R^2 maps provide an additional means to identify artefacts and areas with potentially compromised T1 accuracy, which allowed critical assessment of the quality of T1-maps to increase the reliability of T1-mapping compared to some of the standard CMR modalities. Intra- and inter-observer variability of T1 measurements was assessed by two operators blinded to the clinical data; one slice of T1-map per subject was randomly pre-selected and analysed for all subjects in the study.

4.2.3 Statistical Analysis

Results are presented as inter-individual mean±SD with differences considered significant when p is <0.05 as assessed by unpaired 2-tailed Student T-tests. Receiver operator characteristic (ROC) analysis was performed to identify cut-off values of T1 and T2-weighted methods for their ability to distinguish between normal and affected myocardial segments. Myocardial segments in patients were considered to be affected by oedema if there were acute wall motion abnormalities (wall motion score >1) in this clinical population as defined above, while segments in controls with normal wall motion were considered unaffected. As patient segments with normal wall motion may or may not be affected by oedema, these segments were not included in the ROC analyses in order to identify optimal cut-off values for the methods studied. Significance of ROC analyses was assessed using the method of Delong et al. (41) (MedCalc, version11.5.1.0, www.medcalc.org). Intra- and inter-observer reproducibility of T1 mapping measurements were assessed by using the Bland-Altman method (42).

4.3 Results

4.3.1 Study Population Characteristics

Patient characteristics are presented in Table 4.1. Twenty-one patients (2 males, 61±10 years) and 21 age-matched healthy controls (8 males, age 55±13 years) were included. Patients with Takotsubo cardiomyopathy had a mean Troponin I of 8.26 ug/L (0.84-36.80 ug/L) and patients with regional oedema had a mean Troponin I of 4.28 ug/L (0.15-12.69 ug/L). Ten out of the 12 patients with Takotsubo cardiomyopathy and six out of the 9 patients with acute regional oedema had a clear stress precipitant (emotional or physical), while the rest had no clear precipitant.

4.3.2 CMR Findings

The median duration between symptoms and CMR was 3 days (0-9 days). CMR findings are summarised in Tables 4.1 and 4.2. The mean LVEF for both patients with Takotsubo cardiomyopathy (61±10%) and regional oedema (66±9%) were significantly lower than controls (75±6%; both p<0.01). None had significant LGE.

Compared to controls, patients as a group had significantly higher mean myocardial T1 values, mean myocardial T2 $SI_{myo:skeletal}$ by dark-blood and bright-blood T2w-CMR. There was good correlation between mean myocardial T1 values and T2 SI ratios using dark-blood and bright-blood T2w-CMR (r=0.78 and 0.68, p<0.001; Figures 4.1A and B). There was also good correlation between dark-blood and bright-blood T2w-CMR (r=0.70, p<0.001; Figure 4.1C). There was moderate negative correlation between LVEF and mean T1 values (r=-0.52, p<0.001), T2 $SI_{myo:skeletal}$ by dark-blood T2w-CMR (r= -0.48, p<0.002) but not with bright-blood T2W-CMR (r=-0.19, p=0.23).

4.3.3 Receiver operating characteristic analysis

From the 42 subjects, 205 matching slices (111 patient and 94 control slices) across cine, T1-mapping, dark-blood T2 and bright-blood T2 sequences were available (Figure 4.2). Good coverage of the LV was achieved (median 5 matching short axis slices across all sequences tested, range 3-6 slices per case), yielding 1230 segments.

To maximise the accuracy of the threshold values to detect acute myocardial oedema, each segment was strictly assessed for image quality before inclusion into the final ROC analysis. On cine imaging, 21/1230 (1.7%) segments corresponding to the LVOT were rejected; on T1-maps, 142/1230 (11.5%) segments were excluded due to off-resonance artefacts, poor T1 fit as evidenced by the R^2 maps (see Supplemental Material), patient

Table 4.1 Patient characteristics

Patient #	Age (yrs)	Gender	Precipitating factor (symptoms)	Time to CMR (days)	EF (%)	Diagnosis	Wall motion abnormality	TnI*	STIR T2 SI	ACUT2E T2 SI	T1 (ms)
1	79	F	ES (ACP, P)	4	51	Takotsubo	Mid-apical AK	3.11	1.88	2.37	1043
2	56	F	Sz (ACP)	7	50	Takotsubo	Mid-apical AK	15.00	1.95	1.97	1065
3	70	F	PS (ACP)	2	64	Takotsubo	Mid-apical HK/AK	4.63	2.04	1.94	1051
4	60	F	Nil (ACP)	2	71	Takotsubo	Apical severe HK	19.98	1.89	2.20	1044
5	63	F	PS (D)	0	59	Takotsubo	Mid ventricular AK	4.46	1.57	1.85	1001
6	58	F	PS (ACP, D)	1	46	Takotsubo	Mid-apical AK	6.35	2.12	1.97	1032
7	42	M	Sz (ACP)	1	37	Takotsubo	Mid-apical HK/AK	5.00	1.93	1.64	1047
8	52	F	ES (ACP)	1	79	Takotsubo	Mid inferolateral & anteroseptal	22.75	2.29	2.56	1055
9	73	F	ES (ACP)	1	55	Takotsubo	Mid-apical HK/AK	10.86	1.91	2.18	1075
10	47	F	ES (ACP)	5	52	Takotsubo	Mid-apical HK/AK	0.84	2.57	2.43	1179
11	62	F	ES (ACP)	1	34	Takotsubo	Mid-apical HK/AK	36.80	1.90	2.14	1111
12	77	F	Nil (ACP)	4	66	Takotsubo	Mid ventricular AK	5.18	1.67	2.35	1100
13	47	F	Nil (ACP)	3	65	Regional edema	Inferolateral AK	1.30	1.57	1.98	993
14	66	F	ES (ACP)	2	51	Regional edema	Anterior,antero-septal AK	11.40	1.49	1.86	984
15	65	F	Nil (ACP)	1	62	Regional edema	Mid-apical inferolateral AK	12.69	1.48	1.85	1015
16	57	M	PS (ACP, D)	0	75	Regional edema	Distal anteroseptal HK	0.15	1.38	1.69	917
17	78	F	ES (ACP)	2	58	Regional edema	Mid inferior, inferolateral, inferoseptal AK	0.85	1.94	2.17	1133
18	59	F	ES (ACP)	4	67	Regional edema	Mid-apical anterior & anteroseptal	5.83	2.15	3.16	1113
19	54	F	ES (ACP)	1	66	Regional edema	Mid septum	2.63	1.56	2.07	999
20	63	F	Nil (ACP)	6	67	Regional edema	Mid-apical anterior & anteroseptum	3.46	2.02	2.13	1234
21	55	F	PS (ACP)	6	81	Regional edema	Mid anterior/ anteroseptal	0.21	1.86	2.28	1048

*Upper limit <0.04 ug/L for TnI. ACP = acute chest pain; TnI = Troponin I; T2 SI = T2 signal intensity (myo:skeletal); EF = ejection fraction; D = dyspnea; P = palpitations; PS = Physical stress; ES = Emotionalstress; Sz = Seizure. HK = hypokinesis; AK = akinesis. None of the patients demonstrated significant late gadolinium enhancement or coronary stenosis.

Table 4.2 Mean myocardial T1 and T2 SI ratios per-subject according to groups and segmental wall motion.

ShMOLLI T1 value (ms)	Controls	Takotsubo	Regional edema	All patients
Normal wall motion	944±17	1026±24 (p<0.001)	1032±86 (p<0.02)	1029±59 (p<0.001)
Abnormal wall motion	n/a	1101±78 (p<0.001)	1135±120 (p<0.001)	1113±94 (p<0.001)
Group average	944±17	1064±51 (p<0.001)	1051±98 (p<0.01)	1059±73 (p<0.001)
STIR T2 $SI_{myo:skeletal}$	Controls	Takotsubo	Regional edema	All patients
Normal wall motion	1.52±0.14	1.79±0.25 (p<0.01)	1.65±0.22 (p=0.14)	1.73±0.24 (p<0.001)
Abnormal wall motion	n/a	2.16±0.34 (p<0.001)	1.96±0.48 (p=0.05)	2.09±0.40 (p<0.001)
Group average	1.52±0.14	1.98±0.26 (p<0.001)	1.72±0.28 (p=0.08)	1.87±0.29 (p<0.001)
ACUT2E T2 $SI_{myo:skeletal}$	Controls	Takotsubo	Regional edema	All patients
Normal wall motion	1.77±0.19	1.93±0.26 (p=0.09)	1.97±0.23 (p=0.04)	1.95±0.24 (p<0.02)
Abnormal wall motion	n/a	2.34±0.37 (p<0.001)	2.49±0.50 (p<0.001)	2.40±0.41 (p<0.001)
Group average	1.77±0.19	2.13±0.27 (p<0.001)	2.08±0.29 (p<0.02)	2.11±0.27 (p<0.001)

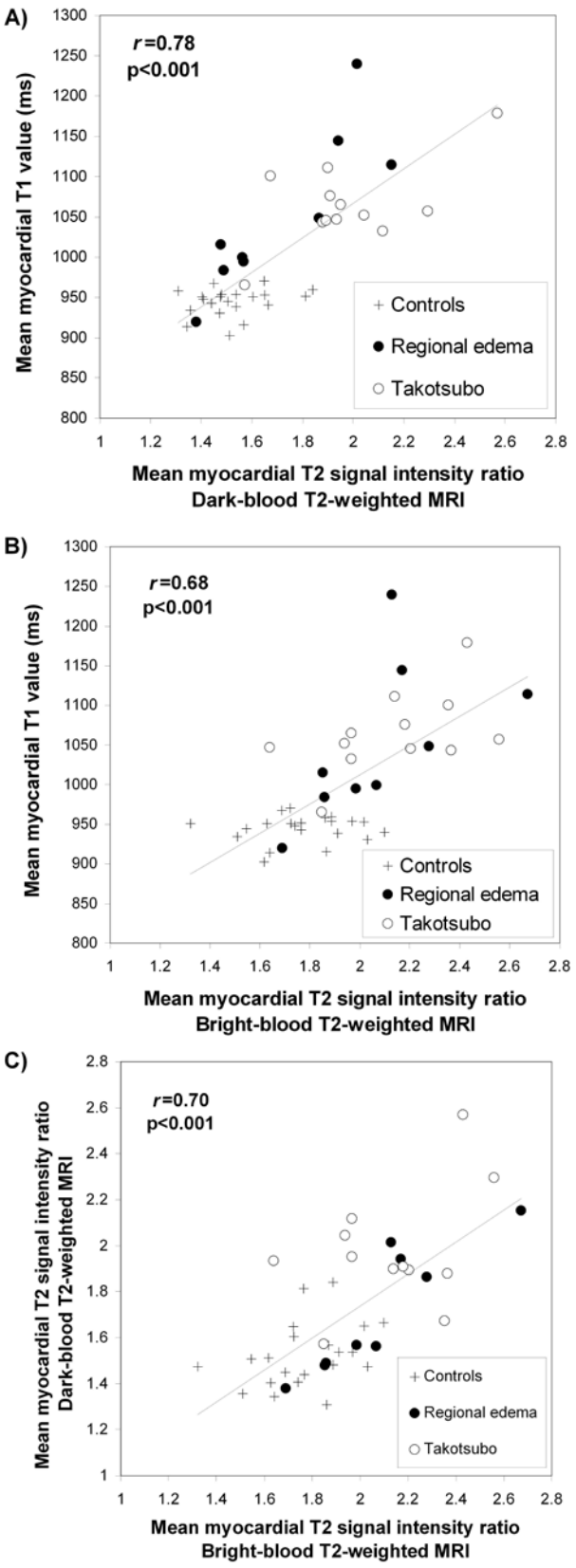


Figure 4.1 Relationship between: **(A)** myocardial T1 values and T2 signal intensity (SI) ratio* derived from dark-blood T2W-CMR; **(B)** myocardial T1 values and T2 SI ratio derived from bright-blood T2W-CMR; **(C)** myocardial T2 SI ratio dark-blood vs. bright-blood T2W-CMR. *T2 SI ratio=$SI_{myocardium}/SI_{skeletal\ muscle}$

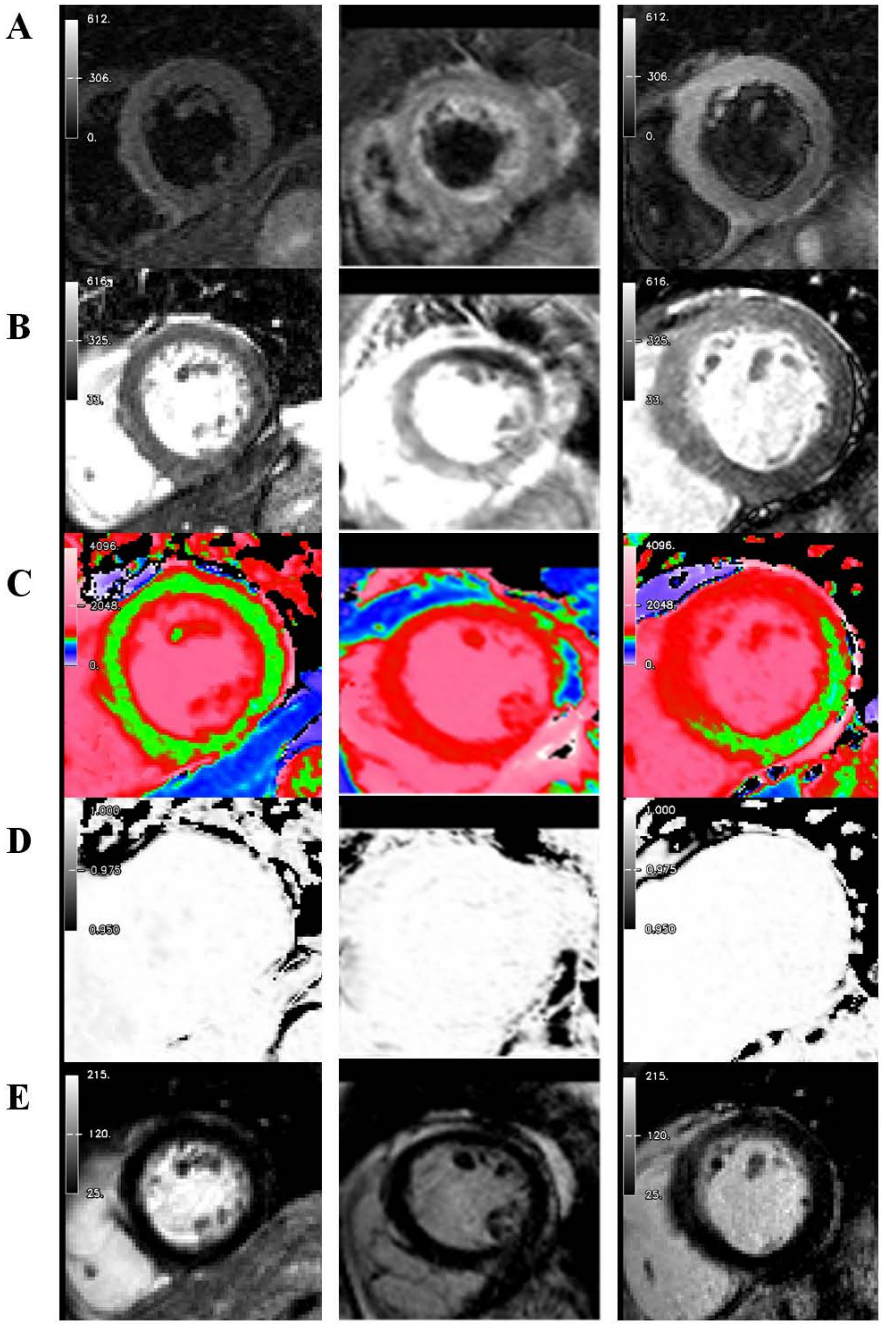


Figure 4.2 CMR imaging modalities used for comparison – representative images in short-axis slices from: **(*Left panel*)** Normal volunteer **(*Middle panel*)** Patient with Takotsubo cardiomyopathy. Note high T2 signal and T1values in an apical slice. (***Right panel***) Patient with regional oedema in the anterior wall territory. Note high T2 signal and T1 values in the anterior, anterolateral wall and anterior septum. **Rows: (A)** Dark-blood T2-weighted images (reference ROIs in skeletal muscle and remote myocardium not shown). **(B)** Bright-blood T2-weighted images. **(C)** Colour ShMOLLI T1-maps. Green denotes normal myocardium. Red denotes increased T1 values **(D)** R^2 maps of ShMOLLI inversion recovery fit used to verify the quality of T1-maps. White denotes perfect T1 reconstruction. **(E)** LGE imaging.

movement or low SNR; on dark-blood STIR imaging, 94/1230 (7.6%) segments were rejected due to insufficient image quality or artefacts; on bright-blood ACUT2E imaging, 26/1230 (2.1%) segments were rejected due to LVOT anatomy and off-resonance artefacts. This yielded 1005 segments of good quality (453 control and 552 patient segments, 230 of which had abnormal wall motion).

ROC analysis (Figure 4.3) showed that for the detection of acute myocardial oedema, T1-mapping demonstrated excellent diagnostic performance with a significantly larger area-under-the-curve (AUC=0.94) compared to dark-blood and bright-blood T2W-CMR, whether the reference ROI was remote myocardium or skeletal muscle ($p<0.04$ for all comparisons). A T1 threshold of 990 ms most optimally differentiated segments affected by oedema from normal segments, with a sensitivity and specificity of 92%. This T1 threshold reproduced the proportion of the number of abnormal to control segments used to construct this ROC curve. We also performed ROC analyses based on patient groups to examine how T1-mapping performed against the T2 methods in detecting regional or global oedema when different reference ROIs were used.

In acute regional oedema, where remote myocardium is more appropriate as a reference ROI for the T2-weighted methods, ROC analysis (Figure 4.4A) showed that both T1-mapping and bright-blood ACUT2E had equally excellent diagnostic performance (AUC=0.92 vs. 0.96, respectively, $p=0.21$); both were significantly better than dark-blood STIR (AUC=0.80, $p<0.03$ for both comparisons) in the detection of regional oedema.

In Takotsubo cardiomyopathy where an entire myocardial slice may be diffusely oedematous, skeletal muscle is a more appropriate reference ROI for the T2 methods, and ROC analysis (Figure 4.4B) showed that both T1-mapping and dark-blood STIR had equally excellent diagnostic performance (AUC=0.95 vs.0.92, respectively, $p=0.12$) over bright-blood ACUT2E (AUC=0.83, $p<0.0001$ for both comparisons) in the detection of global oedema.

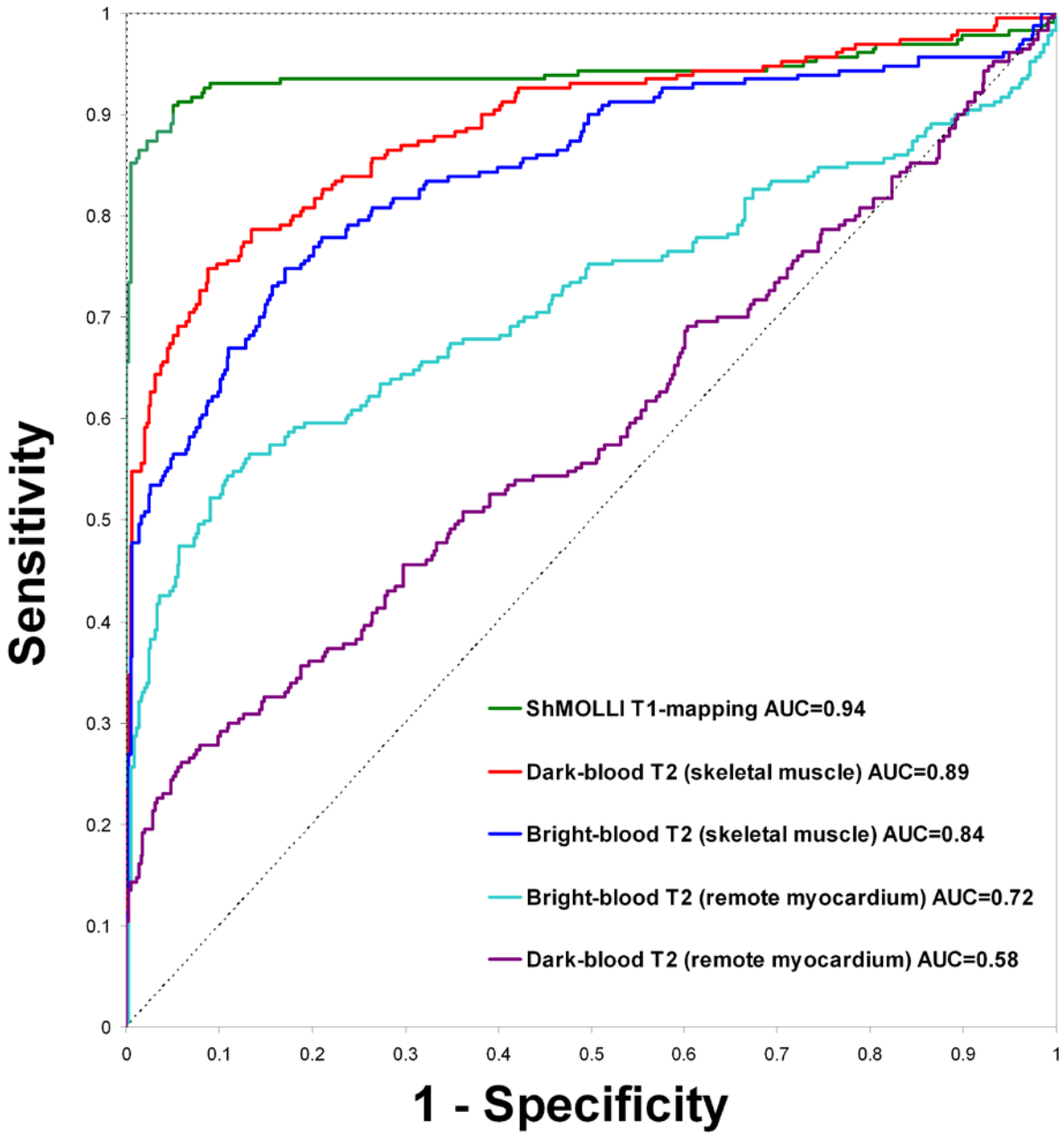


Figure 4.3 Receiver operator characteristic curves for the detection of acute myocardial oedema by ShMOLLI T1-mapping, dark-blood T2W-CMR and bright-blood T2W-CMR. For T2-weighted methods, reference regions of interest for comparison of myocardial signal intensity are specified in brackets. AUC=area-under-the-curve.

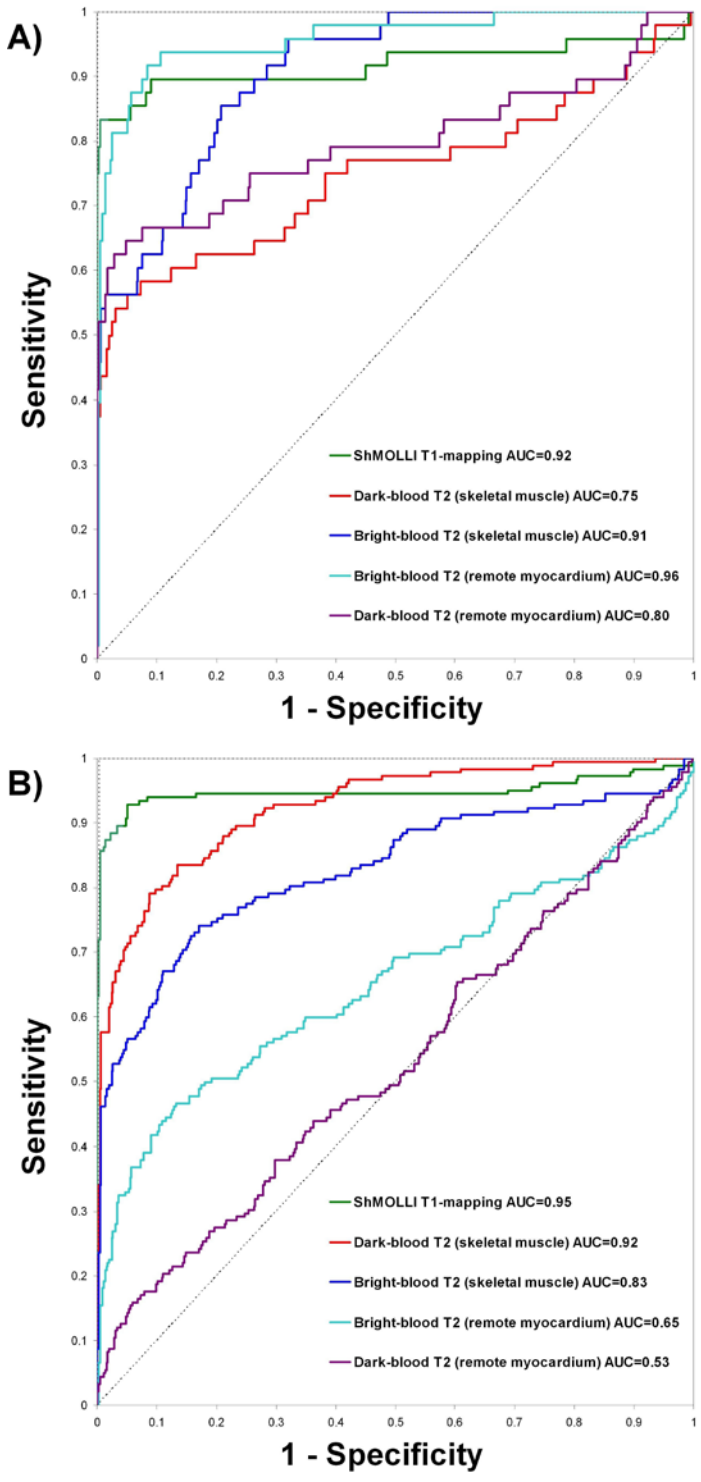


Figure 4.4 ROC curves for the detection of acute myocardial oedema according to patient groups using ShMOLLI T1-mapping, dark-blood T2W-CMR and bright-blood T2W-CMR. **(A)** Patients with regional oedema vs. controls. **(B)** Patients with Takotsubo cardiomyopathy vs. controls. AUC=area-under-the-curve.

Finally, to check for bias against any of the methods, when all 1230 segments (including segments affected by artefacts) were used, all of the original relative relationships were preserved, with T1-mapping maintaining a significantly larger AUC of 0.87 compared to the T2-weighted methods (Figure 4.5). Relative relationships amongst methods were also preserved for ROC analyses according to patient groups (Figure 4.6A and B).

4.3.4 Intra- and inter-observer agreement of T1-mapping

There was excellent correlation (r>0.991) and agreement between T1 estimates obtained between both blinded operators. Bland Altman analysis of intra- and interobserver variability showed that the percentage difference in T1 values was ± 0.5% (±5.6 ms) and the 95% CI for the differences was ± 1.1% of the average T1 (±11.1ms). There were no statistically significant differences between intra- and interobserver variability.

4.4 Discussion

In this study, we have found that T1 is elevated in regions with abnormal wall motion and that these regions co-localise with regions with elevated signal in T2-weighted images. There is strong correlation between myocardial T1 and T2 SI ratios. Further, T1-mapping detected myocardial involvement beyond that identified by wall motion abnormality. We have demonstrated for the first time that non-contrast T1-mapping detects acute myocardial oedema with high diagnostic accuracy compared to conventional dark-blood and newer bright-blood T2W-CMR at 1.5T.

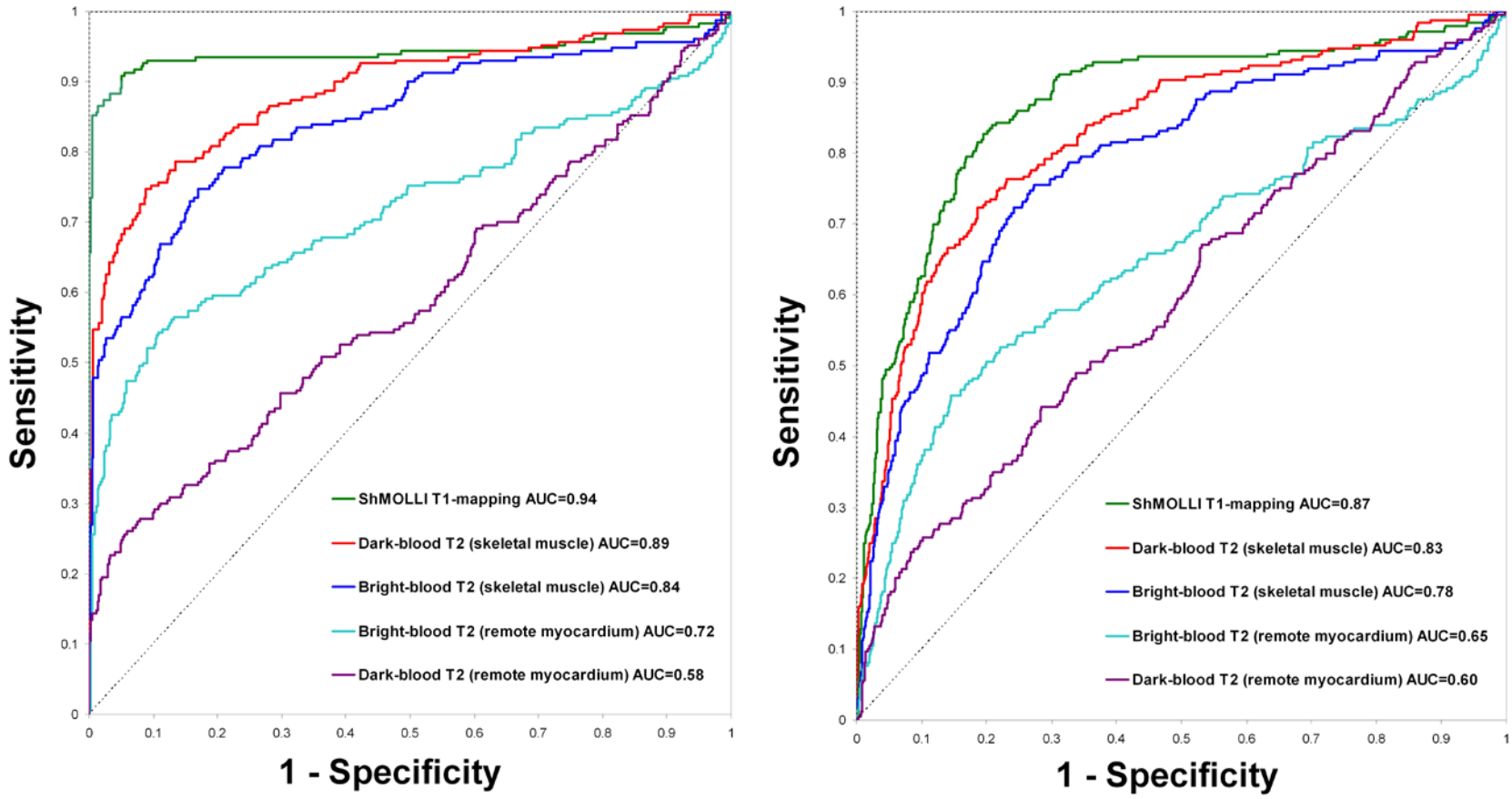


Figure 4.5 ROC curves for the detection of acute myocardial oedema by ShMOLLI T1-mapping, dark-blood T2W-CMR and bright-blood T2W-CMR using only segments of good quality for all methods (***left panel***), and using all available segments, including segments previously rejected for artefacts for all methods (***right panel***). This shows that ShMOLLI T1-mapping retains its superiority despite the re-inclusion of segments affected by artefacts. All comparisons are statistically significant ($p<0.03$). AUC=area-under-the-curve.

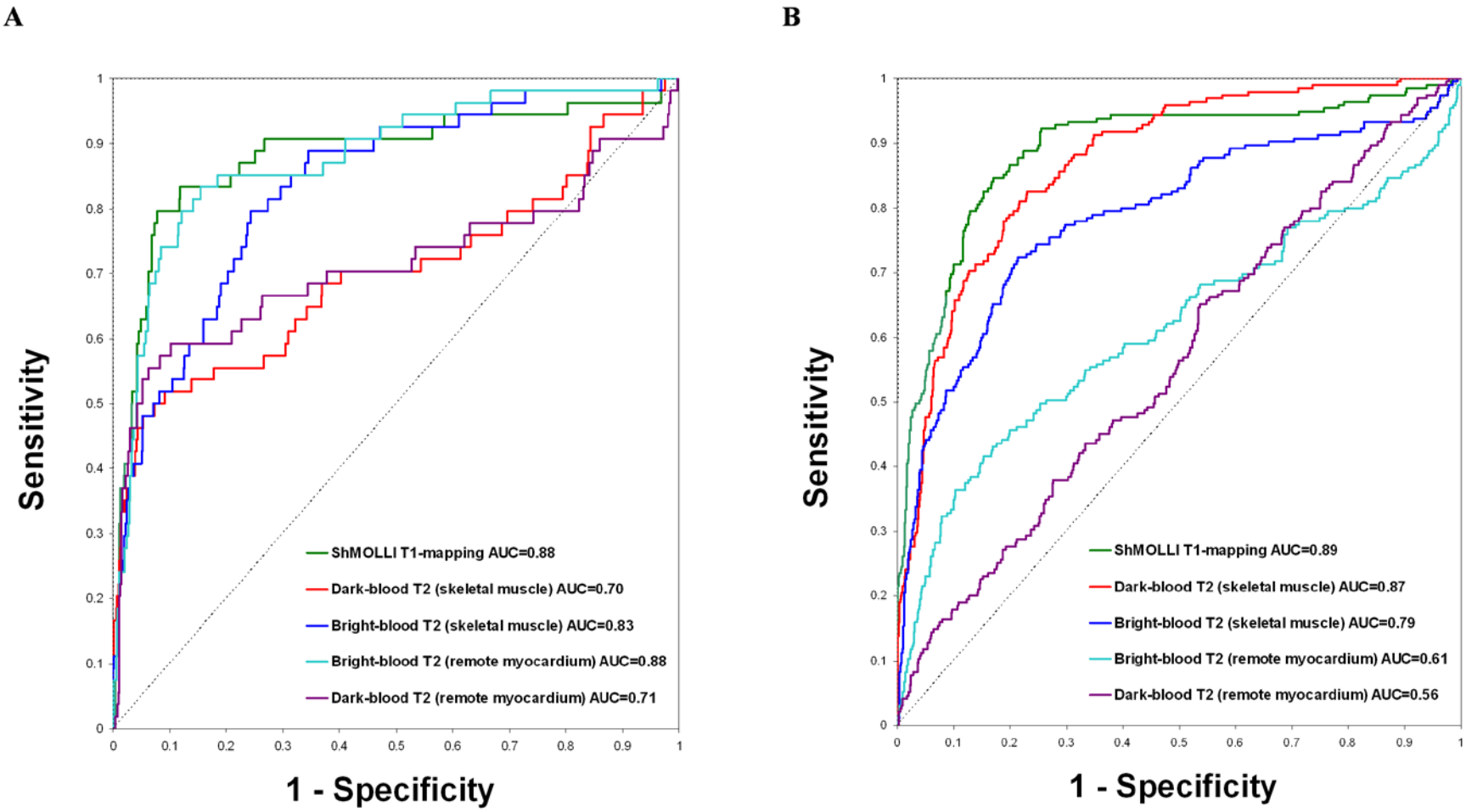


Figure 4.6 Receiver operator characteristic curves according to patient groups for the detection of acute myocardial oedema using all segments, including segments previously rejected for artefacts for all methods. (A) Patients with regional oedema vs. controls. (B) Patients with Takotsubo cardiomyopathy vs. controls. AUC=area under the curve.

4.4.1 CMR for the detection of acute myocardial oedema

Given that oedema is a generic tissue response to acute insults, oedema imaging appears to be a highly suitable tool for assessing acute myocardial injury. The “gold standard” for defining myocardial oedema on imaging, however, is controversial (43). Experimental animal models using fluorescent microspheres to delineate myocardium area-at-risk in acute MI correlated to T2W-CMR imaging (34); however, topographic correlation between T2W images and histopathologic validation of pure myocardial oedema without infarction in humans is lacking, largely due to the difficulty in accurately measuring oedema in histopathologic samples. We thus decided to study patients presenting with cardiac conditions known to involve acute oedema but without co-existing infarction or other pathology detected by LGE. In Takotsubo cardiomyopathy and acute myocardial stunning, inflammation and oedema are main features described on human endomyocardial biopsies and animal models (44-46). Although patients with regional oedema did not fulfil criteria for the typical patterns of Takotsubo cardiomyopathy, and possible mechanisms may include transient ischaemic plaque events leading to myocardial necrosis (as evidenced by the positive troponins) (47), the cases precipitated by an emotionally stressful event may represent an atypical form of stress-induced cardiomyopathy not fitting the traditional description of apical ballooning or other morphologic variants commonly described (40). There was no viral history to suggest a myocarditic process. The common feature for all patients in this study is that all had acute wall motion abnormalities associated with oedema without infarction on CMR. While not proven histologically in our cohort, it is highly likely that segments with acute wall motion abnormality would demonstrate features of acute oedema. Our assumption was strongly supported by the fact that segments with abnormal wall motion showed numerically higher average T2 SI ratio and T1 values than controls.

4.4.2 ShMOLLI T1-mapping: a novel method for imaging myocardial oedema

The ShMOLLI technique for fast T1-mapping (17) overcomes many of the limitations of both conventional MOLLI T1-mapping and dark-blood T2w-CMR. Compared to MOLLI, ShMOLLI is ~50% shorter in breath-hold times; it is also heart rate- and T1-independent over a wide range of T1 values, and thus is more accurate in measuring long T1s in oedema and at fast heart rates (17). Compared to dark-blood T2w-CMR , ShMOLLI is robust to tachycardia (shown in simulation and phantoms for rates up to 100 bpm (17) and tested in clinical subjects with sinus tachycardia and atrial fibrillation at ventricular rates of up to 150 bpm (unpublished own data). It does not suffer from signal dropout due to through-plane cardiac motion and breath-holds are considerably shorter.

Bright-blood T2 is excellent for detecting large areas of regional oedema when there is obvious normal myocardium to be used as a reference, as shown recently (33) and in this work. The main challenge of extending bright-blood T2 imaging for the detection of diffuse oedema was the variability of the image quality of reference skeletal muscle, which was often affected by off-resonance artefacts, bright signals from adjacent fat, bright blood vessels within the muscle or signal dropouts. For this reason, STIR outperformed bright-blood ACUT2E in this setting as STIR images have a more homogenous signal across the field of view, and thus the quality of the skeletal muscle was generally better, more consistent and more reliable. This study suggests that bright-blood T2 may not always be suitable as a replacement method for conventional dark-blood T2w-CMR.

T1-mapping using ShMOLLI has now been shown to be highly sensitive to acute changes in myocardial water characteristics which, up to this point, have been evaluated mainly using T2W-CMR. From a mechanistic point of view, T1-mapping and T2-weighted MRI likely detect acute myocardial injury via distinct, but complementary and overlapping

mechanisms. Interestingly, we detected significant T1 elevation even in patient segments with normal wall motion (Table 4.2), a finding accompanied also by significantly higher T2 SI in segments with normal wall motion in Takotsubo patients (by dark-blood STIR but not bright-blood ACUT2E) as well as in patients with regional oedema (by bright-blood ACUT2E but not dark-blood STIR). This suggests that T1-mapping may be the more sensitive technique in detecting acute myocardial changes in both global and regional pathologies, and/or detects myocardial changes beyond that identified by wall motion abnormality and the T2-weighted methods tested. Previous experimental work demonstrated that T1 relaxation times are prolonged in regionally ischaemic tissue from dog hearts, and while largely reflective of increased free water content of the ischaemic tissue, T1 changes exceeded the changes in water content as the duration of ischaemia was increased (9). The prolongation of T1 values was found to be unrelated to changes in metabolic parameters such as tissue content of oxygen, carbon dioxide, hydrogen ions, lactate, adenosine triphosphate or phosphocreatine (9). Rather, it was postulated that T1 changes may be related to changes in both total water content as well as the relative amounts of water in intracellular and extracellular compartments. Furthermore, changes in sodium and potassium contents and their distribution may impact on the motional freedom of water protons, contributing to prolongation of T1 values in ischaemic tissue (9). Indeed, both of these processes are part of oedema evolution in ischaemic injury to the myocardium (31). Thus, while increased T1 values in acutely injured myocardium may largely reflect water characteristics, there may be additional changes that are more readily detected by T1-mapping and to which T2W methods are less sensitive. The precise nature of what these changes are that prolong T1 values will need to be further investigated, but ShMOLLI T1-mapping is a distinct yet complementary technique to T2W-CMR, which adds to our current repertoire of available sequences for assessing acute myocardial injury.

T1-mapping holds potential to quantify both extent and severity of disease and may provide further insights into conditions where T2W-CMR has proven useful. These include quantifying myocardial salvage in acute MI, determining the age of myocardial injury, diagnosing acute myocarditis and cardiac transplant rejection. It may also be useful in describing subacute conditions where myocardial inflammation is implicated, such as cardiac sarcoidosis (48), amyloidosis, and hypertrophic cardiomyopathy (35). T1-mapping has also been shown to detect changes in chronic cardiac conditions involving diffuse fibrosis (49-51), which is characterised by increased collagen and aqueous content within the myocardium, leading to interstitial expansion.

Unlike the T2W methods examined, ShMOLLI T1-mapping does not require *a-priori* knowledge of where affected and unaffected myocardium (if any) should be for image analysis; it reports absolute T1 values, obviating the need for a reference ROI, and thus has an excellent performance in different models of oedema, whether regional or global. Accordingly, T1-mapping can be useful in pathologies where oedema maybe diffuse, patchy or not immediately obvious to the eye. Immediate visualisation of the extent of injury may be facilitated by dedicated colour schemes based on quantitative thresholds, an example of which is shown in Figure 4.2.

4.4.3 Quality and reliability of ShMOLLI T1-maps

As our T1-mapping method is novel, we aimed to be as accurate as possible in setting the most optimal cut-off value for detecting oedema and thus were stringent on selecting only the best segments (without any or with only minimal artefacts) to include in the analysis. This was one of the reasons for the apparently higher rejection rate for T1-mapping compared to other modalities. T1-maps were assessed for quality and reliability in three ways: visual inspection of the T1-map itself, visual inspection of all seven of the raw T1 images for potential artefacts,

and the use of R^2 maps to ensure that the T1 fit is robust for all segments on the T1-map. The feature of R^2 maps is described in detail with examples in Appendix 1 and serve as a more objective way to detect segments with poor T1 fit that may not be obvious to the eye; T2-weighted methods tested in this study, on the other hand, do not have this added feature for quality assurance and so their rejection rate may be underestimated. We consider the fact that ShMOLLI T1-mapping has multiple ways for detecting regions with potentially compromised T1 values a strength of the method which makes it more robust, especially to observer bias. ACUT2E is also a relatively novel method that has been validated in acute MIs (33), but not in detecting global oedema or non-ischaemic pathologies; sometimes, it is unclear whether darker areas within the myocardium are due to SSFP artefacts (as in Figure 4.2B, middle panel) or whether it is representative of normal myocardium (as in Figure 4.2B (right panel) versus signal drop-out/artefact in the inferolateral wall (less likely in this case). These reasons contribute to the apparently higher rejection rate of T1-mapping, but do not reflect that the method is artefact-prone; rather, we were strict on selecting only the best segments for the purpose of establishing T1 thresholds with the greatest accuracy.

As presented in the Results section, to check for bias against any of the methods tested, when we re-included all rejected segments affected by artefacts, it was reassuring to note that all of the original relative relationships on the ROC analysis were preserved, with T1-mapping maintaining its superior diagnostic performance with a significantly larger AUC of 0.87 compared to the T2-weighted methods (Figure 4.5). Relative relationships amongst methods were also preserved for ROC analyses according to patient groups (Figure 4.6A and B).

4.5 Limitations

ShMOLLI T1-mapping sometimes demonstrated typical SSFP susceptibilities to off-resonance artefacts and partial volumes effects, especially in very apical slices. These may be circumvented with frequency shifting and potentially by wide-band SSFP. As artefacts may cause falsely high or low T1 values, it is important to have methods for assessing the quality and robustness of T1-maps, such as those used in this study (see Appendix 1). ShMOLLI underestimates the true T1 value by 4%, but in a consistent manner (17) so corrected T1 values can be easily derived.

As discussed, it is challenging to establish an in-vivo and histopathologic reference gold standard for acute myocardial oedema; thus, this study used acute regional wall motion abnormality without evidence of infarction as the best clinical surrogate for oedema in a carefully selected study population. Pre-contrast increase in myocardial T1 value is non-specific and may be seen in a number of conditions, including acute myocardial injury, chronic infarct scar (20) and cardiac amyloidosis (52), and thus must be interpreted within the clinical context. Moreover, changes of T1 and T2 within the myocardium are dependent on different mechanisms, but the two are closely related. The precise mechanisms leading to increased T1 relaxation times in acutely injured myocardium remain to be established.

Thirdly, T2-mapping is another technique which may be used to detect oedema (53) but was not studied in this work. We did, however, compare T1-mapping to the state-of-the-art bright-blood ACUT2E sequence (16), which has recently been shown to be superior to conventional dark-blood STIR imaging in acute MI (33). Future work will have to directly compare T1 and T2 mapping techniques.

4.6 Conclusion

ShMOLLI T1-mapping is a novel, quantitative method that we have now clinically validated for detecting acute global and regional myocardial oedema. A T1 cut-off of 990 ms has a high diagnostic performance, with a sensitivity and specificity of 92%, compared to dark-blood and bright-blood T2W-CMR. T1-mapping using ShMOLLI holds potential to quantify both extent and severity of myocardial oedema and may provide further insights into conditions where T2W-CMR has proven useful.

Chapter 5

The Diagnostic Performance of T1-mapping and T2-weighted Cardiovascular Magnetic Resonance in Acute Myocarditis

5.1 Introduction

Given that inflammation and oedema are integral components in the pathophysiology of acute myocarditis, T1-mapping should be able to serve as a new diagnostic criterion for acute myocarditis. Acute myocarditis is common, accounting for up to 75% of patients presenting with chest pain, raised troponin but non-obstructive coronary arteries (54), 12% of young adults presenting with sudden death (55) and 9% of patients who develop dilated cardiomyopathy (56). It is challenging to diagnose, often requiring a combination of clinical assessment and diagnostic tests. Cardiovascular magnetic resonance (CMR) is the imaging tool of choice due to its ability for multiparametric tissue characterisation, as established in recent consensus guidelines (14).

Currently, three CMR methods are available to help diagnose acute myocarditis: dark-blood T2-weighted (T2W) imaging for oedema, T1-weighted imaging pre- and post-contrast for hyperaemia, and late gadolinium enhancement (LGE) to detect the patterns of myocyte necrosis (14). Although CMR is a powerful tool, there are some recognised limitations related to technical factors, image analysis and the mechanism of signal detection for each method in diagnosing myocarditis(14,37). Using a combined CMR approach of at least two out of these three criteria can improve diagnostic accuracy (14).

Novel CMR techniques are constantly being developed, some of which may be suitable for the evaluation of myocarditis. For instance, bright-blood T2W imaging has been shown to be superior to dark-blood T2W imaging for detecting the area-at-risk in acute myocardial infarction (AMI) (16,33,37). T1-mapping is superior to T2W techniques in detecting area-at-risk in AMI (39) and, as presented in chapter 4, acute oedema (57). These methods are promising but have not been systematically validated in the assessment of acute myocarditis.

In this prospective study, we performed multi-parametric tissue characterisation in patients with suspected acute myocarditis (14) using novel and conventional CMR techniques, including dark-blood T2W-CMR, bright-blood T2W-CMR, T1-mapping and LGE imaging. We present the diagnostic performance of these techniques to detect and diagnose acute myocarditis.

5.2 Methods

5.2.1 Study population.

This is a prospective study enrolling consecutive patients with suspected myocarditis (15,17) from two tertiary care centres (John Radcliffe Hospital, Oxford and Milton Keynes Hospital, Milton Keynes, United Kingdom). All patients had:

(a) acute chest pain;

(b) elevation in cardiac troponin I level (>0.04 ug/L);

(c) history of recent systemic viral disease or absence of significant (>50%) obstructive coronary artery disease (CAD) on coronary angiography or absence of risk factors for CAD or age <35 years.

Exclusion criteria included contraindications to CMR, previous myocardial infarction, previous myocarditis or any chronic cardiac conditions. Patients who demonstrated myocardial infarction as evidenced by an ischaemic pattern of LGE (i.e. an isolated area involving the subendocardium) or an obvious alternative diagnosis on CMR (such as Takotsubo or hypertrophic cardiomyopathy) were also excluded. Healthy volunteers with no cardiac history or known cardiac risk factors, not on cardiovascular medications and with a normal ECG underwent CMR as controls. All subjects gave written informed consent and ethical approval was granted for all study procedures.

5.2.2 CMR image acquisition and analysis

CMR studies were performed within 14 days of symptoms using a single 1.5T MR system (Avanto, Siemens Healthcare, Germany) including cine, dark-blood T2W-CMR, bright-blood T2W-CMR, T1-mapping and LGE imaging, with matching short-axis images. These are described in detail in chapters 2 and 3.

Image Analysis

Image quality was assessed and matching short axis slices were compared across cine, ShMOLLI T1-mapping, dark-blood T2W, bright-blood T2W and LGE imaging. For the T2W methods, given that myocarditis is often a global and patchy disease with often no easily identifiable “normal remote myocardium”, only skeletal muscle was used as a reference ROI, as per common practice (14). Details are described in chapters 2 and 3.

For all quantitative analysis of T2W, LGE and T1-map images, only regions of myocardium with a contiguous area of ≥40 mm^2 above the specified thresholds were considered relevant. This corresponds to 10 adjacent pixels for the STIR method, in accordance with currently proposed recommendations (14), to reduce the detection of noise as positive findings. To determine the sensitivity and specificity for each threshold, an average involvement of ≥5% of segmental myocardium above the described threshold per subject was considered a positive finding by each method.

5.2.3 Statistical Analysis

Normality of data was tested using the Kolmogorov-Smirnov test. Normally-distributed data are presented as mean±SD; non-parametric data are presented as median (interquartile range). Unpaired samples between groups were assessed by the unpaired 2-tailed Student *t*

tests, or the Mann-Whitney *U* test for non-parametric data. To determine the presence of significant differences in subject groups when using multiple CMR methodologies, ANOVA analysis was performed with Bonferroni corrected post-hoc comparisons. For non-parametric data, we used the Friedman test; the Kruskal-Wallis one-way analysis of variance with post-hoc pairwise comparisons was made using the Mann-Whitney U test as appropriate. Correlation was assessed using the Pearson "*r*" and Spearman "ρ" coefficient as appropriate. Receiver operator characteristic (ROC) analysis was performed to compare the diagnostic performance of the CMR methods in detecting myocardial changes in patients compared to controls. Significance of ROC analyses was assessed using the method of Delong et al. (41) (MedCalc, version11.5.1.0, www.medcalc.org). All statistical tests were two-tailed, with p-values of less than 0.05 considered statistically significant.

5.3 Results

5.3.1 Study population characteristics

There were 50 patients (age 41.5±16.0 years, 22% females) and 45 age- and gender-matched controls (age 41.5±14.0 years, 22% females). Patients enrolled demonstrated a wide range of Troponin I levels from 0.15 to >60 ug/L (median 5.15 ug/L). The majority (n=36/50; 72%) underwent coronary angiography which demonstrated non-obstructive coronary arteries; coronary artery disease was excluded on clinical grounds for fourteen (n=14/50; 28%) due to young age, no CAD risk factors or a history of recent systemic viral or inflammatory illness (14). Patients underwent CMR at a median of 3 days (range 0-13 days) from presentation. A majority of the patients (n=46, 92%) had a recent systemic viral (n=41, 82%) or inflammatory (n=5, 10%) illness, while the rest (n=4) did not have any clear viral, infectious or inflammatory precipitant.

5.3.2 Detection of myocardial changes by CMR in acute myocarditis

CMR findings are shown in figure 5.1 and summarised in table 5.1. Patients had significantly lower LV ejection fraction compared to controls (EF 63±12% vs. 72±6%, p<0.01). Patients had significantly higher T2 SI ratio, as measured by both dark-blood T2W and bright-blood T2W imaging, as well as significantly higher mean myocardial T1 values and LGE SI ratio compared to controls. The pattern of LGE was predominantly subepicardial (95.6%) and midwall (84.4%), localised most frequently to the lateral wall (97.9%) and inferior wall (95.6%), as compared to the septum (60.0%) and anterior wall (35.6%). None of the 50 patients demonstrated an isolated ischaemic pattern of LGE to suggest myocardial infarction as the aetiology of the acute presentation.

5.3.3 Relationship between myocardial T1 and other measures of acute myocardial injury.

Average myocardial T1 values correlated well with LVEF (r=0.58) and better than measures of global myocardial oedema by dark-blood T2W (r=0.36) or bright-blood T2W imaging (r=0.38; all correlations p<0.002). Mean myocardial T1 showed moderate correlations with relative T2 SI changes by both dark-blood and bright-blood T2W imaging (r=0.47-0.55), and LGE (r=0.61). T1 values were significantly higher in segments with abnormal wall motion (1063±85ms), increased dark-blood T2 SI ratio (1063±70ms) and LGE (1058±83ms) compared to controls.

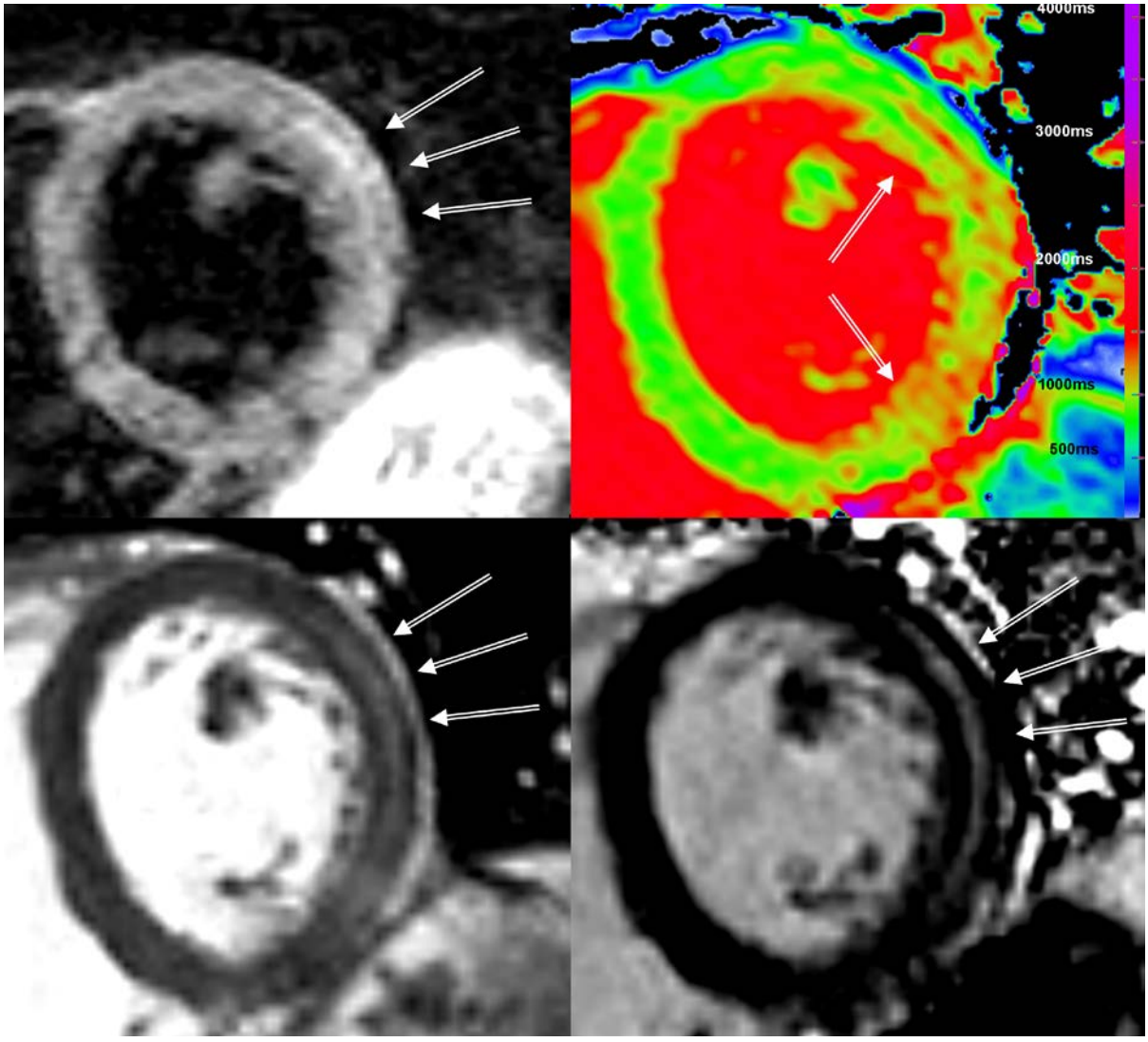


Figure 5.1 Acute myocarditis. **(Top left)** Dark-blood T2W imaging demonstrating increased signal intensity in the mid lateral wall (white arrows). **(Bottom left)** Bright-blood T2W imaging demonstrating increased signal intensity in the mid lateral wall (white arrows). **(Top right)** ShMOLLI T1-map demonstrating increased T1 values (1100-1200 ms) in the lateral wall (white arrows). **(Bottom right)** LGE imaging demonstrating mid-wall enhancement in the lateral wall (white arrows).

Table 5.1 CMR findings in patients with acute myocarditis compared to controls.

CMR	Controls	Patients
Ejection fraction (%)	72±6%	63±12%*
Dark-blood T2 SI ratio	1.56±0.15	1.73±0.27*
Bright-blood T2 SI ratio	1.84±0.17	2.02±0.33*
Myocardial T1 (ms)	941±18 ms	1010±65 ms*
LGE (%)	0% (0%, 2%)	11% (5%, 21%)*

*signifies statistical significance $p<0.01$. Dark-blood T2 SI ratio and bright-blood T2 SI ratio = $SI_{myocardium}/SI_{skeletal\ muscle}$; LGE (%) = median volume fraction of late gadolinium enhancement per subject; interquartile range in brackets. SI = signal intensity.

5.3.3 Diagnostic performance of CMR methods in the detection of acute myocarditis.

Both T1-mapping and LGE imaging demonstrated excellent and equivalent diagnostic performance, with an area-under-the-curve (AUC) of 0.96 and 0.95, respectively (p=ns) and significantly outperformed any of the T2W methods tested (Figure 5.2). To check for bias against any of the methods, ROC analysis was repeated using all data including segments affected by artefacts. All of the above relative relationships were preserved, with no significant change in the AUC for each method (all $\leq$0.02).

The diagnostic performance of each CMR tissue criterion and their combinations are summarised in table 5.2. T1-mapping, using a cut-off of T1 ≥ 990ms as established in the previous study in chapter 4 for detecting acute oedema (14), demonstrated very good performance with a sensitivity (SN), specificity (SP), diagnostic accuracy, positive predictive value (PPV) and negative predictive values (NPV) of 90%, 91%, 91%, 92% and 89%, respectively. The T2W methods showed good diagnostic performance within ranges published in the literature, whereas LGE had high specificity (97%) and PPV (97%) with a lower sensitivity (74%) compared to T1-mapping.

Using a combination approach, T1-mapping together with either dark-blood or bright-blood T2W imaging achieved a higher specificity (89% and 100%, respectively), but at the expense of lower sensitivity (52% and 67%, respectively), compared to T1-mapping alone. Combining LGE with any of the other methods did not significantly improve specificity compared to LGE alone, but lost sensitivity significantly. Consistent with current literature, a combination approach, using any 2 out of the 4 now available criteria, improved diagnostic performance, to SN (87%), SP (100%), and accuracy (88%). Interestingly, combining T1-mapping with any of the T2W methods replicated the diagnostic performance of LGE alone.

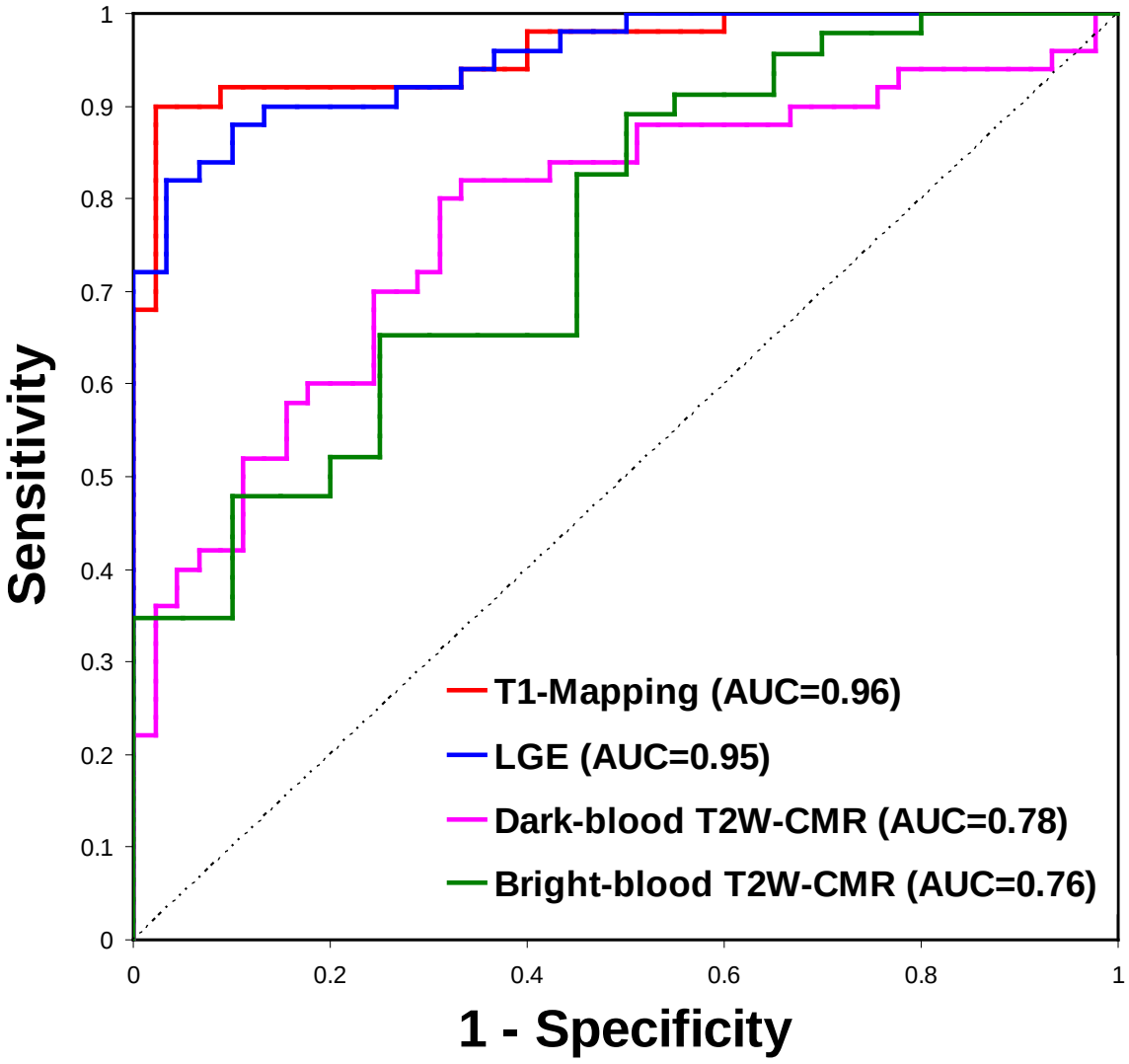


Figure 5.2: Diagnostic performance of T1-mapping compared to T2W and LGE imaging in the detection of acute myocarditis. AUC = area-under-the-curve; LGE = late gadolinium enhancement; SD = standard deviation. T1 mapping is similar to LGE and both significantly outperformed T2W imaging.

Table 5.2 Diagnostic performance of CMR tissue criteria in the detection of suspected acute myocarditis.

Tissue Criteria	Sensitivity (%)	Specificity (%)	Accuracy (%)	PPV (%)	NPV (%)
Individual					
T1-mapping*	90	91	91	92	89
Dark-blood T2†	52	84	67	79	61
Bright-blood T2‡	67	55	64	78	42
LGE§	74	97	83	97	69
Combination					
T1-Mapping and Dark-blood T2	52	98	74	96	65
T1-Mapping and Bright-blood T2	67	100	77	100	57
LGE and T1-mapping	70	97	80	97	66
LGE and Dark-blood T2	48	97	66	96	53
LGE and Bright-blood T2	50	100	55	100	18
Any 2 out of 4	87	100	88	100	45
T1 and any T2W method	76	100	83	100	65

* Myocardial injury is detected when T1 is ≥ 990 ms;
† Edema is diagnosed when the T2 SI ratio ($T2\ SI_{\text{myocardium : skeletal muscle}}$) is ≥ 2.0;
‡ Edema is diagnosed when the T2 SI ratio ($T2\ SI_{\text{myocardium : skeletal muscle}}$) is ≥ 2.2 (equivalent to >2 SD of normal; see Table 2);
§ LGE is detected when myocardial SI is ≥ 2 SD above mean SI of normal myocardium.
For each technique, only contiguous areas of myocardium ≥40 mm^2 above the stated threshold were considered relevant; involvement of ≥5% of any segment on a per-subject basis was the threshold used for comparison of methods.
CMR = cardiovascular magnetic resonance; LGE = late gadolinium enhancement; T2W = T2-weighted; PPV = positive predictive value; NPV = negative predictive value; SI = signal intensity; SD = standard deviation.

5.4 Discussion

In this work, we have demonstrated for the first time that quantitative CMR by T1-mapping has an excellent diagnostic performance in detecting changes in acute myocarditis over a wide range of presentations in common clinical practice. Further, a combined approach using T1-mapping and any T2W-CMR technique can further improve specificity and replicates the diagnostic performance of LGE alone, without the need for exogenous contrast agents. Using a combination approach of any 2 out of the 4 criteria improved overall diagnostic performance to a sensitivity, specificity and accuracy to 87%, 100% and 88%, respectively.

The CMR methods tested in this study all have advantages and limitations. From the technical standpoint, factors that lead to the failure of a method to diagnose acute myocarditis may be categorized into (1) compromised image quality during acquisition (patient movement, poor breath-holding, tachyarrhythmia); (2) suboptimal post-processing techniques; (3) noise and the selection of thresholds.

5.4.1 Dark-blood T2-weighted imaging

Dark-blood T2W-CMR is widely-used for clinical oedema imaging. In addition to following recommended parameters (14), optimal image quality relies on a regular heart rhythm with a ventricular rate within a relatively normal range, appropriate selection of the repetition time (TR) tailored to the patient's heart rate and the ability of the patient to breath-hold. Excessive tachycardia, irregular rhythms such as atrial fibrillation and poor breath-holding render dark-blood T2W images non-diagnostic most of the time. Dark-blood T2W images are known for signal drop-out especially in the basal inferolateral wall, where myocarditis typically manifests. When myocarditis is global, the use of "normal remote" myocardium as a reference, which may not be available, leads to significant underestimation

of the extent of myocardial injury (Figure 5.3). The use of skeletal muscle circumvents this problem until skeletal muscle is also inflamed, which occurs in some cases of myocarditis (58) and also seen in this work. While our methods did not specifically target skeletal muscle T1 with shim or SSFP image quality control over that area, patients with myocarditis demonstrated significantly higher T1 values in skeletal muscle with greater variability (822±55 ms) compared to controls (803±32 ms, p=0.04). In this cohort of 50 patients, there were 3 cases in which the dark-blood T2 oedema ratio relative to skeletal muscle was < 2.0 (1.78±0.11) despite reasonable image quality, but the average myocardial T1 was significantly increased (1158±11ms, see example in Figure 5.4). This can be explained by skeletal muscle inflammation, supported by significantly increased T1 values in the skeletal muscle regions in these 3 patients (941±104ms, over 4 SD above the normal cohort). The finding of increased T1 values in skeletal muscle on T1-mapping is consistent with skeletal muscle inflammation demonstrated in patients presenting with acute myocarditis using pre- and post-contrast T1-weighted imaging (58). Thus, in 6% of our cohort, conventional T2W imaging was unable to diagnose oedema in myocarditis even when using skeletal muscle as a reference, with the remainder of the patients potentially affected by the same mechanism, only to a lesser degree, as supported by the overall increase in T1 values in patient skeletal muscle. All of these factors contribute to the underperformance of dark-blood T2W imaging in the detection of oedema in a systemic disease such as acute myocarditis.

5.4.2 Bright-blood T2-weighted imaging

Newer bright-blood T2w imaging offers some practical advantages: breath-holds are shorter (typically under 10 seconds), and is more forgiving in cases of tachyarrhythmias or patient movement. Better signal- and contrast-to-noise ratios seemed to improve visualisation of focal signal changes, especially in large acute lesions such as ST-elevation myocardial

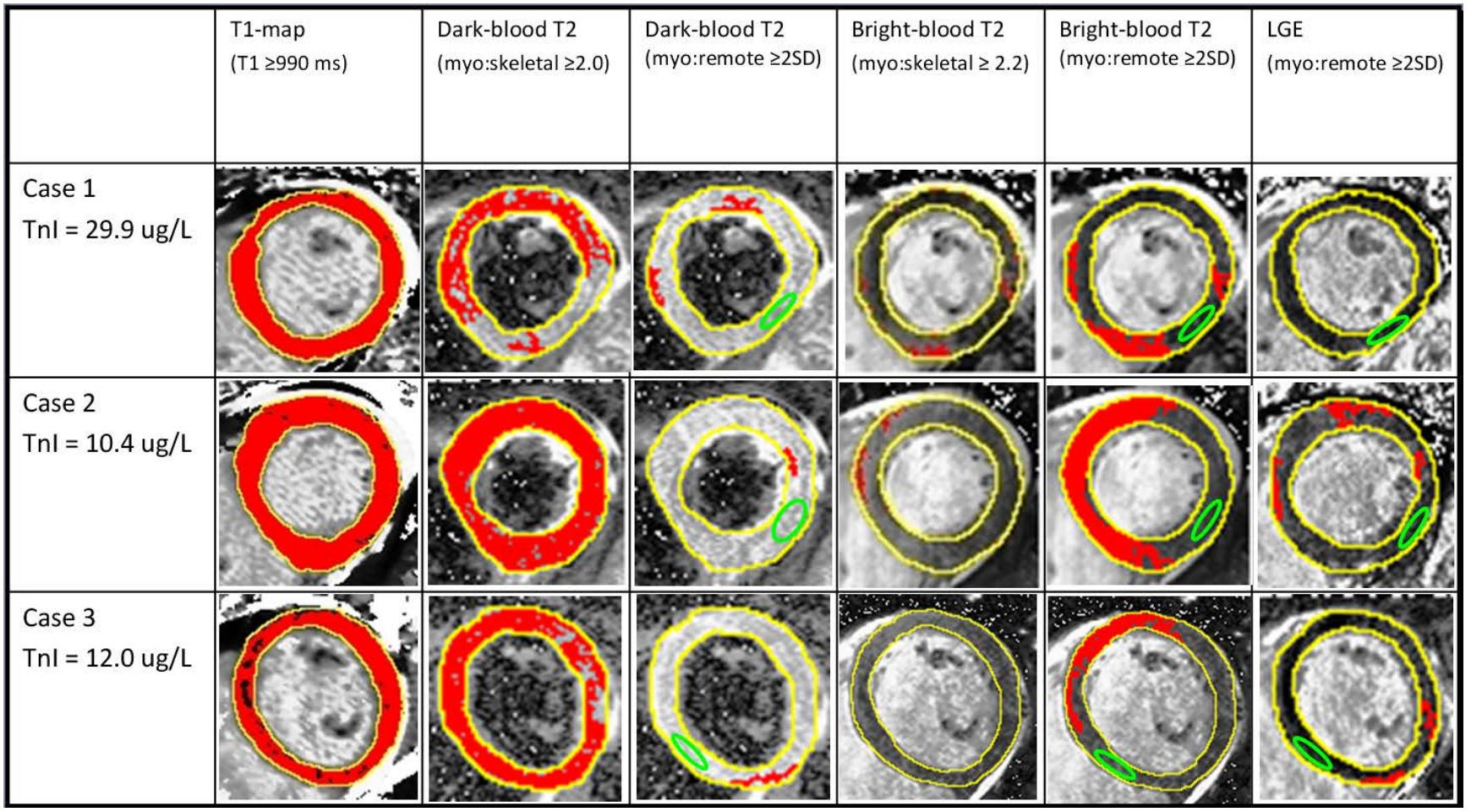


Figure 5.3 Three cases of acute myocarditis with global oedema but only mild LGE. CMR methods based on reference ROIs significantly underestimate the areas of myocardial injury. Red indicates areas of myocardium with values above the standard threshold for each CMR method. Green contour marks the positioning of myocardial reference ROI. Skeletal muscle ROI not shown. TnI = Troponin I (ug/L)

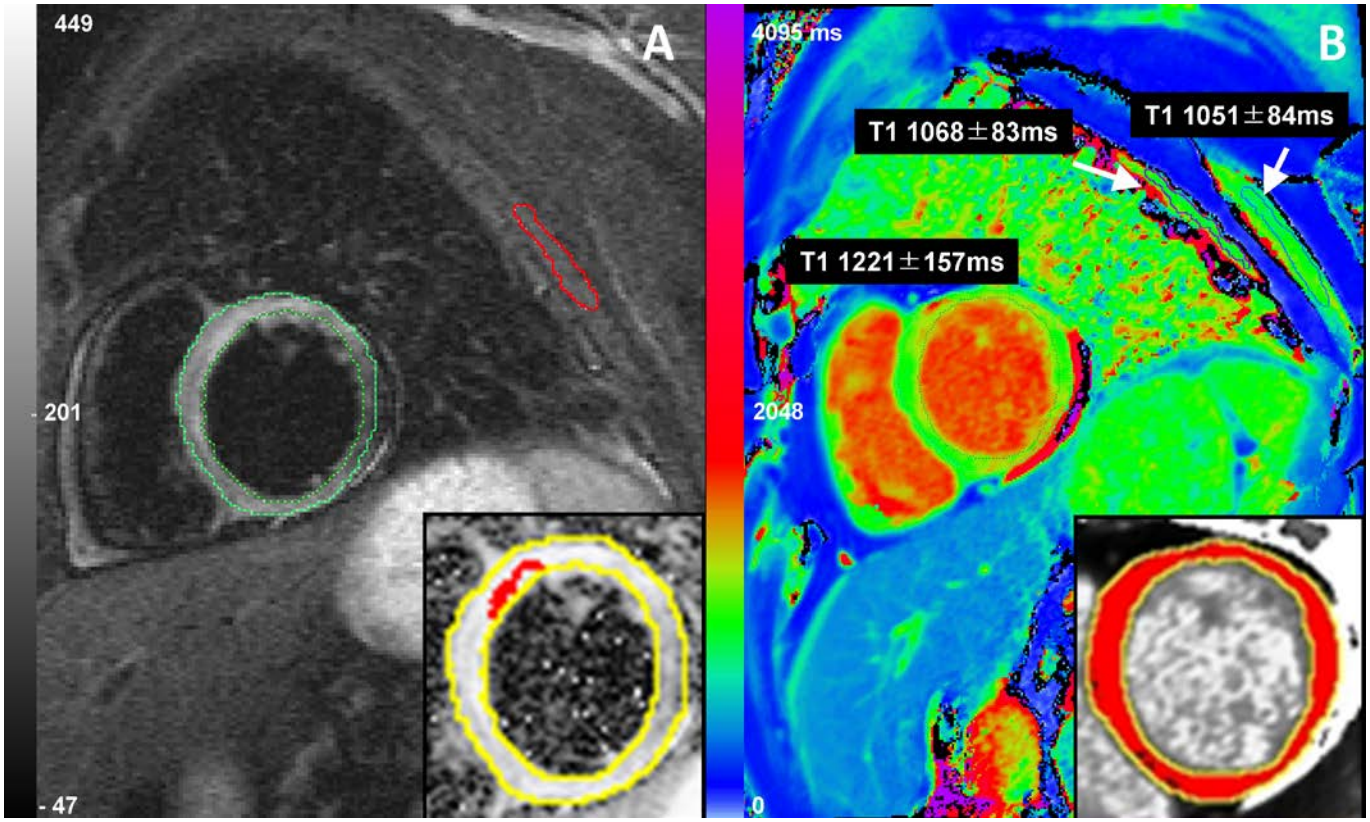


Figure 5.4 A case of acute severe myocarditis demonstrating the effect of skeletal muscle inflammation on dark-blood T2W-CMR using skeletal muscle as a reference region to detect global oedema in the myocardium. This patient had an initial ejection fraction of 37%, elevated C-reactive protein level of 94.6 [normal 0-8 mg/L) and white blood cell count 17.9 x 10^9/L with recurrent ventricular tachycardia in hospital. (A) Dark-blood T2W imaging shows visible increase in myocardial T2 SI. Inset: computer-aided analysis of the T2W image using skeletal muscle as a reference (red contour) failed to adequately detect significant increase in T2 SI ratio ≥2.0 relative to skeletal muscle within the myocardium (green contour). (B) T1-map of the corresponding slice in the same patient. Purple contour (top right) outlines skeletal muscle (T1= 1068±83 ms) corresponding to that on the T2W image; an adjacent region of skeletal muscle (blue contour) also showed high T1 values (1051±84 ms). Inset: computer-aided analysis of the T1-map, demonstrating global increase in myocardial T1 value (1221±157ms).

infarction (33); however, the detection of small, focal patchy oedema in acute myocarditis was more challenging. When normal unaffected myocardium could be reliably identified, bright-blood T2W imaging tended to display these changes well. Visual detection of global oedema, on the other hand, was less obvious to the eye on bright-blood T2W images, and the use of skeletal muscle as the reference ROI can often be limited by artefacts and noise over the region of the muscle, in addition to the same issue surrounding skeletal muscle inflammation as with dark-blood T2W imaging discussed above (57). As demonstrated in chapter 4, for cases of global oedema, dark-blood T2W imaging has a superior diagnostic performance over bright-blood T2W imaging (57).

5.4.3 Late Gadolinium Enhancement (LGE) imaging

LGE imaging has excellent CNR, making it one of the most robust CMR methods for visualising myocardial lesions, including small focal disease. Acute myocarditis can sometimes demonstrate little LGE and/or predominantly global oedema which tends to be inconspicuous on LGE imaging, such as the cases shown in Figure 5.3, hence the improved diagnostic yield by combining any 2 of 3 CMR methods for diagnosing the disease (14). It is also conceivable that sometimes, the lesions are so small they are beyond the resolution of even LGE contrast imaging. As shown in Table 5.2, combining LGE with T1-mapping did not significantly improve the diagnostic performance of LGE alone, but worsened the overall diagnostic performance of T1-mapping alone; this may be related to the fact that T1-mapping is able to detect changes due to both oedema and myocyte necrosis, and thus can serve to function as a “LGE + T2W” combination, only with much better sensitivity, diagnostic accuracy and negative predictive value than any of the LGE + T2W combination set out in Table 5.2.

5.4.4 T1-mapping

T1-mapping using ShMOLLI circumvents most of the issues suffered by conventional T2W and LGE imaging. It provides a direct, quantitative means for myocardial characterisation without the need for contrast agents or reference ROIs to detect changes within the myocardium. It has short breath-holds and is robust to even tachyarrhythmias (successful in rapid atrial fibrillation up to average ventricular rates of 150 bpm, unpublished data), making it highly suitable for acute scanning. These advantages confer ShMOLLI T1-mapping its superior diagnostic performance compared to the T2W and LGE methods tested.

5.4.5 Combination approach

The selection of diagnostic thresholds is dependent upon the amount of noise inherent to the technique and represents a trade-off between sensitivity and specificity. Historically, 2 standard deviations (SD) above the normal mean is accepted as a cut-off for identifying abnormally high values; this was applied to the original validation of dark-blood T2W imaging in detecting acute myocarditis (15,39,59) and is commonly used in LGE imaging to identify fibrosis in ischaemic and non-ischaemic heart disease (14,60). As shown in Table 5.2, the commonly accepted threshold of 2SD above normal mean SI for dark-blood T2W imaging is actually a relatively specific threshold with low sensitivity, meaning that low grade disease would easily be undetected. Interestingly, for T1-mapping, while the threshold of T1 ≥ 990ms is a sensitive threshold, it simultaneously represents an even more stringent >2.7 SD above normal T1 values; this is directly due to the fact that normal myocardial T1 values have a tight normal range with relatively small variability in the normal population, contributing to its good diagnostic performance (61). A combined approach of any 2 of the 4 techniques can improve diagnostic performance to a sensitivity 88%, specificity 100% and diagnostic accuracy 88%. Further, without the use of exogenous contrast agents, combining T1-mapping with any of the

T2W techniques closely replicated the diagnostic performance of LGE alone in the detection of acute myocarditis, with a sensitivity 76%, specificity 100% and diagnostic accuracy 83%.

5.5 Limitations

This study was performed using clinical validation for suspected myocarditis rather endomyocardial biopsy (EMB) as a reference standard and as such, lacks direct histopathologic confirmation of the diagnosis. However, in view of the well-documented low sensitivity of EMB for ruling out myocarditis (62-65) to serve as a reliable gold standard, we have chosen to validate the CMR methods using clinical criteria, as performed in multiple previous CMR validation studies (12,14,15,58). A majority of the patients (92%) had a preceding systemic viral or inflammatory illness, which, together with their CMR findings, would be consistent with a diagnosis of myocarditis; a few patients (n=4) did not have a clear infectious or inflammatory precipitant, but none of the 50 patients in the study cohort had an isolated ischaemic pattern of LGE suggestive of myocardial infarction as the presenting diagnosis. Other obvious diagnoses, such as dilated cardiomyopathy, hypertrophic cardiomyopathy or Takotsubo cardiomyopathy, were not included in this study, as outlined in the methods section.

Early gadolinium enhancement (EGE) was not performed for practical reasons as our protocol was already extensive. Therefore, out of three available conventional sequences, we selected dark-blood T2W and LGE imaging since EGE is more time-consuming and its image quality often affected by irregular breathing patterns or arrhythmias (14) commonly encountered in acutely ill patients. As the goal of the study was to validate novel CMR techniques in a cohort defined by clinical features, none of the Lake Louise imaging criteria was used as inclusion criteria when enrolling subjects. Future studies may directly compare

all available CMR methods simultaneously if the testing of method performance against each other were desired.

T2-mapping is another quantitative CMR technique which has been shown to be useful in the diagnosis of acute myocarditis (53). Again, future studies may compare T1-mapping against T2-mapping techniques in the diagnosis of acute myocarditis.

5.6 Conclusion

CMR is a superior imaging modality in the evaluation of suspected myocarditis, offering multiple techniques for myocardial tissue characterisation. In addition to dark-blood T2-weighted, early and late gadolinium enhancement imaging, newer bright-blood T2-weighted imaging and T1-mapping can now be added to the current criteria for the CMR diagnosis of myocarditis. Quantitative T1-mapping has excellent diagnostic performance equivalent to the performance of LGE imaging in this cohort. A threshold of T1 ≥ 990ms involving ≥5% of any segment in a subject has a high diagnostic performance, with a sensitivity, specificity and diagnostic accuracy of 90%, 91% and 91%, respectively. Combining T1-mapping with any of the T2W techniques closely replicated the diagnostic performance of LGE alone in the detection of acute myocarditis, with a sensitivity 76%, specificity 100% and diagnostic accuracy 83%, without the need for exogenous contrast agents. Using any 2 out of the 4 criteria can improve the CMR detection of acute myocarditis, with a sensitivity, specificity and accuracy of 87%, 100% and 88%, respectively.

Chapter 6

Tissue Characterisation of Acute Myocarditis Using T1-mapping: Insights Into Myocardial Injury from Quantitative Cardiovascular Magnetic Resonance

6.1 Introduction

As introduced in chapter 5, acute myocarditis can be detected on CMR using a combination of T2W imaging for oedema, early gadolinium enhancement (EGE) imaging for hyperaemia and late gadolinium enhancement (LGE) for the non-ischaemic pattern of myocyte necrosis. Of these three techniques, LGE is especially powerful with an impressive (up to 500%) contrast between diseased and normal myocardium, allowing detection of even small areas of myocardial injury (65,66) and differentiation between ischaemic and non-ischaemic aetiologies of myocardial disease (3). In myocarditis, LGE is a frequent finding (88%), associated with active myocarditis on histopathology, often patchy and subepicardial with one or several foci, frequently localised to the lateral free wall (65).

However, there are some limitations in using LGE alone in the diagnosis of acute myocarditis. Small, focal areas of myocarditis, especially early on in the disease process, may not always be large enough to be detected with the pixel size used. Myocarditis in some patients is characterised by predominant global oedema rather than frank myocyte necrosis, resulting in negative findings on LGE imaging. Diffuse myocarditis either may not be apparent on LGE imaging, or may not be objectively detectable given that LGE requires normal myocardium as a reference region of interest (ROI) for comparison. Additionally, although the risk is low, gadolinium-based contrast agents are associated with the rare but serious complication of nephrogenic systemic fibrosis (NSF), especially in patients with significant renal impairment (GFR<30 cc/min). Thus, it would be ideal if there were a CMR method which could provide similar information but without the need for exogenous contrast agents.

T1-mapping is an ideal candidate given its equivalent diagnostic performance to LGE in diagnosing acute myocarditis, as shown in chapter 5, and the fact that it allows direct tissue characterisation without the need for reference ROIs. In this study, our hypothesis is two-fold: (1) given that T1-mapping has an excellent sensitivity (90%) and specificity (91%) for

detecting acute myocarditis, it should be able to detect larger areas of myocardial involvement as well as very small areas of injury compared to conventional T2W and LGE techniques; (2) as T1-mapping is also a quantitative technique for tissue characterisation without the need for contrast agents, it should be possible to extract information similar to those provided by LGE imaging (such as patterns of injury) using T1-mapping. We therefore applied quantitative analyses to T1-maps for detailed tissue characterisation in patients with acute myocarditis, and compared findings to T2W and LGE imaging.

6.2 Methods

6.2.1 Study Population

This is described in Chapter 5.

6.2.2 CMR image acquisition and analysis

These are described in chapters 2, 3 and 5. In this chapter, for the T2W methods, reference regions using both skeletal muscle and remote myocardium were applied in order to evaluate all current methodologies of CMR image analysis in the assessment of this disease model - acute myocarditis.

6.2.3 Statistical analysis

These are described in chapter 5.

6.3 Results

6.3.1 Study Population characteristics

The study population characteristics were provided in Chapter 5 and summarised in table 6.1.

For the analysis in this chapter, patients were further divided into subgroups according to their diagnostic certainty of acute myocarditis based on conventional CMR findings, as CMR specialists would interpret the images: the presence or absence of (1) oedema on dark-blood T2W imaging, and; (2) hyper-enhancement on LGE imaging (table 6.2). This allows testing of the performance of T1-mapping in each group in the context of their diagnostic certainty in a clinical setting.

Group I patients (oedema+, LGE+) (n=34/50; 68%) demonstrated both oedema and LGE, with a median Troponin I of 9.80 ug/L (IQR 3.50, 19.20) and a significantly lower EF than controls (60±13% vs. 72±6%, p<0.001).

Group II patients (oedema- LGE+) (n=11/50; 22%) demonstrated only LGE patterns consistent with acute myocarditis (14); none demonstrated oedema on dark-blood T2W-CMR due to: non-diagnostic image quality as a result of poor breath-holding (n=2); tachyarrhythmia (n=2); and not meeting current T2 SI cut-off values for global or regional oedema despite good image quality (n=7). Group II patients overall had a significantly lower median Troponin I of 0.65 ug/L (IQR 0.26, 6.79) than Group I patients and a mean EF no different from controls (72±10% vs. 72±6%, p=0.71).

Group III patients (oedema-, LGE-) (n=5/50; 10%) did not demonstrate either oedema or LGE on CMR. Two patients with difficulty breath-holding had non-diagnostic dark-blood T2W and LGE (including single shot LGE) imaging, while the other three patients did not demonstrate findings despite good image quality. These patients had a significantly lower Troponin I of 0.48 ug/L.

Table 6.1 Baseline characteristics of the study population

	Normal Volunteers (n=45)	All patients (n=50)	Patient Subgroup I (Oedema+, LGE+) (n=34)	Patient Subgroup II (Oedema-, LGE+) (n=11)	Patient Subgroup III (Oedema-, LGE-) (n=5)
Age (years)	41.5 ± 14.0	41.5 ± 16.0	38.6 ± 16.9	45.6 ± 12.2	53.0 ±11.7
Female, n (%)	10 (22.2)	11 (22.0)	6 (17.6)	4 (36.4)	1 (20.0)
Troponin I (ug/L)	n/a	5.15 (1.22, 14.20)	9.80 (3.50, 19.20)	0.65 (0.26, 6.79)	0.48 (0.23, 2.04)
Coronary angiogram performed, n (%)	n/a	36 (72.0)	22 (64.7)	9 (81.8)	5 (100.0)
Median (IQR) time from symptoms to CMR (days)	n/a	3 (1, 6)	2 (1, 4)	3 (3, 8)	3 (2, 4)

Values are mean ± SD, n (%), or median (interquartile range). LGE = late gadolinium enhancement. IQR = interquartile range. CMR = cardiovascular magnetic resonance. There was no statistical difference in age and gender between controls and patients. Patient subgroup I has significantly higher Troponin I levels compared to patient subgroups II and III ($p<0.001$); all other characteristics were not statistically different amongst patient subgroups.

Table 6.2 CMR findings according to patient groups compared to controls.

CMR Method	**Controls**	**All patients (n=50)**	Group I (Oedema+, LGE+)	Group II (Oedema-, LGE+)	Group III (Oedema-, LGE-)
Ejection fraction (%)	72 ± 6	63 ± 12 (p<0.001)	60 ± 13 (p<0.001)	72 ± 10	61 ± 4 (p<0.001)
Global myocardial SI* (Dark-blood T2W-CMR)	1.56 ± 0.15	1.73 ± 0.27 (p=0.0002)	1.81 ± 0.28 (p<0.0001)	1.62 ± 0.15 (ns)	1.49 ± 0.15 (ns)
Regional myocardial SI† (Dark-blood T2W-CMR)	1.03 ± 0.05	1.08 ± 0.07 (p<0.0002)	1.10 ± 0.07 (p<0.0001)	1.06 ± 0.04 (p<0.036)	0.99 ± 0.04 (ns)
Global myocardial SI* (Bright-blood T2w-CMR)	1.84 ± 0.17 (n=20)	2.02 ± 0.33 (p<0.006; n=46)	2.09 ± 0.33 (p=0.001; n=31)	1.89 ± 0.38 (ns; n=10)	1.87 ± 0.14 (ns)
Regional myocardial SI† (Bright-blood T2w-CMR)	1.05 ± 0.07 (n=20)	1.14 ± 0.10 (p<0.0001; n=46)	1.16 ± 0.09 (p<0.0001; n=31)	1.15 ± 0.11 (p<0.021; n=10)	1.00 ± 0.03 (p<0.043)
Global myocardial T1 (T1-mapping)	941 ± 18 ms	1010 ± 65 ms (p<0.0001)	1027 ± 62 ms (p<0.0001)	987 ± 59 ms (ns)	941 ± 31 ms (ns)
LGE (%) ‡	1 % (0%, 2%) (n=30)	16 ± 16 % (p<0.0001)	17% (10%, 24%) (p<0.0001)	8% (4%, 12%) (p<0.002)	2% (0%, 3%) (p<0.005)

All p-values refer to the difference from normal controls. Bonferroni-corrected significance level is p<0.009 (p<0.05/6 comparisons); ns=p>0.05

*Global myocardial T2 SI ratio = $SI_{myocardium}/SI_{skeletal\ muscle}$; † Regional myocardial T2 SI ratio = $SI_{myocardium}/SI_{remote\ myocardium}$

‡ LGE (%) = median volume fraction of LGE per subject; interquartile range (IQR) in brackets.

Dark-blood and bright-blood T2-weighted CMR

The presence of myocardial oedema, as evidenced by significant increase in relative myocardial T2 SI, was detected by conventional dark-blood T2W imaging in Group I (oedema+, LGE+), but not Group II (oedema-, LGE+) or Group III (oedema-. LGE-) patients compared to controls, whether the reference ROI was skeletal muscle or remote myocardium (table 6.2). Similarly, newer bright-blood T2W imaging detected significant increase in myocardial T2 SI in Group I (oedema+, LGE+), but not Group II (oedema-, LGE+) or Group III (oedema-. LGE-) patients compared to controls, whether the reference ROI was skeletal muscle or remote myocardium. Bright-blood T2W imaging showed moderate correlations to dark-blood T2W imaging in the detection of myocardial oedema ($r=0.60$ for T2 $SI_{myocardium:skeletal}$, and $r=0.33$ for T2 $SI_{myocardium:remote}$; both $p<0.01$).

Late gadolinium enhancement imaging

Significant LGE was present in Group I (oedema+, LGE+) and Group II (oedema-, LGE+) but not Group III (oedema-, LGE-) patients compared to controls (Tables 6.2 and 6.3). The pattern of LGE was predominantly subepicardial and midwall, localised most frequently to the lateral wall and inferior wall, in both Groups I and II patients. None of the 50 patients demonstrated an isolated ischaemic pattern of LGE to suggest myocardial infarction as the aetiology of the acute presentation.

T1-mapping

The overall mean myocardial T1 was significantly higher in Group I (oedema+, LGE+), but not Group II (oedema-, LGE+) or Group III (oedema-. LGE-) patients compared to controls (1027±62 vs. 987±59, 941±31 and 941±18ms, respectively; $p<0.0001$; Table 6.2). Focal areas

Table 6.3 Extent and distribution of LGE in patients with acute myocarditis.

	All patients n=50 (100%)	Group I (Oedema+, LGE+) n=34 (100%)	Group II (Oedema-, LGE+) n=11 (100%)	Group III (Oedema-, LGE-) n=5 (100%)
Presence of LGE	45 (90%)	34 (100%)	11 (100%)	0 (0%)
Extent				
Subepicardial	43 (95.6%)	33 (97.1%)	10 (90.9%)	0 (0.0%)
Midwall	38 (84.4%)	27 (79.4%)	11 (100.0%)	0 (0.0%)
Subendocardial	5 (11.1%)	5 (14.7%)	0 (0.0%)	0 (0.0%)
Transmural	24 (53.3%)	20 (58.8%)	4 (36.4%)	0 (0.0%)
Distribution				
Lateral wall	44 (97.8%)	33 (97.1%)	11 (100.0%)	0 (0.0%)
Inferior wall	43 (95.6%)	33 (97.1%)	10 (90.9%)	0 (0.0%)
Septal wall	27 (60.0%)	20 (58.8%)	7 (63.6%)	0 (0.0%)
Anterior wall	16 (35.6%)	15 (44.1%)	1 (9.1%)	0 (0.0%)

LGE = late gadolinium enhancement.

of injury measured by T1-mapping showed good correlation with those measured by LGE (ρ=0.72, p<0.0001) and with Troponin I level ρ=0.82, p<0.0001).

6.3.2 Quantification of myocardial injury in acute myocarditis using CMR.

Examples of the typical extent and distribution of myocardial injury in myocarditis detected by each method are shown according to subject groups in Figure 6.1. The quantitative extent of myocardial injury by each method is presented in Figure 6.2, and summarised in Table 6.4.

Overall, T1-mapping detected a significantly larger extent of myocardial injury in all patient subgroups compared to controls (p<0.0001), and compared to all T2W methods and LGE imaging in all patient subgroups (p<0.001). Further, in Group III (oedema-, LGE-) patients, T1-mapping was able to detect small focal areas of injury in 4 of the 5 cases (see Figure 6.3).

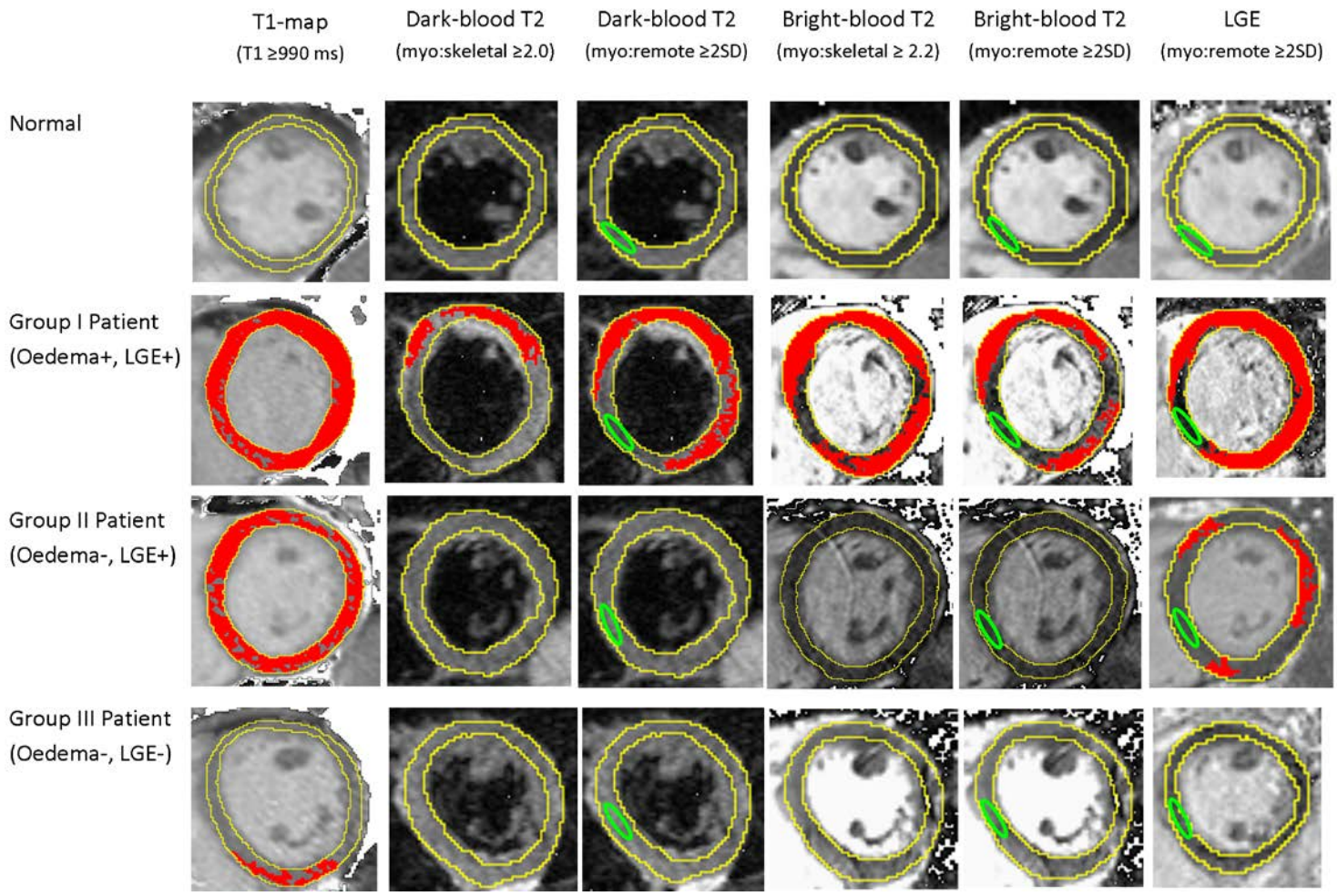


Figure 6.1 Areas of acute myocardial injury (red) as detected by computer-aided analysis of T1-maps, T2W and LGE images in patients with acute myocarditis compared to a normal subject. T1-mapping ≥990 ms (> 2.7 SD above normal myocardial T1) detected larger areas of injury than T2W and LGE imaging. Red indicates areas of myocardium with values above the stated threshold for each CMR method. Green contour marks the position of reference region of interest (ROI). Skeletal muscle ROI not shown.

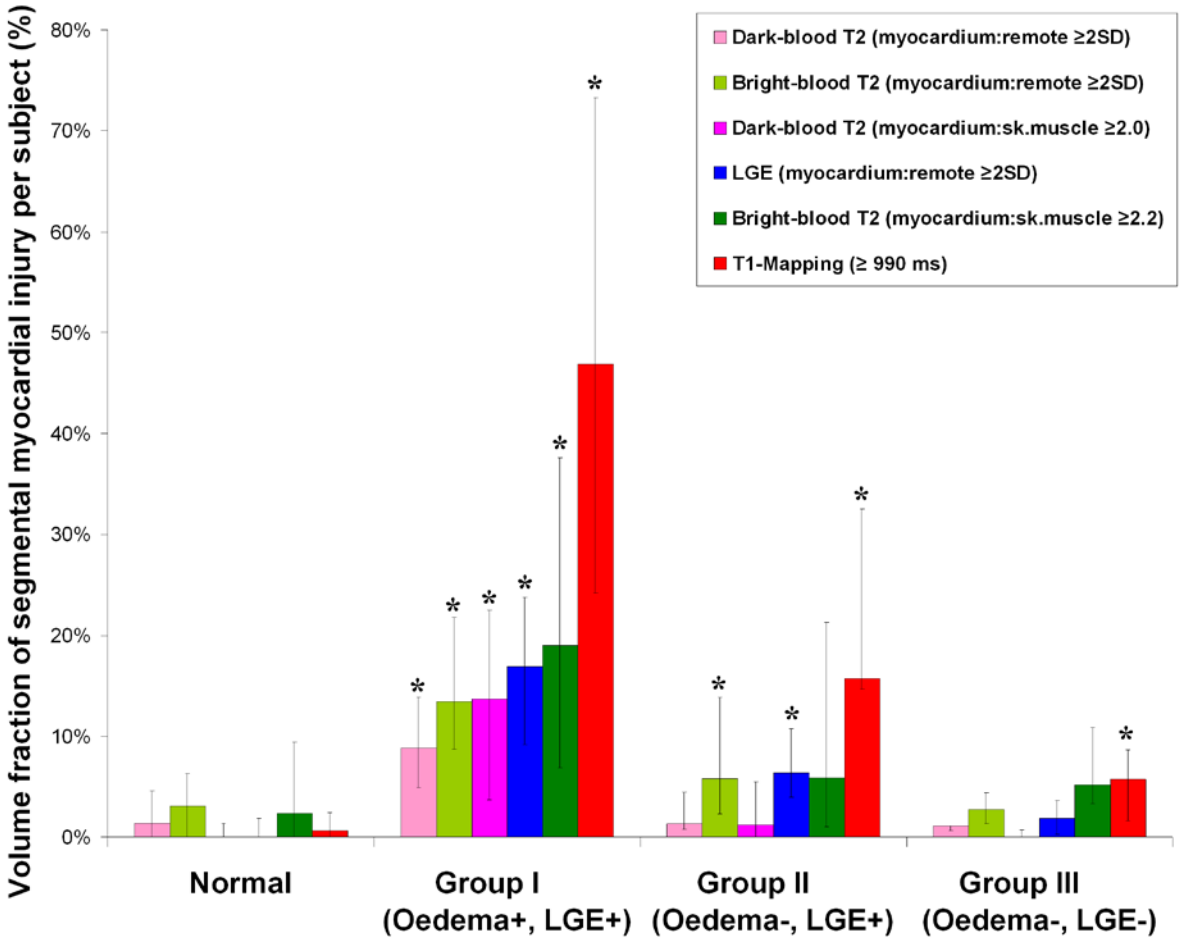


Figure 6.2 Median volume fraction of myocardial injury detected by T2W, LGE imaging and T1-mapping in normal controls and patients with acute myocarditis. T1-mapping detected a significantly larger extent of myocardial injury in all patient subgroups compared to controls (all p<0.0001), and compared to all T2W methods and LGE imaging in all patient subgroups (all p<0.001). Asterisks mark a significant difference compared to controls. Error bars are representative of interquartile ranges. T2W = T2-weighted; CMR = cardiovascular magnetic resonance; LGE = late gadolinium enhancement; IQR = interquartile range.

Table 6.4. Volume fraction of myocardial injury detected by T2W-CMR, T1-Mapping and LGE in patients with acute myocarditis compared to controls.

CMR Method	Median (IQR) volume fraction of segmental myocardial injury per subject (%)				
	Controls	**All patients**	Group I Patients	Group II Patients	Group III Patients
Dark-blood T2W-CMR (myocardium : skeletal muscle SI ratio ≥2.0)	0 (0, 1) (n=45)	7 (1, 20) (n=50)	14 (4, 22) (n=34)	1 (0, 6) (n=11)	0 (0, 1) (n=5)
Dark-blood T2W-CMR (myocardium: remote SI ratio ≥ 2 SD)	1 (0, 5) (n=45)	6 (1, 12) (n=50)	9 (5, 14) (n=34)	1 (1, 4) (n=11)	1 (1, 1) (n=5)
Bright-blood T2W-CMR (myocardium : skeletal muscle SI ratio ≥ 2.2)	2 (0, 9) (n=20)	14 (5, 29) (n=46)	19 (7, 38) (n=31)	6 (1, 21) (n=10)	5 (3, 11) (n=5)
Bright-blood T2W-CMR (myocardium: remote SI ratio ≥ 2 SD)	3 (0, 6) (n=20)	11 (5, 17) (n=46)	13 (9, 22) (n=31)	6 (2, 14) (n=10)	3 (1, 4) (n=5)
T1-mapping (T1>990 ms)	1 (0, 2) (n=45)	32 (16, 67) (n=50)	47 (24, 73) (n=34)	16 (15, 33) (n=11)	6 (2, 9) (n=5)
LGE (myocardium: remote SI ratio ≥ 2 SD)	0 (0, 2) (n=30)	11 (5, 21) (n=50)	17 (10, 24) (n=34)	8 (4, 12) (n=11)	2 (0, 3) (n=5)

T2W = T2-weighted; CMR = cardiovascular magnetic resonance; LGE = late gadolinium enhancement; IQR = interquartile range; SD = standard deviation

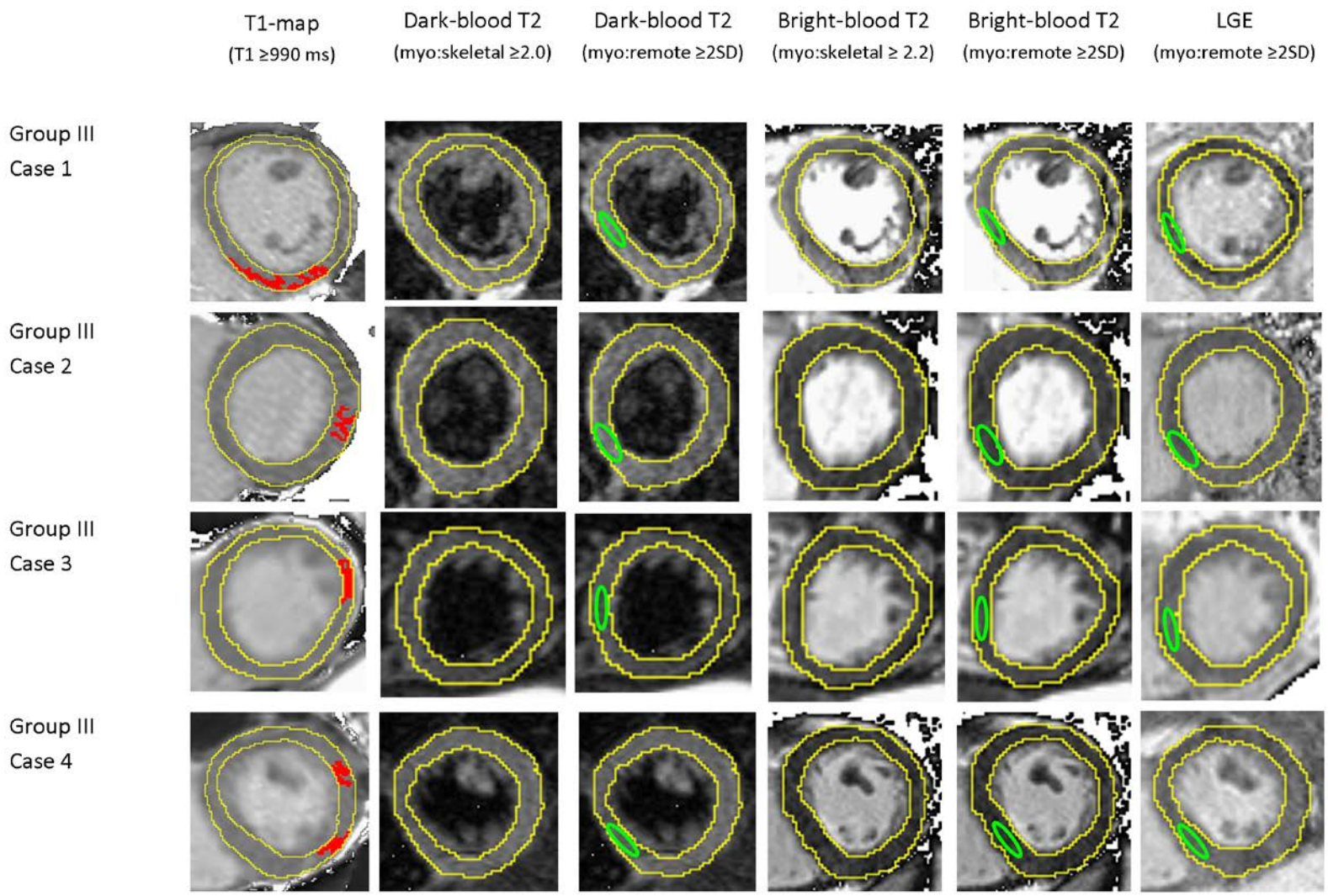


Figure 6.3 Quantitative CMR analysis of four Group III patients (oedema-, LGE-) with small rises in Troponin I. T1-mapping was able to detect small focal areas of injury in 4 out of the 5 patients in this group (marked by red overlay). Green contour marks the positioning of reference region of interest (ROI). Skeletal muscle ROI not shown

6.3.3 Patterns of myocardial injury revealed by T1-mapping using incremental thresholds.

In the preceding section, we have presented that T1-maps using the threshold of ≥ 990 ms (57), despite being >2.7 SD above normal T1 values, can detect a larger extent of myocardial injury compared to T2W or LGE methods (Figure 6.2), often demonstrating global myocardial involvement in acute myocarditis. Interestingly, to reveal the underlying pattern of myocardial injury, similar to that typically seen on LGE imaging, T1-maps using incremental thresholds can be particularly useful (Figure 6.4).

In cases of severe myocarditis (Figure 6.4, second row), T1 ≥ 990 ms revealed global myocardial injury; however, using incremental thresholds, it became evident that the most severe areas of injury (T1>1200 ms) were localised to the lateral wall in a midwall or subepicardial pattern. On the other hand, some patients presented with low-grade myocarditis with low troponin levels (Figure 6.4, bottom row); while using a T1 threshold of 1200 ms would have been too high to detect the changes, the threshold of T1 ≥ 990 ms allowed immediate visualisation of the area of injury to the inferolateral wall in a predominantly subepicardial or midwall pattern.

Thus, having a range of T1 thresholds (starting at 990 ms) allows the detection and characterisation of both low grade and severe myocarditis without compromising on either (1) the ability to detect the area of injury, or (2) to reveal the underlying pattern of injury, than relying on only one fixed threshold like many conventional methods.

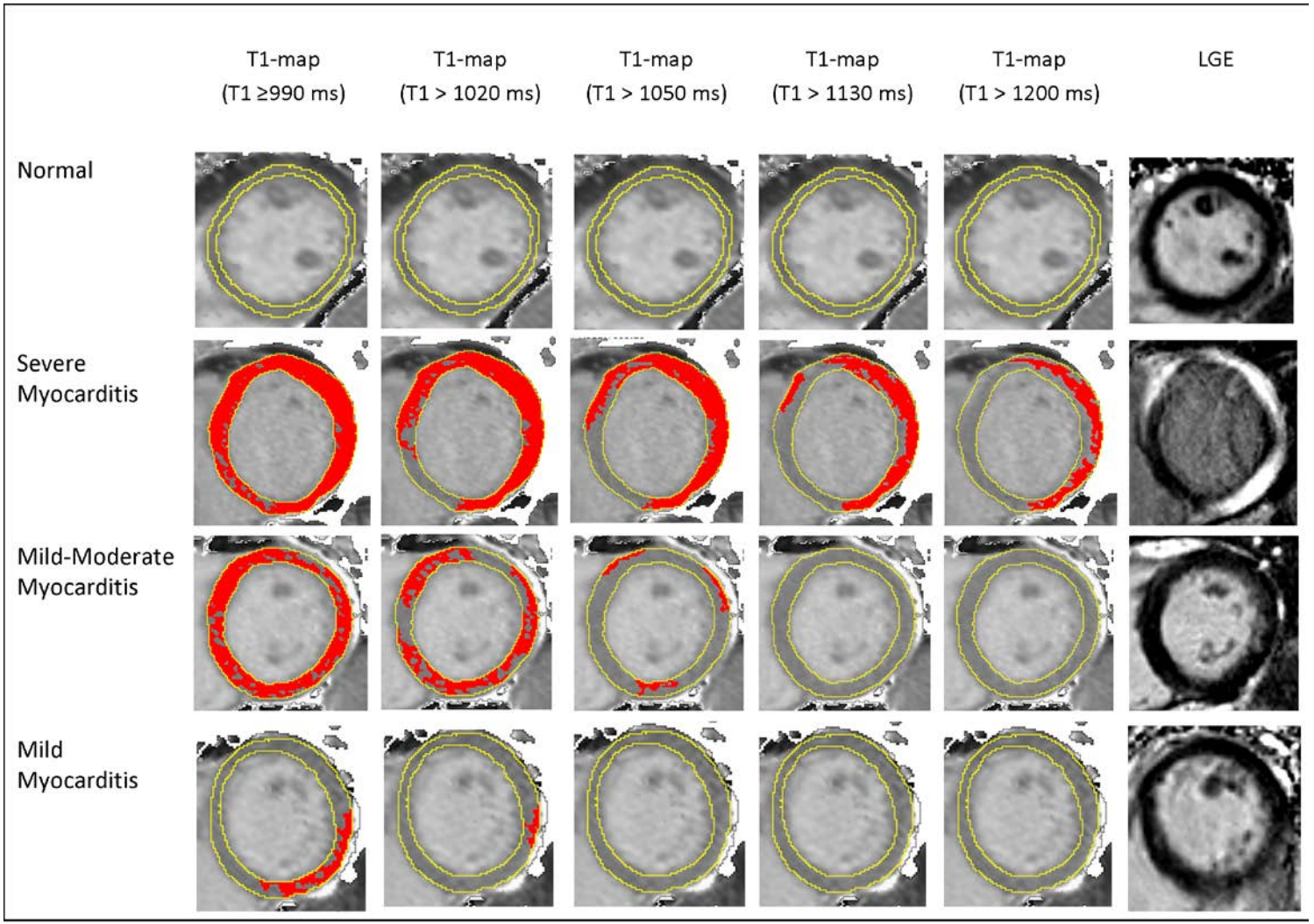


Figure 6.4 Computer-aided analyses of T1-maps using incremental thresholds to demonstrate the pattern of most severe injury in acute myocarditis across a spectrum of clinical presentation. Red indicates areas of myocardium with a T1 value above the stated threshold.

6.4 Discussion

In this work, we have shown for the first time, that native T1-mapping, without the use of exogenous contrast agents, are able to demonstrate patterns of non-ischaemic injury in acute myocarditis. T1-mapping detects a larger extent of myocardial injury than T2W and LGE methods, and is able to detect even small areas of focal injury not detected by T2W and LGE imaging. Only one patient out of 50, who had a very small Troponin I rise (0.15 ug/L) and underwent CMR 5 days after presentation, did not reveal any findings using all methods.

6.4.1 Insights from T1 characterisation of acute myocarditis

Consistent with the current understanding of acute myocarditis, the findings of significantly increased T2 SI and T1 in these patients support that oedema and inflammation major components in the acute pathophysiological process (14). While acute oedema is known to increase native T1 relaxation times (9,57), there may be additional changes, such as the distribution of free water fractions in the intra- and extra-cellular compartments, that are more readily detected by T1-mapping (9) than T2W methods. This and the fact that T1-mapping directly quantifies myocardial changes without the need for reference ROIs may explain why T1-mapping was able to detect larger areas of myocardial involvement than T2W imaging. The exact underlying pathophysiological processes that lead to changes in T1 relaxation times, however, will have to be investigated in future studies.

Additionally, T1-mapping using incremental thresholds permits visualisation of patterns of injury with simultaneous grading of disease severity. In many cases, a T1 threshold of ≥ 990ms demonstrated that acute myocarditis is a global process involving territories supplied by more than one coronary artery, and within which there are focal areas of more severe injury with even higher T1 values. These areas are characterised by a predominantly

subepicardial/midwall pattern or focal islands of high T1 within the myocardium, typically in the lateral or inferior wall. These observations are consistent with published literature that acute myocarditis starts as a focal process which then spreads globally (12). Once seeded within the myocardium, the wave front of myocardial injury appeared to spread by direct extension away from the focus of most severe injury (for example, in both a clockwise and counter-clockwise direction on a slice), until the entire myocardium is involved (Figure 6.4). This temporal pattern of injury may be confirmed in future studies by performing T1-mapping at serial time points within the first 14 days of acute myocarditis, similar to the original study using early gadolinium imaging which demonstrated this process (12). Even in some cases of severe myocarditis, while it may appear on LGE imaging that one segment of the myocardium such as the inferior septum is spared, using serial T1-maps (Figure 6.4, second row), it became evident that the entire myocardium was involved, only that the inferior septum was less severely injured, likely because it is diametrically opposite and furthest away from the initial focus of injury in the basal lateral wall. This is supported by the findings that, while patient segments with LGE had significantly higher T1 values (1058±83ms), patient segments without LGE still demonstrated average T1 values >2SD above normal T1 values (983±62 vs. 941±18ms in controls), suggesting that these areas were also likely involved, but to a milder degree. Thus, T1-maps with incremental thresholds not only display the areas of most severe injury, showing the predominant non-ischaemic pattern, but they also provide additional insights such as the wave fronts and true extent of myocardial involvement.

6.4.2 Clinical Implications

T1-mapping with incremental thresholds revealing patterns of myocardial injury has important clinical implications, as there is now a way to extract information similar to LGE imaging without the need for exogenous contrast agents. In the future, it may be possible to perform a

contrast-free CMR protocol for the diagnosis of acute myocarditis. For instance, it may be feasible to perform cine, T2W imaging and T1-mapping to start. If a diagnosis were apparent from these images, then perhaps gadolinium administration may be omitted or reserved for cases in which the diagnosis is still uncertain. This approach is supported by our findings presented in Table 5.2 in chapter 5, where the combination of T1-mapping with any T2W method replicates the diagnostic performance of LGE alone. However, such an approach should be tested against other cardiac pathologies in a wide spectrum of clinical population to further investigate the ability of T1-mapping to distinguish diseases in combination with other CMR techniques. It does hold promise and may be particularly useful for patients in whom gadolinium contrast is contraindicated.

6.6 Conclusion

Acute myocarditis can typically be diagnosed using a combination of clinical assessment and CMR tissue characterisation. While T2W and LGE imaging can detect oedema and myocyte necrosis, respectively, T1-mapping offers information and insights into acute myocarditis beyond what both of these techniques can provide, such as the detection of larger areas of injury and also locating small areas of injury otherwise not detected by conventional techniques. More importantly, T1 mapping with incremental thresholds (starting at ≥ 990 ms) allows tailoring of diagnostics to the individual rather than relying on fixed thresholds. It permits the detection of areas and patterns of injury in both mild and severe cases of myocarditis similar to the type of information obtained from LGE imaging that often aid in clinical decision making, but without the need for exogenous contrast agents. In the future, it may be feasible to perform contrast-free CMR protocols in the diagnosis of myocarditis; future work will have to test this approach in variety of cardiac pathologies.

Chapter 7

General conclusions and future directions

Cardiovascular magnetic resonance, with its superior capabilities in advanced multiparametric tissue characterisation, is in a prime position to provide more insight into the wide range of cardiac phenotypes and possible aetiologies commonly encountered in clinical practice. In addition to conventional CMR techniques for tissue characterisation such as T2-weighted imaging for oedema and late gadolinium enhancement imaging for patterns of scarring and fibrosis, myocardial T1-mapping, by way of the novel ShMOLLI method, has advanced from a previously primary research tool to a clinically applicable technique. Together with our cardiac physics team, we have successfully developed a T1-mapping method that:

1. breached the breath-hold barrier for clinical T1-mapping to under 10 seconds – this directly translates to better patient tolerability and fewer respiratory motion artefacts, leading to better image quality, improving diagnostic yield.

2. is heart rate independent – this renders the ShMOLLI method more robust to tachyarrhythmias such as excessive sinus tachycardia, atrial fibrillation and frequent premature ectopic beats, all frequently encountered in acutely ill patients.

3. has less error in measuring high T1 values than the conventional method – this means improved accuracy in estimating long T1 such as in myocardial oedema.

4. has a tight normal range with little variability in the normal population, making it one of the best imaging biomarkers suitable for detecting disease states.

5. can detect different models of myocardial oedema, whether regional or global, by direct tissue quantification without the need for reference regional of interests as required by conventional T2-weighted imaging. T1-mapping thus is likely to be useful in other cardiac pathologies where oedema or increase water content is part of the pathophysiological process.

6. detects larger and additional areas of injury compared to T2W and LGE techniques in the assessment of acute myocarditis, revealing a truer extent of myocardial involvement and diagnosing cases when conventional methods are non-revealing.

7. has a high diagnostic performance equivalent to that of late gadolinium enhancement imaging in the detection of acute myocarditis. Additionally, ShMOLLI T1-mapping provides information similar to that of LGE imaging but without the need for exogenous contrast agents. This may benefit patients with contraindications to gadolinium-based contrast agents.

T1-mapping holds great promise in sophisticated, quantitative tissue characterisation of myocardial diseases. These may include non-ischaemic cardiomyopathy and ischaemic heart disease. Future studies should include the testing of T1-mapping in distinguishing different cardiac conditions in a wide clinical population. Histopathologic correlation to T1-mapping may help elucidate the underlying mechanisms of T1 changes in the human myocardium during disease states. Follow-up and prognostic data for T1-mapping will help further

establish the method as clinically useful and informative for both patients and clinicians, hopefully improving patient care and outcomes.

Index of Tables and Figures

Table 3.1 Assessment of myocardium by T1-mapping and LGE at 3T in acute STEMI treated by 1^{o} PCI **p. 51**
Table 4.1 Patient characteristics. **p. 64**
Table 4.2 Mean myocardial T1 and T2 SI ratios per-subject according to groups and segmental wall motion. **p. 65**
Table 5.1 CMR findings in patients with acute myocarditis compared to controls. **p. 88**
Table 5.2 Diagnostic performance of CMR tissue criteria in the detection of suspected acute myocarditis. **p. 91**
Table 6.1 Baseline characteristics of the study population **p.104**
Table 6.2 CMR findings according to patient groups compared to controls. **p.105**
Table 6.3 Extent and distribution of LGE in patients with acute myocarditis. **p.107**
Table 6.4. Volume fraction of myocardial injury detected by T2W-CMR, T1-Mapping and LGE in patients with acute myocarditis compared to controls. **p.111**

Figure 1.1 T1 relaxation curve of normal human myocardium at 1.5 Tesla **p.15**
Figure 1.2 (A) T1 relaxation curves of fat, myocardium and blood. (B) Colour T1-map **p.17**
Figure 2.1 Dark-blood T2-weighted image with myocardial contours (green contours) and regions of interests over remote myocardium (blue contour) and skeletal muscle (red contour). **p.30**
Figure 2.2 Bright-blood T2-weighted image with myocardial contours (green contours) and regions of interests over remote myocardium (blue contour) and skeletal muscle (red contour). **p.31**
Figure 2.3 Late gadolinium image with myocardial contours (green contour) and region of interest over remote myocardium (blue contour) **p.32**
Figure 3.1 ECG-gated pulse sequence schemes for simulation of A) MOLLI and B) ShMOLLI at a heart rate of 60 bpm **p.37**
Figure 3.2 ShMOLLI conditional data analysis. **p.38**
Figure 3.3 Relationship between T1 measurements for ShMOLLI (top row) and MOLLI (bottom row) **p.42**
Figure 3.4 Representative short axis slice T1 maps of the normal myocardium obtained using MOLLI (top row) and ShMOLLI (bottom row) at 1.5T at the baseline and following Gd administration for perfusion imaging (1st Gd) and after top-up (2nd Gd) at times shown in panel labels **p.44**
Figure 3.5 T1 values for AHA myocardial segments 1-16 (see insert) at 1.5T and 3T using ShMOLLI and MOLLI **p.46**
Figure.3.6 Bland-Altman plot shows good agreement between the average ShMOLLI and MOLLI myocardial T1 values pooled across our material obtained at 1.5T and 3T **p.47**
Figure 3.7 Short-term intra-scan variability of MOLLI vs. ShMOLLI at 1.5T. The Bland-Altman plots demonstrate that the standard deviation (SD) of the differences is the same at 16 ms, with both methods having similar 95% repeat confidence interval at ± 32ms (~3% of resting myocardial T1 values). **p.48**
Figure 3.8 The distribution of T1 in case #1 at 3T using A) MOLLI and B) ShMOLLI reveals two distinct populations of values within the myocardium, which can be fitted using two Gaussian curves, corresponding to injured (long T1) and unaffected (normal T1) myocardium. **p.50**
Figure 3.9 Simulated average relative T1 estimation error (thick lines) with boundaries characterising dependence on heart rate (thin lines) and measurement noise (whiskers) as a function of reference T1ref. **p.53**
Figure 4.1 Relationship between: **(A)** myocardial T1 values and T2 signal intensity (SI) ratio* derived from dark-blood T2W-CMR; **(B)** myocardial T1 values and T2 SI ratio derived from bright-blood T2W-CMR; **(C)** myocardial T2 SI ratio dark-blood vs. bright-blood T2W-CMR. *T2 SI ratio=$SI_{myocardium}/SI_{skeletal\ muscle}$ **p.66**

Figure 4.2 CMR imaging modalities used for comparison – representative images in short-axis slices **p.67**
Figure 4.3 Receiver operator characteristic curves for the detection of acute myocardial oedema by ShMOLLI T1-mapping, dark-blood T2W-CMR and bright-blood T2W-CMR. **p.69**
Figure 4.4 ROC curves for the detection of acute myocardial oedema according to patient groups using ShMOLLI T1-mapping, dark-blood T2W-CMR and bright-blood T2W-CMR. **p.70**

Figure 4.5 ROC curves for the detection of acute myocardial oedema by ShMOLLI T1-mapping, dark-blood T2W-CMR and bright-blood T2W-CMR **p.72**
Figure 4.6 Receiver operator characteristic curves according to patient groups for the detection of acute myocardial oedema using all segments, including segments previously rejected for artefacts for all methods. **p.73**
Figure 5.1 Acute myocarditis. **p.87**
Figure 5.2: Diagnostic performance of T1-mapping compared to T2W and LGE imaging in the detection of acute myocarditis. **p.90**
Figure 5.3 Three cases of acute myocarditis with global oedema but only mild LGE. CMR methods based on reference ROIs significantly underestimate the areas of myocardial injury. **p.94**
Figure 5.4 A case of acute severe myocarditis demonstrating the effect of skeletal muscle inflammation on dark-blood T2W-CMR using skeletal muscle as a reference region to detect global oedema in the myocardium. **p.95**
Figure 6.1 Areas of acute myocardial injury (red) as detected by computer-aided analysis of T1-maps, T2W and LGE images in patients with acute myocarditis compared to a normal subject. **p.109**
Figure 6.2 Median volume fraction of myocardial injury detected by T2W, LGE imaging and T1-mapping in normal controls and patients with acute myocarditis. **p.110**
Figure 6.3 Quantitative CMR analysis of four Group III patients (oedema-, LGE-) with small rises in Troponin I. **p.112**
Figure 6.4 Computer-aided analyses of T1-maps using incremental thresholds to demonstrate the pattern of most severe injury in acute myocarditis across a spectrum of clinical presentation. **p.114**

Appendix 1: R^2 maps

Supplemental Methods for Chapter 4

Image Post-processing

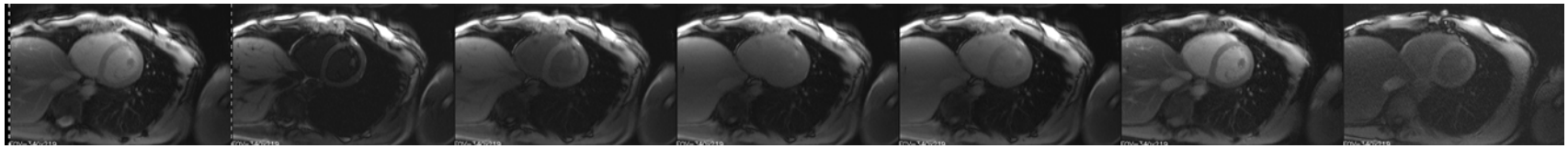
Quality assessment of T1-maps – the use of R^2 maps

The R^2 map is a pixel-wise indicator of the quality of the T1-map, and is dependent on a number of factors, including SNR, partial volume effects, off-resonance frequency shifts, motion or any other sources of error. These factors are not additive across the image and generally have different impact on R^2. As such, there is no specific R^2 value for a particular error source. Low R^2 may indicate T1 bias or just increased T1 variation.

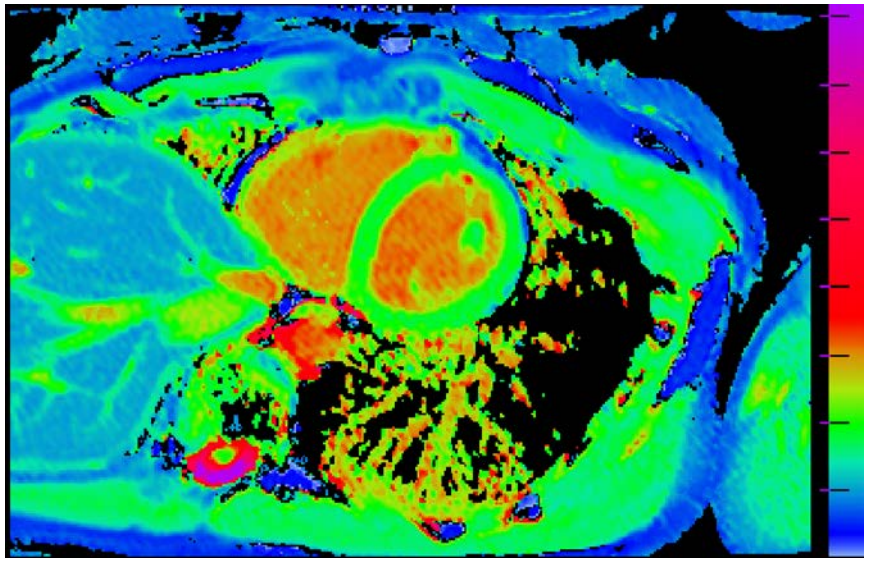
The R^2 map is a visual aid for detection of artefacts. For instance, a T1-map with T1 values having excellent fit to the T1 recovery curve model will have an R^2 map free of artefacts (see figures below). On the other hand, a T1-map with poor fit to the T1 recovery curve (such as due to breathing or mistriggering during acquisition) will have recognizable regions of dark pixels on the edges of myocardium on its R^2 map (see figures below). Similarly, dark SSFP bands encroaching on the myocardium may also produce artefacts on the T1 map and R^2 map (see figures on next pages). Segments significantly affected by poor T1 fit as evidenced on the R^2 maps were rejected, much like segments affected by artefacts on images acquired using other sequences may be rejected on a visual and qualitative basis.

R^2 maps provide an additional means to identify areas with potentially compromised T1 accuracy. These tools allow critical assessment of the quality of T1-maps generated, which led to an overall higher rejection rate for T1-mapping compared to other modalities studied. However, even with re-inclusion of all segments affected by artefacts, T1-mapping retained superiority in diagnostic performance. Thus, additional tools to assess for artefacts and inaccuracies serve to increase the reliability of T1-mapping compared to some of the standard CMR modalities.

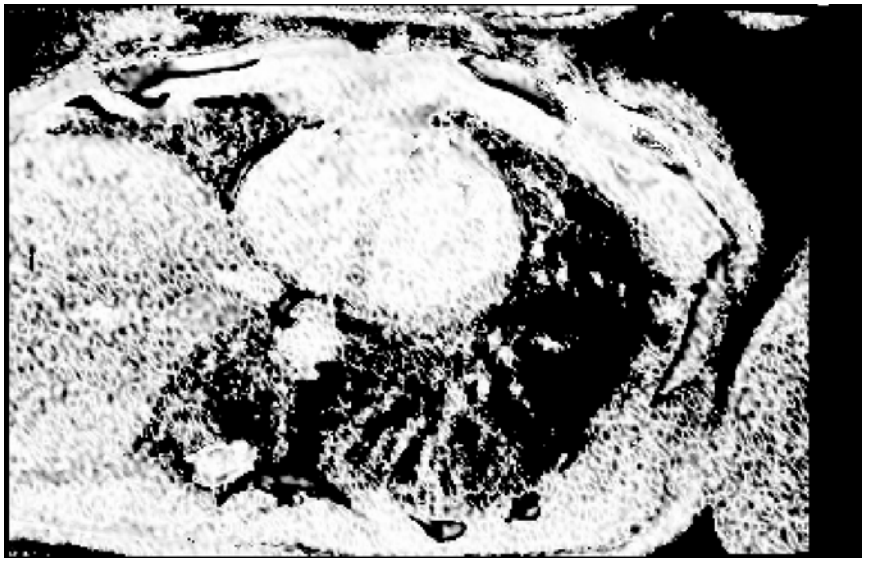
ShMOLLI T1-mapping - No artefacts



Raw T1 images

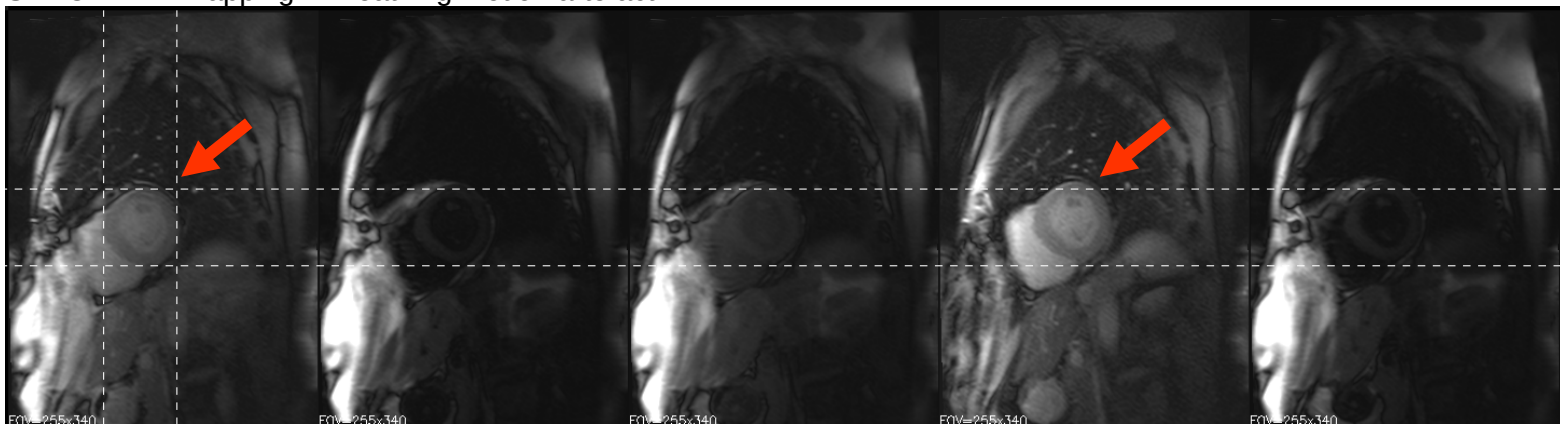


Coloured T1-map

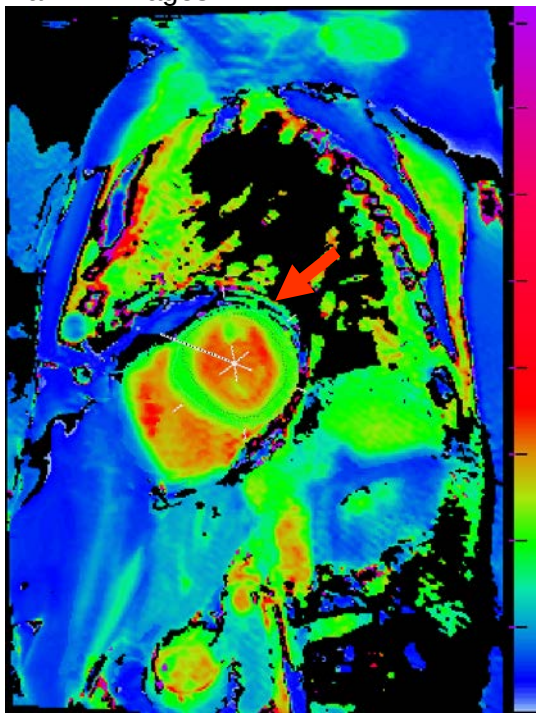


R^2 map

ShMOLLI T1-mapping – Breathing motion artefact



Raw T1 images

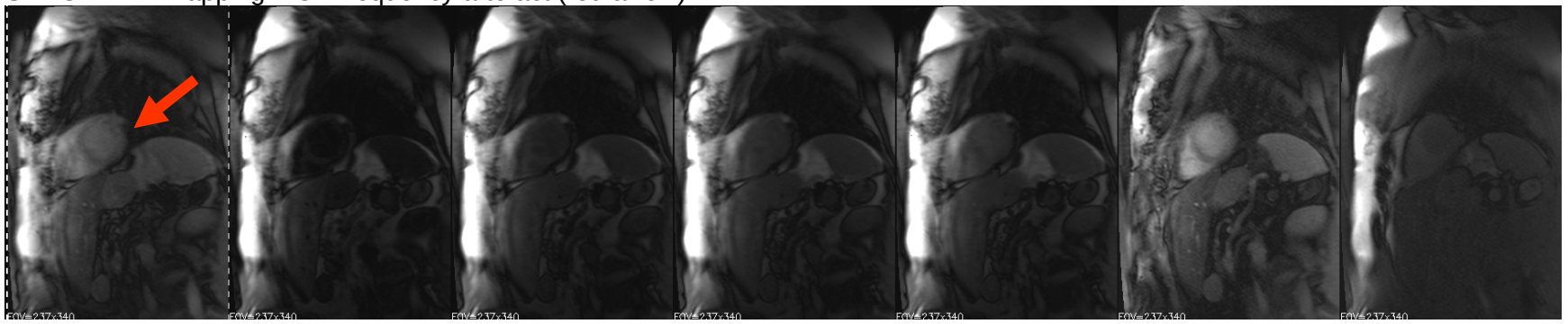


Coloured T1-map



R^2 map

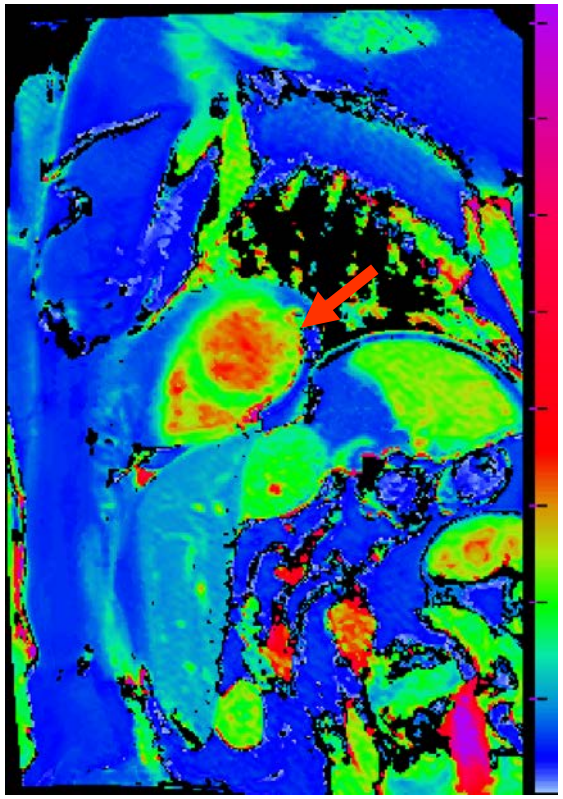
ShMOLLI T1-mapping – Off-frequency artefact (red arrow)



Raw T1 images



Raw T1 image

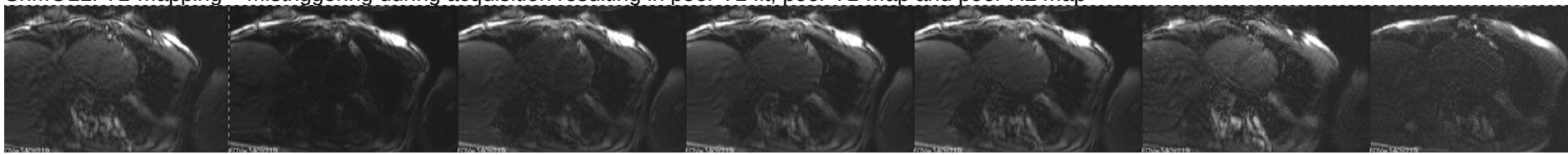


Coloured T1-map

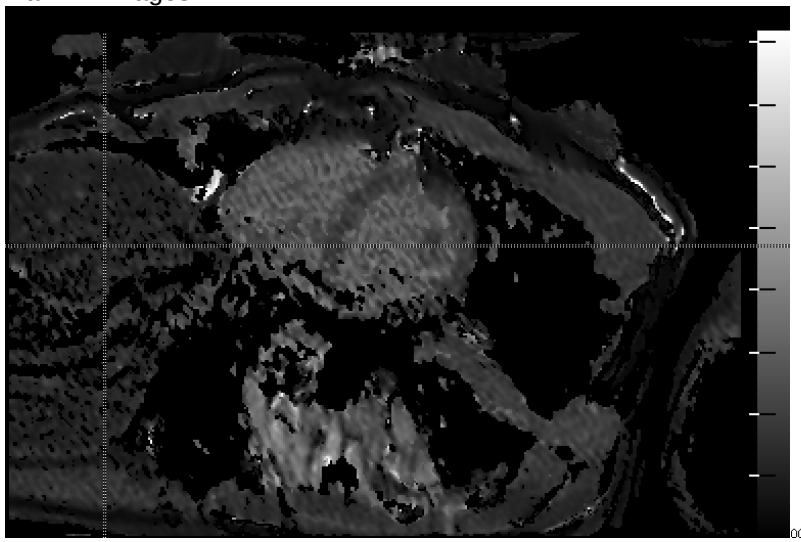


R^2 map

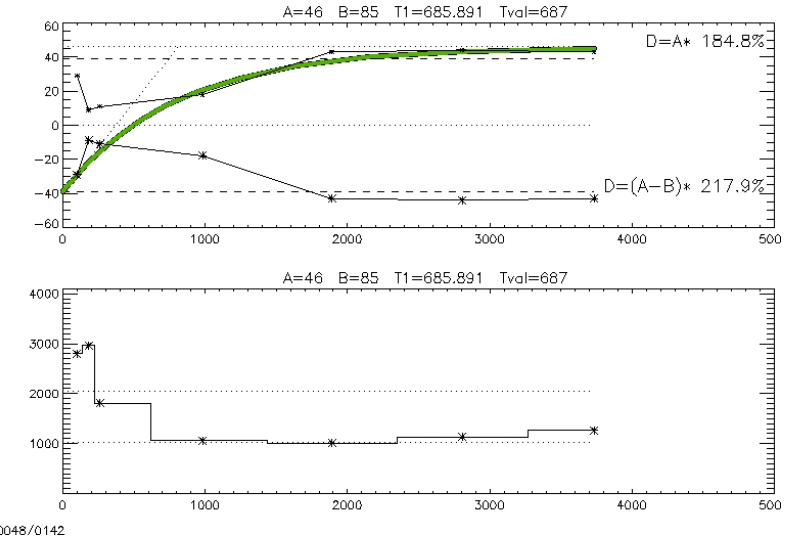
ShMOLLI T1-mapping – Mistriggering during acquisition resulting in poor T1 fit, poor T1-map and poor R2 map



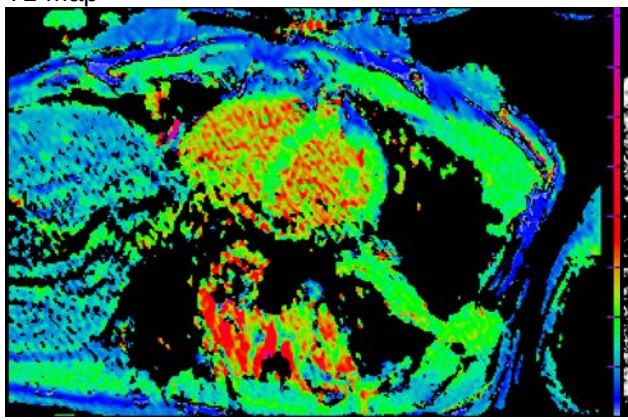
Raw T1 images



T1-map



T1 curve fitting



Coloured T1-map



R^2 map

Appendix 2: Published abstracts

1. **VM Ferreira**; SK Piechnik; E Dall'Armellina; TD Karamitsos; JM Francis; RP Choudhury; MG Friedrich; MD Robson; S Neubauer. T1-mapping accurately detects acute myocardial edema: a comparison to T2-weighted cardiovascular magnetic resonance imaging. Poster presentation. SCMR 15th Annual Scientific Sessions, Orlando, 2012.

2. **VM Ferreira**; SK Piechnik; E Dall'Armellina; TD Karamitsos; JM Francis; RP Choudhury; A Kardos; MG Friedrich; MD Robson; S Neubauer. The Diagnostic Performance of Non-contrast T1-Mapping in Patients with Acute Myocarditis on Cardiovascular Magnetic Resonance Imaging. SCMR 15th Annual Scientific Sessions, Orlando, 2012.

3. **VM Ferreira**; SK Piechnik; E Dall'Armellina; TD Karamitsos; JM Francis; RP Choudhury; A Kardos; MG Friedrich; MD Robson; S Neubauer. T1-mapping has a high diagnostic performance in patients presenting with acute myocarditis: a cardiovascular magnetic resonance study. British Cardiovascular Society Annual Conference 2012 May 28-30.

4. SK Piechnik, **V Ferreira**, AJ Lewandowski, N Ntusi, D Sado, V Maestrini, SK White, M Lazdam, R Banerjee, MB Hofman, J Moon, S Neubauer, P Leeson, MD Robson. Age and gender dependence of pre-contrast T1-relaxation times in normal human myocardium at 1.5T using ShMOLLI**.** SCMR 15th Annual Scientific Sessions, Orlando, 2012.

5. E Dall'Armellina, SK Piechnik, **V Ferreira**, JM Francis, MD Robson, F Cuculi, R Kharbanda, AP Banning, RP Choudhury, T Karamitsos, S Neubauer. Characterization of acute myocardial infarction by pre-contrast T1 mapping**.** SCMR 15th Annual Scientific Sessions, Orlando, 2012.

6. S Dass, J Suttie, SK Piechnik, **V Ferreira**, C Holloway, MD Robson, H Watkins, T Karamitsos, S Neubauer. Non-contrast T1 mapping characterizes the myocardium beyond that achieved by late gadolinium enhancement in both hypertrophic and dilated cardiomyopathy**.** SCMR 15th Annual Scientific Sessions, Orlando, 2012.

7. S Bull, SK White, SK Piechnik, A Flett, **V Ferreira**, M Loudon, JM Francis, S Neubauer, J Moon, S Myerson. Pre-contrast T1 mapping for detection of myocardial fibrosis in asymptomatic and symptomatic aortic stenosis**.** SCMR 15th Annual Scientific Sessions, Orlando, 2012.

8. T Karamitsos, SM Banypersad, D Sado, V Maestrini, **V Ferreira**, SK Piechnik, MD Robson, PN Hawkins, S Neubauer, J Moon. Pre-contrast ShMOLLI T1 mapping in cardiac AL amyloidosis**.** SCMR 15th Annual Scientific Sessions, Orlando, 2012.

9. **VM Ferreira**; SK Piechnik; E Dall'Armellina; TD Karamitsos; JM Francis; RP Choudhury; A Kardos; MG Friedrich; MD Robson; S Neubauer. Non-contrast T1-Mapping is a Novel Diagnostic Tool for Acute Myocarditis on Cardiovascular Magnetic Resonance Imaging. Oral presentation. *Scientific Sessions of the American Heart Association Scientific Sessions*, Orlando, 2011.

10. **VM Ferreira**; SK Piechnik; E Dall'Armellina; TD Karamitsos; JM Francis; RP Choudhury; MG Friedrich; MD Robson; S Neubauer. T1-Mapping is Superior to T2-weighted Cardiovascular Magnetic Resonance Imaging for the Detection of Acute Reversible Myocardial Injury. Poster presentation. *Scientific Sessions of the American Heart Association Scientific Sessions*, Orlando, 2011.

11. **VM Ferreira**, SK Piechnik, E Dall'Armellina, T Karamitsos, JM Francis, MG Friedrich, MD Robson, S Neubauer. Quantification of acute myocardial injury in patients presenting with chest pain, positive troponins and non-obstructive coronary arteries by ShMOLLI T1-Mapping, edema and late gadolinium imaging. Poster. *SCMR/EuroCMR Joint Scientific Sessions*, Nice, 2011

12. E Dall'Armellina; S Piechnik; **V Ferreira**; TD Karamitsos, JM Francis; F Cuculi; C Forfar; BD Prendergast; AP Banning; KM Channon; RK Kharbanda; MD Robson; RP Choudhury; S Neubauer. CMR T1 mapping at 3T characterizes the extent of acute ischaemic myocardial injury: comparison to standard techniques. Oral presentation. *Scientific Sessions of the American Heart Association Scientific Sessions*, Orlando, 2011.

13. S Dass; JJ Suttie; S Piechnik; **V Ferreira;** C Holloway; TD Karamitsos; MD Robson; H Watkins; S Neubauer. In Both Hypertrophic and Dilated Cardiomyopathy, Non-contrast T1 Mapping provides Myocardial Tissue Characterization beyond that achieved by Late Gadolinium Enhancement. Oral presentation. *Scientific Sessions of the American Heart Association Scientific Sessions*, Orlando, 2011.

14. E Dall'Armellina, SK Piechnik, **VM Ferreira,** TD Karamitsos, JM Francis, MD Robson, RP Choudhury, S Neubauer. Quantification of acute myocardial injury in STEMI patients post revascularization at 3Tesla – Comparison of T1-mapping, late gadolinium and edema imaging *SCMR/EuroCMR Joint Scientific Sessions*, Nice, 2011

15. SK Piechnik, E Dall'Armellina, **VM Ferreira**, MD Robson. Gaussian modelling for operator-independent and threshold-free volumetric segmentation of phase sensitive inversion recovery late gadolinium enhanced images**.** *Journal of Cardiovascular Magnetic Resonance* 2011, 13 (Suppl 1):P43 (2 February 2011)

16. **Ferreira VM**, Dall'Armellina E, Robson MD, Piechnik SK, Neubauer S. A Novel Sequence for Cardiac T1-Mapping at 3T – Shortened Modified Look-Locker Inversion Recovery (ShMOLLI): From Theory to Practice. In: 5th BSCMR Annual Meeting 24th March 2010 (Poster).

17. SK. Piechnik, **VM Ferreira**, E Dall'Armellina, LE. Cochlin, S Neubauer, MD Robson. ShMOLLI: Shortened Modified Look Locker Inversion Recovery for Cardiac T1 Mapping – from Theory to Normal Human Myocardium. *ISMRM-ESMRMB Joint Annual Meeting*, Stockholm, 2010.

18. SK. Piechnik, E Dall'Armellina, **VM Ferreira**, LE Cochlin, JE Schneider, S Neubauer, MD Robson. Quantitative T1 and T2 Measurements of Tissue Characteristics in Myocardial Infarction – Pilot Results at 3T. *ISMRM-ESMRMB Joint Annual Meeting*, Stockholm, 2010.

19. Piechnik SK, **Ferreira VM**, Dall'Armellina E, Neubauer S, Robson MD: Validation of the Shortened Modified Look Locker Inversion recovery (Sh-MOLLI) sequence for cardiac gated T1 mapping - normal human myocardium*. SCMR Thirteenth Annual Scientific Sessions*, Phoenix, 2010

20. Piechnik SK, **Ferreira VM,** Dall'Armellina E, Cochlin LE, Robson MD: Shortened Modified Look Locker Inversion recovery (Sh-MOLLI) cardiac gated mapping of T1 - Theory and phantom verification. *26th Annual Scientific Meeting, ESMRMB*, Antalya, 2009.

Appendix 3: Publications

1. **VM Ferreira**; SK Piechnik; E Dall'Armellina; TD Karamitsos; JM Francis; RP Choudhury; MG Friedrich; MD Robson; S Neubauer. Non-Contrast T1-Mapping Detects Acute Myocardial Edema with High Diagnostic Accuracy: A Comparison to T2-weighted Cardiovascular Magnetic Resonance Imaging. *Journal of Cardiovascular Magnetic Resonance* 2012, 14**:**42. Highly Accessed status achieved within 14 days of publication.

2. SK Piechnik; **VM Ferreira**; E Dall'Armellina; LE Cochlin; A Greiser; S Neubauer; MD Robson. Shortened Modified Look-Locker Inversion recovery (ShMOLLI) for clinical myocardial T1-mapping at 1.5 and 3 T within a 9 heartbeat breathhold. *Journal Cardiovascular Magnetic Resonance* 2010, 12: 69.

3. E Dall'Armellina; S Piechnik; **V Ferreira**; QL Si, M Robson; JM Francis; F Cuculi; RK. Kharbanda; AP Banning; RP Choudhury; TD Karamitsos; S Neubauer. Cardiovascular magnetic resonance by non-contrast T1 mapping allows assessment of severity of injury in acute myocardial infarction. *Journal Cardiovascular Magnetic Resonance* published online 6 Feb 2012 ahead of print DOI: 10.1186/1532-429X-14-15

4. S Dass, JJ Suttie, SK Piechnik, **VM Ferreira**, CJ Holloway, R Banerjee, M Mahmod, L Cochlin, TD Karamitsos, MD Robson, H Watkins, S Neubauer. Myocardial Tissue Characterization using Magnetic Resonance Non-Contrast T1 Mapping in Hypertrophic and Dilated Cardiomyopathy. Manuscript accepted for publication in *Circulation Cardiovascular Imaging* September 2011

5. E Dall'Armellina, N Karia, A Lindsay, TD Karamitsos, **V Ferreira**, MD Robson, P Kellman, JM Francis, C Forfar, B Prendergast, AP Banning, KM Channon, RK Kharbanda, S Neubauer and RP Choudhury. Dynamic Changes of Edema and Late Gadolinium Enhancement after Acute Myocardial Infarction and their Relationship to Functional Recovery and Salvage Index. *Circulation Cardiovascular Imaging* 2011 May 1; 4(3): 228-36.

6. TD Karamitsos, S Bull, **V Ferreira**, N.J Alp, S Neubauer.Acute Myocarditis Mimicking Reverse Takotsubo Cardiomyopathy. *Circulation* 2011;123;226-227

7. DC Hutchings; D Adlam; **V Ferreira**; TD Karamitsos; KM Channon. Takotsubo Cardiomyopathy in association with endogenous and exogenous thyrotoxicosis. *QJM* (2011) 104 (5):433-435.

Bibliography

1. Leading Causes of Death. Centers for Disease Control and Prevention Accessed 6 September, 2012. ;http://www.cdc.gov/nchs/fastats/lcod.htm.
2. Internet. Accessed September 06. Leading causes of death, 2010. Office for National Statistics.
3. Shah DJ, Judd RM, R.J. K. Myocardial viability. Clinical Magnetic Resonance Imaging. 3rd edition. 2006;Edelman R.R., Hesselink J.R., Zlatkin M.B., and Crues J.V. (Eds), Elsevier, New York, NY.
4. Bloch F. Nuclear induction. Physical Review (Physics) 1946;70:460-473.
5. Bottomley PA, Foster TH, Argersinger RE, Pfeifer LM. A review of normal tissue hydrogen NMR relaxation times and relaxation mechanisms from 1-100 MHz: Dependence on tissue type, NMR frequency, temperature, species, excision, and age. Med. Phys. 1984;11:425-448.
6. Look DC, Locker DR. Time saving in measurement of NMR and EPR relaxation times. Rev. Sci. Instrum. 1970;41:250-251.
7. Messroghli DR, Radjenovic A, Kozerke S, Higgins DM, Sivananthan MU, Ridgway JP. Modified look-locker inversion recovery (MOLLI) for high-resolution T 1 mapping of the heart. Magn. Reson. Med. 2004;52:141-146.
8. Been M, Thomson BJ, Smith MA, et al. Myocardial involvement in systemic lupus erythematosus detected by magnetic resonance imaging. Eur. Heart J. 1988;9:1250-1256.
9. Williams ES, Kaplan JI, Thatcher F. Prolongation of proton spin lattice relaxation times in regionally ischemic tissue from dog hearts. J. Nucl. Med. 1980;21:449-453.
10. Larson DM, Menssen KM, Sharkey SW, et al. "False-positive" cardiac catheterization laboratory activation among patients with suspected ST-segment elevation myocardial infarction. Journal of the American Medical Association 2007;298:2754-2760.
11. Assomull RG, Lyne JC, Keenan N, et al. The role of cardiovascular magnetic resonance in patients presenting with chest pain, raised troponin, and unobstructed coronary arteries. European Heart Journal 2007;28:1242-1249.
12. Friedrich MG, Strohm O, Schulz-Menger J, Marciniak H, Luft FC, Dietz R. Contrast media-enhanced magnetic resonance imaging visualizes myocardial changes in the course of viral myocarditis. Circulation 1998;97:1802-1809.
13. Simonetti OP, Finn JP, White RD, Laub G, Henry DA. "Black blood" T2-weighted inversion-recovery MR imaging of the heart. Radiology 1996;199:49-57.
14. Friedrich MG, Sechtem U, Schulz-Menger J, et al. Cardiovascular Magnetic Resonance in Myocarditis: A JACC White Paper. J. Am. Coll. Cardiol. 2009;53:1475-1487.
15. Abdel-Aty H, Boye P, Zagrosek A, et al. Diagnostic performance of cardiovascular magnetic resonance in patients with suspected acute myocarditis: Comparison of different approaches. J. Am. Coll. Cardiol. 2005;45:1815-1822.
16. Aletras AH, Kellman P, Derbyshire JA, Arai AE. ACUT2E TSE-SSFP: A hybrid method for T2-weighted imaging of edema in the heart. Magn. Reson. Med. 2008;59:229-235.
17. Piechnik SK, Ferreira VM, Dall'Armellina E, et al. Shortened Modified Look-Locker Inversion recovery (ShMOLLI) for clinical myocardial T1-mapping at 1.5 and 3 T within a 9 heartbeat breathhold. J. Cardiovasc. Magn. Reson. 2010;12:69.
18. Messroghli DR, Plein S, Higgins DM, et al. Human myocardium: Single-breath-hold MR T1 mapping with high spatial resolution - Reproducibility study. Radiology 2006;238:1004-1012.

19. Messroghli DR, Niendorf T, Schulz-Menger J, Dietz R, Friedrich MG. T1 mapping in patients with acute myocardial infarction. J. Cardiovasc. Magn. Reson. 2003;5:353-359.
20. Messroghli DR, Walters K, Plein S, et al. Myocardial T1 mapping: Application to patients with acute and chronic myocardial infarction. Magn. Reson. Med. 2007;58:34-40.
21. Marks B, Mitchell DG, Simelaro JP. Breath-holding in healthy and pulmonary-compromised populations: effects of hyperventilation and oxygen inspiration. J. Magn. Reson. Imaging 1997;7:595-7.
22. Solano JP, Gomes B, Higginson IJ. A comparison of symptom prevalence in far advanced cancer, AIDS, heart disease, chronic obstructive pulmonary disease and renal disease. J. Pain Symptom Manage. 2006;31:58-69.
23. Messroghli DR, Greiser A, FrÃ¶hlich M, Dietz R, Schulz-Menger J. Optimization and validation of a fully-integrated pulse sequence for modified look-locker inversion-recovery (MOLLI) T1 mapping of the heart. J. Magn. Reson. Imaging 2007;26:1081-1086.
24. Nelder JA, Mead R. A simplex method for function minimization. The Computer Journal 1965;7:308.
25. Cochlin L, Blamire A, Styles P. Dependence of T1 and T2 on high field strengths in doped agarose gels; facilitating selection of composition for specific T1/T2 at relevant field. Proceedings of 11th Annual ISMRM Meeting. Toronto, Canada. 2003:885.
26. Cerqueira MD, Weissman NJ, Dilsizian V, et al. Standardized myocardial sementation and nomenclature for tomographic imaging of the heart: A Statement for Healthcare Professionals from the Cardiac Imaging Committee of the Council on Clinical Cardiology of the American Heart Association. Circulation 2002;105:539-542.
27. Kim RJ, Wu E, Rafael A, et al. The use of contrast-enhanced magnetic resonance imaging to identify reversible myocardial dysfunction. N. Engl. J. Med. 2000;343:1445-1453.
28. Piechnik SK, Ferreira VM, Dall'Armellina E, Cochlin LE, Robson MD. Shortened Modified Look Locker Inversion recovery (Sh-MOLLI) cardiac gated mapping of T1 - Theory and phantom verification. 26th Annual Scientific Meeting, ESMRMB Antalya, Turkey, 2009:485.
29. Sharma P, Socolow J, Patel S, Pettigrew RI, Oshinski JN. Effect of Gd-DTPA-BMA on blood and myocardial T1 at 1.5T and 3T in humans. J. Magn. Reson. Imaging 2006;23:323-30.
30. Been M, Ridgeway JP, Douglas RHB. Characterisation of acute myocardial infarction by gated magnetic resonance imaging. Lancet 1985;2:348-350.
31. Friedrich MG. Myocardial edema - a new clinical entity? Nature Reviews Cardiology 2010;7:292-296.
32. Abdel-Aty H, Zagrosek A, Schulz-Menger J, et al. Delayed enhancement and T2-weighted cardiovascular magnetic resonance imaging differentiate acute from chronic myocardial infarction. Circulation 2004;109:2411-2416.
33. Payne AR, Casey M, McClure J, et al. Bright-blood T2-weighted MRI has higher diagnostic accuracy than dark-blood short tau inversion recovery MRI for detection of acute myocardial infarction and for assessment of the ischemic area at risk and myocardial salvage. Circulation: Cardiovascular Imaging 2011;4:210-219.
34. Aletras AH, Tilak GS, Natanzon A, et al. Retrospective determination of the area at risk for reperfused acute myocardial infarction with T2-weighted cardiac magnetic resonance imaging: Histopathological and displacement encoding with stimulated echoes (DENSE) functional validations. Circulation 2006;113:1865-1870.
35. Abdel-Aty H, Simonetti O, Friedrich MG. T2-weighted cardiovascular magnetic resonance imaging. J. Magn. Reson. Imaging 2007;26:452-459.
36. Dall'Armellina E, Karamitsos TD, Neubauer S, Choudhury RP. CMR for characterization of the myocardium in acute coronary syndromes. Nature Reviews Cardiology 2010;7:624-636.
37. Kellman P, Aletras AH, Mancini C, McVeigh ER, Arai AE. T2-prepared SSFP improves diagnostic confidence in edema imaging in acute myocardial infarction compared to turbo spin echo. Magn. Reson. Med. 2007;57:891-897.

38. Arai AE. Magnetic resonance imaging for area at risk, myocardial infarction, and myocardial salvage. J. Cardiovasc. Pharmacol. Ther. 2011;16:313-320.
39. Dall'Armellina E, Piechnik S, Ferreira V, et al. Cardiovascular magnetic resonance by non contrast T1 mapping allows assessment of severity of injury in acute myocardial infarction. J. Cardiovasc. Magn. Reson. 2012;14:15.
40. Eitel I, Von Knobelsdorff-Brenkenhoff F, Bernhardt P, et al. Clinical characteristics and cardiovascular magnetic resonance findings in stress (takotsubo) cardiomyopathy. JAMA - Journal of the American Medical Association 2011;306:277-286.
41. DeLong ER, DeLong DM, Clarke-Pearson DL. Comparing the areas under two or more correlated receiver operating characteristic curves: a nonparametric approach. Biometrics 1988;44:837-845.
42. Bland JM, Altman DG. Statistical methods for assessing agreement between two methods of clinical measurement. Lancet 1986;1:307-310.
43. Wince WB, Kim RJ. Molecular imaging: T2-weighted CMR of the area at riskg-a risky business? Nature Reviews Cardiology 2010;7:547-549.
44. Abdel-Aty H, Cocker M, Friedrich MG. Myocardial edema is a feature of Tako-Tsubo cardiomyopathy and is related to the severity of systolic dysfunction: Insights from T2-weighted cardiovascular magnetic resonance. Int. J. Cardiol. 2009;132:291-293.
45. Eitel I, Lücke C, Grothoff M, et al. Inflammation in takotsubo cardiomyopathy: insights from cardiovascular magnetic resonance imaging. Eur. Radiol. 2010;20:422-431.
46. Bragadeesh T, Jayaweera AR, Pascotto M, et al. Post-ischaemic myocardial dysfunction (stunning) results from myofibrillar oedema. Heart 2008;94:166-171.
47. Thygesen K, Alpert JS, Jaffe AS, et al. Third universal definition of myocardial infarction. Eur. Heart J.;33:2551-2567.
48. Vignaux O, Dhote R, Duboc D, et al. Clinical significance of myocardial magnetic resonance abnormalities in patients with sarcoidosis: A 1-year follow-up study. Chest 2002;122:1895-1901.
49. Iles L, Pfluger H, Phrommintikul A, et al. Evaluation of Diffuse Myocardial Fibrosis in Heart Failure With Cardiac Magnetic Resonance Contrast-Enhanced T1 Mapping. J. Am. Coll. Cardiol. 2008;52:1574-1580.
50. Flett AS, Hayward MP, Ashworth MT, et al. Equilibrium contrast cardiovascular magnetic resonance for the measurement of diffuse myocardial fibrosis: Preliminary validation in humans. Circulation 2010;122:138-144.
51. Sparrow P, Messroghli DR, Reid S, Ridgway JP, Bainbridge G, Sivananthan MU. Myocardial T1 mapping for detection of left ventricular myocardial fibrosis in chronic aortic regurgitation: pilot study. AJR. American journal of roentgenology 2006;187.
52. Krombach GA, Hahn C, Tomars M, et al. Cardiac amyloidosis: MR imaging findings and T1 quantification, comparison with control subjects. J. Magn. Reson. Imaging 2007;25:1283-1287.
53. Thavendiranathan P, Walls M, Giri S, et al. Improved detection of myocardial involvement in acute inflammatory cardiomyopathies using T2 mapping. Circulation: Cardiovascular Imaging 2011;5:102-110.
54. Monney PA, Sekhri N, Burchell T, et al. Acute myocarditis presenting as acute coronary syndrome: Role of early cardiac magnetic resonance in its diagnosis. Heart 2010;97:1312-1318.
55. Doolan A, Langlois N, Semsarian C. Causes of sudden cardiac death in young Australians. Med. J. Aust. 2004;180:110-112.
56. Felker GM, Thompson RE, Hare JM, et al. Underlying causes and long-term survival in patients with initially unexplained cardiomyopathy. N. Engl. J. Med. 2000;342:1077-1084.

57. Ferreira V, Piechnik S, Dall'Armellina E, et al. Non-contrast T1-mapping detects acute myocardial edema with high diagnostic accuracy: a comparison to T2-weighted cardiovascular magnetic resonance. J. Cardiovasc. Magn. Reson. 2012;14:42.
58. Laissy JP, Messin B, Varenne O, et al. MRI of acute myocarditis: A comprehensive approach based on various imaging sequences. Chest 2002;122:1638-1648.
59. Kim RJ, Fieno DS, Parrish TB, et al. Relationship of MRI delayed contrast enhancement to irreversible injury, infarct age, and contractile function. Circulation 1999;100:1992-2002.
60. Dall'Armellina E, Karia N, Lindsay AC, et al. Dynamic Changes of Edema and Late Gadolinium Enhancement after Acute Myocardial Infarction and Their Relationship to Functional Recovery and Salvage Index. Circulation: Cardiovascular Imaging 2011.
61. Piechnik S, Ferreira V, Lewandowski A, et al. Age and gender dependence of pre-contrast T1-relaxation times in normal human myocardium at 1.5T using ShMOLLI. J. Cardiovasc. Magn. Reson. 2012;14:P221.
62. Baughman KL. Diagnosis of myocarditis death of Dallas criteria. Circulation 2006;113:593-595.
63. Hauck AJ, Kearney DL, Edwards WD. Evaluation of postmortem endomyocardial biopsy specimens from 38 patients with lymphocytic myocarditis: Implications for role of sampling error. Mayo Clin. Proc. 1989;64:1235-1245.
64. Mavrogeni S, Spargias C, Bratis C, et al. Myocarditis as a precipitating factor for heart failure: Evaluation and 1-year follow-up using cardiovascular magnetic resonance and endomyocardial biopsy. Eur. J. Heart Fail. 2011;13:830-837.
65. Mahrholdt H, Goedecke C, Wagner A, et al. Cardiovascular Magnetic Resonance Assessment of Human Myocarditis: A Comparison to Histology and Molecular Pathology. Circulation 2004;109:1250-1258.
66. Simonetti OP, Kim RJ, Fieno DS, et al. An improved MR imaging technique for the visualization of myocardial infarction. Radiology 2001;218:215-223.